Order Number 8926395

Wave overtopping and partial standing waves

Umeyama, Motohiko, Ph.D.

University of Hawaii, 1989

U·M·I
300 N. Zeeb Rd.
Ann Arbor, MI 48106

WAVE OVERTOPPING AND PARTIAL STANDING WAVES

A DISSERTATION SUBMITTED TO THE GRADUATE DIVISION OF
THE UNIVERSITY OF HAWAII IN PARTIAL FULFILLMENT
OF THE REQUIREMENTS FOR THE DEGREE OF

DOCTOR OF PHILOSOPHY

IN OCEAN ENGINEERING

May 1989

by

Motohiko Umeyama

Dissertation Committee:

Franciscus Gerritsen, Chairman
Charles L. Bretschneider
Ping Cheng
Hans-Jurgen Krock
Harold G. Loomis

ACKNOWLEDGEMENTS

I would like to thank my advisor, Professor Franciscus Gerritsen, for his assistance, encouragement and advice to pursue this research. I appreciate the dissertation committee as well. I am deeply grateful.

The hydraulic model study was conducted at the Hydraulic Laboratory of Civil Engineering, College of Industrial Technology, Nihon University. The author is very grateful to Nihon University for their permission to use the university facilities at Narashino. I wish to thank Dr. S. Endo, research associate Mr. M. Ochiai and their senior students for aid in construction of the model and measurements of surface displacement, analysis of data, and their support in conducting the experiments.

ABSTRACT

In this study, first the surface displacement of standing waves is derived from the finite amplitude approximation when the wave elevation exceed a breakwater with a vertical wall. Some important phenomena related to wave motion are also studied. Second, a basic concept is explained to obtain a total amount of wave overtopping, considering the property of standing waves in front of the vertical wall. Third, computer experiments are carried out in order to estimate the surface displacement of waves and the total amount of wave overtopping. These calculations are compared with the results of laboratory experiments.

A perturbation method representing a non-linear gravity water waves is applied to the vertical displacement of the water surface and the velocity potential to derive a standing wave equation at wave overtopping. The author gives consideration to the solution of Goda and Abe (1968), who dealt with the standing wave as a combination of incident wave, reflective wave and bound wave (secondary effect by two waves) and calculated the surface displacement for various wave conditions. In this study this method is expanded to predict the temporal and spatial free surface displacement, the reflection effect, and the effect to the incident wave height in front of the breakwater when the crest level of the breakwater is lowered below the maximum wave elevation and the wave overtopping takes place.

In addition to the non-linear treatment of the standing wave, the wave crest and trough levels and the variation of mean water level are studied to ascertain the interaction of waves and structure in non-overtopping and overtopping conditions.

A theoretical investigation is conducted to study the behavior of wave overtopping in the presence of a vertical wall. A hypothesis is proposed to calculate the quantity of overtopping water during an entire wave period. The hypothesis is based on the energy equation. The total amount of wave overtopping is calculated by integrating a function of the free surface elevations of perfect and partial standing waves at the vertical wall.

Experiments were performed to verify the theories in a two-dimensional wave channel where a vertical breakwater model was placed. The surface displacement of partial standing waves was measured at several points between the breakwater and 150cm from the breakwater.

The surface displacements, calculated using the finite amplitude method are shown to be in agreement with test data for which the crest levels of the breakwater were chosen 4cm, and 8cm above still water level, and above maximum wave elevations. The comparison of results of the numerical method of wave overtopping with data obtained from measurements by another investigator, shows a reasonable agreement despite the simple hypothesis that was assumed.

TABLE OF CONTENT

LIST OF TABLES

LIST OF FIGURES

LIST OF SYMBOLS

a : first order amplitude of surface elevation

a_* : first order amplitude of surface elevation of reflective wave

B : width of channel

b_{mn} : coefficient of elevation

c : abbreviation for cosh kh

C_1 : correction factor to wave frequency due to finite amplitude effect of progressive waves

C_2 : correction factor to wave frequency due to interaction between progressive and reflective waves

C_f : discharge coefficient

E : energy head

f : vertical displacement of water surface in general

$f_c(\ )$: vertical displacement of surface water measured from z=0 on partial standing wave condition

$f_m(\ )$: vertical displacement of surface water measured from z=0 on perfect standing wave condition

$F(\ )$: flux of momentum

g : acceleration of gravity (=980cm/sec^2)

h : water depth

H_c : height of breakwater from still water level

H_I : incident wave height

H_I' : incident wave height after wave overtopping

H_R : reflected wave height

H_s : standing wave height

k : wave number in general

$\bar{k}$: average of incident and reflected wave numbers

k_A : first order approximation of wave number

K_1 : correction factor to wave number corresponding to C_1

K_2 : correction factor to wave number corresponding to C_2

K_I : ratio between H_I' and H_I $(=\bar{H}_I'/H_I)$

K_R : reflection coefficient $(=H_R/H_I)$

L : wave length in general

P : pressure

q : discharge per unit width

Q : total amount of wave overtopping

R : mean water level of reflected wave from still water level

S_{xx} : radiation stress

t : time

T : wave period

T_f : transfer coefficient

u : horizontal velocity of water particle

v : mean horizontal velocity of overtopping flow

w : vertical velocity of water particle

x : horizontal coordinate

z : vertical coordinate measured from still water level

α_{mn} : coefficient of non-periodic term of velocity potential

β_{mn} : coefficient of velocity potential

δ : non-linear effect on height of set-up from still water level

ε : parameter related to wave amplitude (=ka)

η_c : wave crest height on partial standing wave

η_s : absolute wave trough height in perfect standing wave

η_t : absolute wave trough height in partial standing wave

λ : reflection coefficient

λ_1 : reflection coefficient in wave overtopping condition

λ_2 : ratio between incident wave heights after to before wave overtopping

π : constant (3.14159...)

ρ : water density

σ : angular wave frequency ($2\pi/T$)

τ : dimensionless time (argument)

ϕ : velocity potential

SPECIAL SYMBOLS

$|\ \ |$: absolute value

$O(\ )$: order symbol

CHAPTER I

INTRODUCTION

The protection of shores or harbors from wave attack often depends on structures, the design of which is related to the understanding of physical processes and on being able to predict physical quantities at a given location. The principal function of breakwaters is to prevent the penetration of incident waves into a harbor, but complete stoppage of these waves at the breakwater may not always be required in the design process. When waves travel to the breakwater, they will undergo several processes which will involve energy dissipation, run-up on the seaward face of the structure, and reflection. Where the wave elevation exceeds the crest of the breakwater, wave overtopping takes place. The estimation of wave overtopping is very important when determining the size of breakwaters. More recently, maritime structures have been constructed in deeper water, and the design of these structures often allows wave overtopping, by lowering the design height in order to reduce construction cost. Therefore, as better models are developed, better decisions can be made to improve future coastal and ocean structures and to help the protection of existing structures as well. It is in this spirit that this investigation was carried out. The objective of this study is to analyze phenomena of waves which approach a vertical wall normally, to determine the amount of wave overtopping, and to apply the result to the design of coastal structures such as breakwaters and seawalls. The basic characteristics of motion of waves during wave overtopping are still

obscure, although many studies related to these phenomena have been done theoretically and experimentally. The results of these studies have been applied to the design of breakwaters for beach protection.

The essential problem arising from the interaction of incident waves and structure is related to the reflection of waves and the formation of partial standing waves. The resultant wave pattern can also be influenced by overflow when wave overtopping occurs. Assumptions employed on the partial standing waves are not closely approximated in the vicinity of the structure, although many types of wave theories have been applied to obtain the physics of overtopping waves. The difficulty of this problem relates to the complexity of the hydraulic phenomenon which includes periodic wave motion and flow over a structure at the same time. The surface displacement of the partial standing waves can be determined from incident wave height, wave period and water depth at the location of the structure, in a similar way as developed for perfect standing wave problems. The height of the structure has an influence on the wave overtopping condition.

The amount of wave overtopping has been treated on a two dimensional basis and calculations of quantities have been made per unit length and per wave period. Many studies have been carried out using wave channel tests while others have endeavored to derive a theory based on a weir approach. The treatment of wave overtopping in a numerical model using the weir approach is possible but lacks conformity with the physical phenomenon

because the mechanism of wave overtopping is treated as steady flow. The property of standing waves does not enter in these formulations. Therefore, to deal with the treatment of wave overtopping beyond the vertical boundary, it was decided to develop a numerical model based on the combination of wave and flow effects.

Experiments have been carried out for the surface displacement of overtopping waves in the vicinity of an upright breakwater model set in a two-dimensional wave channel. In addition to the measurements of surface displacement, quantities of wave overtopping which were already measured in another experiment by Horie (1981), have been used to test the validity of the numerical model.

A review of previous studies of the partial standing wave phenomenon, which includes surface displacement, wave crest and trough levels, mean water level changes, and wave overtopping, is presented in Chapter II. The theoretical analysis, which includes a review of the finite amplitude standing wave theories and the application to this study, and the predicting model for the total amount of wave overtopping, are presented in Chapter III. The experimental equipment and procedures are described in Chapter IV. The results of the investigation are presented in Chapter V and the conclusions based upon these are described in Chapter VI.

CHAPTER II

LITERATURE REVIEW

This chapter reviews various types of investigations relevant to the standing wave phenomenon, the wave crest and trough levels, and the process of wave overtopping.

2.1 Standing Wave Theories

Airy (1845) presented the first satisfactory treatment for two dimensional oscillatory waves for the case of a fluid which is frictionless, homogeneous, incompressible, and uniform in depth. In addition, the inertia of the air and the pressure due to a column of air whose height is comparable with that of the waves were neglected, so that the pressure at the surface of the fluid could be assumed to be zero (atmospheric pressure). In the classical theory of standing waves, the equations are linearized and derived from the velocity potential, and the surface displacement is expressed by a superposition of incident wave and fully reflected wave. Under these assumptions the wave height of standing waves is twice as much as that of the incident wave.

Since gravity waves of finite height are governed by non-linearity as proven by experiments and field measurements, theoretical studies related to non-linear waves have been conducted by many scientists and engineers. The theoretical development of waves of finite amplitude is basically the same as that of Airy waves with the exception that the higher order terms are considered important and are retained. Stokes (1847, 1880) considered waves

of small but finite height progressing over still water of finite depth and presented a second order theory. The method used by Stokes was to expand the velocity potential about the still water level, thereby obtaining a non-linear surface condition for the potential on the plane of the still water level which consists of an infinite series containing partial derivatives of the potential. The solution is obtained by successive approximations. Stokes pointed out that for water of finite depth, the restriction on wave steepness is more severe than that of infinite depth. Although Stokes only studied the case of progressive waves, the solving technique has been applied to the standing wave problem by many investigators after the 1950s.

Sainflou (1928) was the first civil engineer who derived a non-linear standing wave theory based on the trochoidal wave theory by St.Venant and Flamant (1888). Sainflou's formula has been preferred for the design of coastal structures owing to its simplicity. However, the trochoidal standing wave theory does not satisfy Laplace's equation because of the rotationality of the fluid. Miche (1944) modified the components of Sainflou's formula and obtained the second order equation for zero mass transport. Both theories have been applied for the calculation of wave forces on a vertical wall. The Sainflou's theory is usually used in the design of upright breakwaters, although the theory of Miche appears to be better.

Penny and Price (1952) carried out a calculation by a Fourier expansion method of fifth order finite amplitude standing waves in infinite depth. They found that the maximum wave steepness to the fifth order would be $(H/L)_{max}=0.218$ in infinitely deep water and

that the maximum crest level above the still water level and the maximum trough level below the still water level would be $(\eta_c/L)_{max}=0.141$ and $(\eta_t/L)_{max}=0.077$. Although they didn't solve the problem of maximum steepness of standing waves in water of finite depth, they estimated the maximum amplitude standing wave with a 90 degree sharp crest angle.

Tadjbaksh and Keller (1960) obtained the third order solution of velocity potential and surface displacement for standing waves in finite depth, using the perturbation method which Stokes derived for the progressive wave problem. Their results do not distinguish the incident and reflected waves. The height of the incident wave is considered to be one-half of the standing wave height in their calculations. It is also shown from their results that the wave length of a wave of finite height not only depends on the water depth, but also on the wave amplitude. The wave length increases with increasing the amplitude in an area shallower than a certain depth and decreases with increasing the amplitude in deeper depth. The frequency effect reversal appears to occur at h/L=0.170. Fultz (1962) verified the value with experiments and got the depth ratio h/L=0.14. The difference from the result of Tadjbaksh and Keller might be considered to be related to the effect of higher order terms which is neglected in the theory. Goda and Kakizaki (1965, 1966) extended the solution of Tadjbaksh and Keller to the fourth order approximation.

For the formation of perfect standing waves, two progressive waves (the incoming and reflected waves) should have exactly equal

wave height and period in a given water depth and move in opposite directions. If the two progressive waves traveling in opposite directions have different wave characteristics, a partial standing wave will be formed. Because most of the theories discussed above deal with only perfect reflection, they cannot explain partial standing waves. Friction on the wall and the bottom should be taken into account in the theory for partial standing waves.

Hamada (1965) reviewed the phenomenon of partially reflected waves and introduced an interactive effect between incident waves and reflective waves to solve a second order finite amplitude standing wave problem, because a superposition of these waves cannot express the phenomenon due to the non-linearity of waves. The solution can be considered in such a way that the original two waves deform themselves by the result of the interaction, and the difference due to the deformation creates the secondary effect to form the partial standing waves. Goda and Abe (1968) extended this to the third order. Their study indicates that as compared with linear wave theory, decrease in wave length and increase in wave height for both the incident and reflective waves occur. The partial standing wave height is therefore a little larger than twice that of the incident wave.

2.2 Wave Crest Level and Trough Level

The crest level of standing waves is generally defined by the following equation;

$$\frac{\eta_m}{H} = 1 + \delta \,, \tag{2. 1}$$

where η_m is the crest level, and H is one half of the standing wave height. The equation includes a term related to a non-linear effect on the height of set-up from the still water level.

Sainflou (1928) derived the value of δ from the trochoidal wave theory and obtained the following equation

$$\delta_S = \frac{1}{2} (kH \coth kh) \,. \tag{2. 2}$$

A higher order solution was developed by Miche as follows.

$$\delta_M = \frac{1}{8} kH(3 \coth^3 kh + \tanh kh) \,. \tag{2. 3}$$

Endo and Miura (1983) measured the crest level of standing waves at a wall of an upright breakwater in a two-dimensional wave channel. According to their laboratory results, a comparison between theoretical and experimental results shows that Miche's theory overestimates crest elevations because of the second order term which Miche added to his derivations. Sainflou's theory underestimated the actual observed crest levels. Endo and Miura

derived an equation for the crest level based on their experiments in the form

$$\frac{\eta_m}{H_I} = 1.0 + \left(14.834 - 42.509 \left(\frac{h}{L}\right) \right) \frac{H_I}{L} \quad , \qquad (2.4)$$

where η_m is the crest level of non-overtopping waves. H_I is the incident wave height and L is the wave length of linear wave theory at water depth h. For the absolute value of the trough level, the following relation was found from the same experiments;

$$\frac{\eta_s}{H_I} = 0.725 + 0.05 \frac{\eta_m}{H_I} \quad , \qquad (2.5)$$

where η_s is the depth of the trough level below mean water level in the non-overtopping condition.

When the crest of the structure is lower than the wave crest level, wave overtopping occurs across the structure. The phenomenon of overtopping waves is different from that of no overtopping waves and quite complex as explained before.

An experimental study was carried out to determine the crest level and the trough level of overtopping waves by Endo and Miura after they obtained experimental results of equations (2.4) and (2.5). The result of the experiments, shown in figure 1, gives the following relation;

$$\frac{\eta_c}{\eta_m} = 0.65 + 0.35 \frac{H_c}{\eta_m} \quad , \qquad (2.6)$$

where η_c is the crest level of overtopping waves and η_m the crest level of non-overtopping waves under the same initial wave conditions, and H_c the height of the structure above the still water level. The absolute value of trough level in the overtopping condition is derived as

$$\frac{\eta_t}{H_I} = 0.725 + 0.05 \frac{H_c}{H_I}, \qquad (2.7)$$

where η_t is the depth of the trough level below mean water level in the overtopping condition.

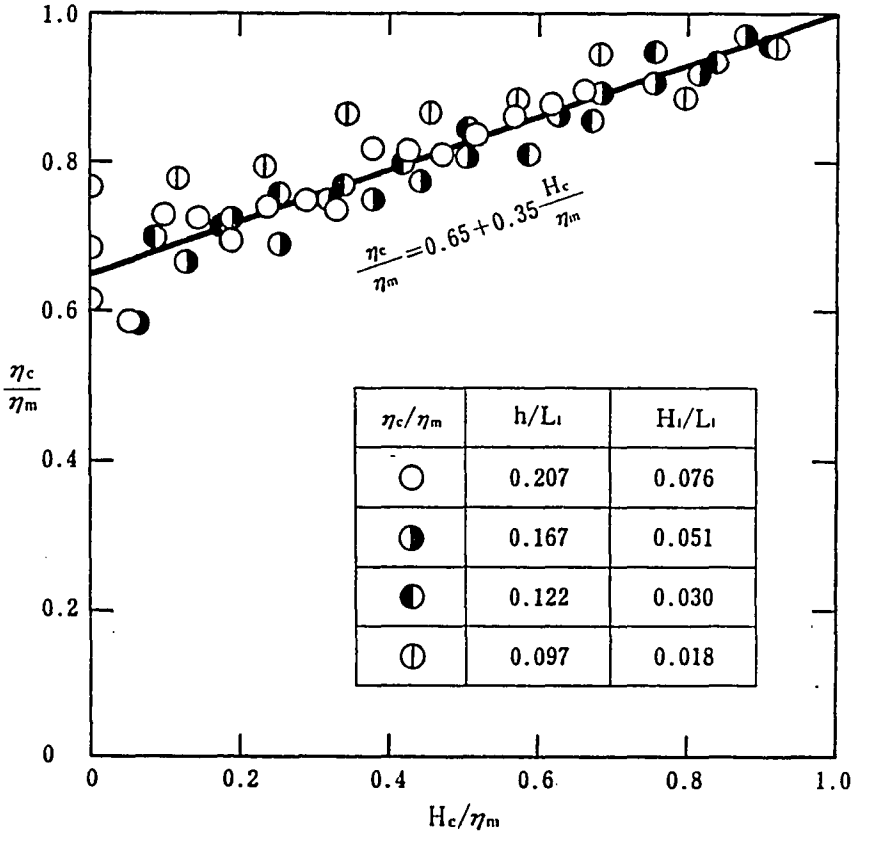

Figure 1, Correlation between wall height and wave crest height in wave overtopping. Endo and Miura (1983)

2.3 Wave Overtopping

When waves exceed the top level of a maritime structure wave overtopping occurs. Serious problems have been inflicted upon the leeward area of the structure. It may be important to know the quantity of water passing over the top of the structure per wave period from wave overtopping. The impulse of the overtopping waves also generates waves in the basin behind the breakwater.

Many facts related to wave overtopping have been discovered experimentally by Saville and Caldwell (1953) for a vertical wall, and by Sibul (1955) for an inclined wall. It is shown in Sibul (1955) that the maximum rate of overtopping occurs when the height of the structure above mean sea level is between 0 and 2/5 of the incident wave height, depending on the wave steepness, and the maximum rate of wave overtopping decreases as the wave steepness increases.

Iwagaki et al (1965) carried out an experimental study whose results were well summarized. The basic idea was to try to connect the amount of wave overtopping with the volume of incoming sinusoidal waves above the still water level. They found two different tendencies for the volume of wave overtopping by the effect of wave height; one is the maximum value of volume of wave overtopping exists at a certain wave height and the volume of wave overtopping decreases with further increase in the wave height, and the other is that the volume of wave overtopping increases with increase in wave height. These relationships are shown in figure 2. They suggest that the design wave height must be determined

carefully not only by taking account of the deep water wave height but also by considering the water depth at the location where the structure will be constructed, because it may not be sufficient for the prevention of wave overtopping to design breakwaters using the largest wave height.

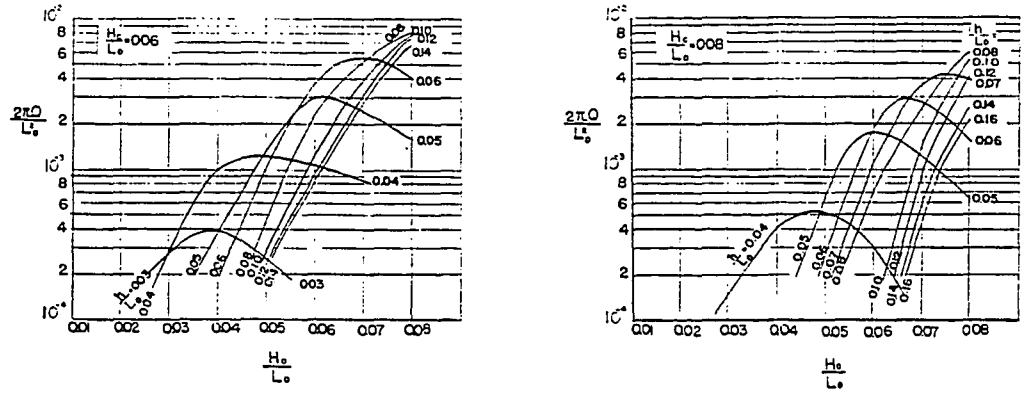

Figure 2, Effect of wave height on wave overtopping
Iwagaki et al (1965)

Another approach is to consider wave overtopping as a phenomenon similar to the flow over a weir with changing water depth as a function of time. The idea to analyze wave overtopping, in which the input is the deep water wave height and wave period and the output is the amount of wave overtopping, was first proposed by Kikkawa et al (1966). Although this theory was fairly simple, this approach could explain some of the features of wave overtopping quite satisfactorily. The investigated forms of volume were obtained for sinuisoidal waves and for linear triangular waves and it was found that the linear triangular waves could be a simple and accurate wave profile for their wave overtopping model. Kikkawa et al (1966, 1968) and Shi-igai and Kono (1970) applied the

simple discharge formula of a weir to the calculation of wave overtopping on a seawall or breakwater. Their theoretical analysis agreed with the experimental results when the wave was assumed linear. The theory includes two parameters which must be determined by experiments. One of parameters relates to the wave profile of partial standing waves at the vertical wall due to wave overtopping and the other relates to the rate of discharge in the formula. Therefore the analysis is not easy to handle until these values are determined precisely for possible actual conditions.

Tsuruta and Goda (1969) used the equation of Kikkawa et al but modified it to obtain other dimensionless parameters for monochromatic waves and a spectrum. The wave overtopping of irregular waves with the assumption of the Reyleigh distribution on a vertical wall was treated as the linear summation of individual wave overtopping. They found that the model could predict the amount of wave overtopping for randomly distributed wave heights with uniform period by using significant wave height.

Takada (1970,1971,1972,1973) carefully studied the existing analyses of wave overtopping and concluded with a resulting analysis which was supported by many laboratory experiments. Although he assumed several wave theories for surface displacement of partial standing waves, he finally used the trapezium profile for the calculation of the volume of wave overtopping.

A report prepared by the Netherlands Government (1974), entitled "Wave Run-Up and Overtopping", provides a comprehensive summary and discussion of existing literature.

Wave overtopping is dependent on many variables, including roughness, water depth at the toe of the breakwater, and incident wave characteristics. The "Shore Protection Manual" (1984) proposes a formula to calculate wave overtopping rates for various slopes and structure types based on wave steepness and relative depth parameters. Formulas given by Weggel (1976) were used as a basis for this method.

CHAPTER III
THEORIES

3.1 Finite Amplitude Partial Standing Waves

The problem of finite amplitude standing waves has been investigated with a perturbation method by some researchers since 1960. In general, these standing wave theories reflect two distinct approaches; one deals with a boundary value problem and the other deals with the result of the composition of a progressive wave, a reflected wave, and the secondary effect by both waves. The boundary value problem such as the one developed by Tadjbaksh and Keller (1960) gives the third order approximations and it is the most commonly employed method for analyzing the standing waves. Goda and Kakizaki (1967) solved the fourth order solutions with the same process. Hamada (1966) and Goda and Abe (1968) employed the finite amplitude standing wave theory introducing a reflection coefficient to satisfy the conservation of energy.

There is no theoretical consideration for partial standing waves after wave overtopping has started, but it was confirmed by Tsuchiya and Yamaguchi (1970) that the surface displacement could be expressed by the finite amplitude standing wave theory. The formula derived by Goda and Abe (1968) is considered to be the most suitable to apply to overtopping waves in the present situation. The surface displacement could be determined with a change in the reflection coefficient by energy dissipation on the wall or on the bottom. The results of the third order theory of Goda and Abe

(1968) by means of a perturbation method will be presented here as the preparation for the calculation of partial standing waves in the wave overtopping condition.

In the irrotational motion, the velocity components of the water particles can be expressed in terms of a velocity potential $\phi(x,z,t)$ such that

$$u = \phi_x , \quad w = \phi_z , \tag{3.1}$$

where u and x are the horizontal velocity and horizontal coordinate, and w and z are the vertical velocity and vertical coordinate, measured upward from the still water level, respectively. ϕ_x and ϕ_z are the partial differential equation with respect to x and z. Figure 3 shows the sketch of the coordinate system.

For incompressible flow and two-dimensional motion, the continuity equation gives

$$u_x + w_z = 0 , \tag{3.2}$$

or, in terms of the velocity potential,

$$\phi_{xx} + \phi_{zz} = 0 . \tag{3.3}$$

Equation (3.3) is known as Laplace's equation.

The pressure requirement at any point in water is given by Bernoulli's equation (neglecting energy losses);

$$\frac{(P - P_0)}{\rho} = -\phi_t - \frac{1}{2}(\phi_x^2 + \phi_z^2) - gz , \tag{3.4}$$

where ρ is the density of water and P_0 is the atmospheric pressure.

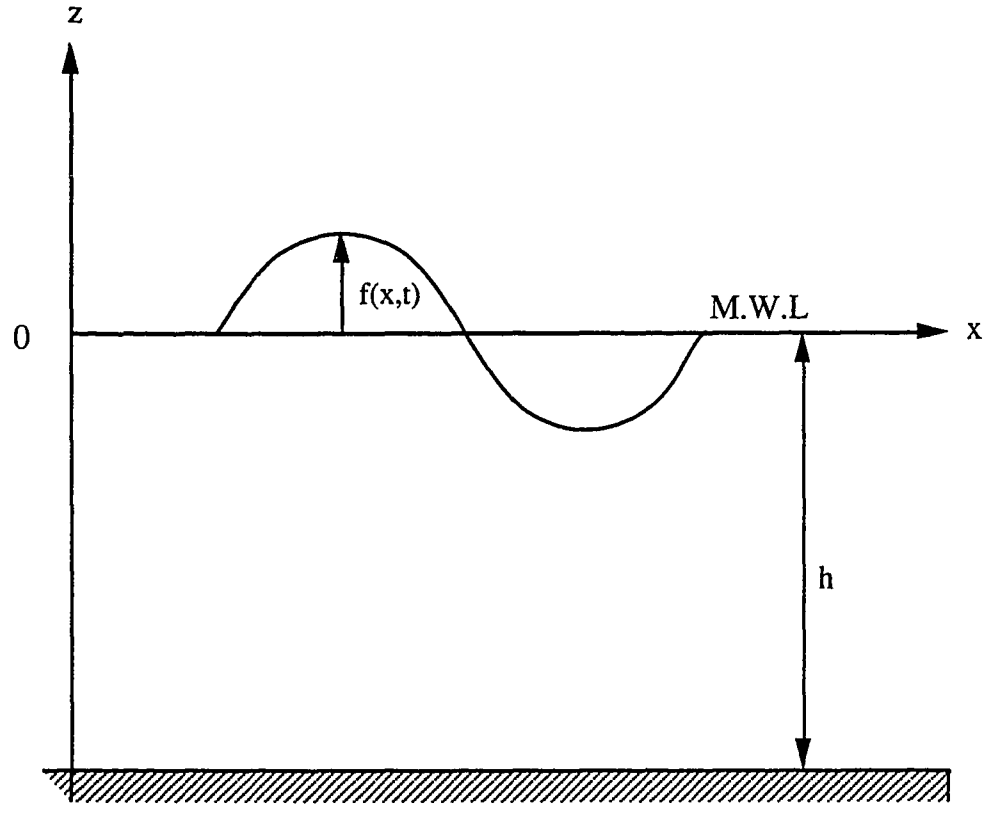

Figure 3, Sketch of coordinate system

At the free surface, P must be P_0 and consequently,

$$gf + \phi_t + \frac{1}{2}(\phi_x^2 + \phi_z^2) = 0 \qquad \text{on } z = f \ , \qquad (3.5)$$

where f= f(x,t) is the vertical displacement of the water surface measured from z=0.

The free surface of the water at any instant must remain a free surface, and a fluid element on this surface must move so that its velocity component normal to the surface is the same as the normal velocity of the surface itself. This condition is described;

$$\phi_z = f_t + f_x \phi_x \qquad \text{on } z = f . \tag{3.6}$$

No fluid can pass through the sea floor, and therefore the bottom boundary condition at the depth h is

$$\phi_z = 0 \qquad \text{on } z = -h . \tag{3.7}$$

As additional conditions, first the conservation of water mass requires

$$\int_0^{2\pi/k} f(x, t)\, dx = 0 . \tag{3.8}$$

Second, the motion must be periodic both in x and t such as

$$\phi(x,z,t+2\pi/\sigma) = \phi(x+2\pi/k,z,t) = \phi(x,z,t) , \tag{3.9}$$

where k is the wave number and σ is the angular frequency.

The theory consists of the composition of third order progressive and reflected waves, and an additional secondary effect. Therefore, we consider the progressive wave theory first. The solution of progressive waves of finite amplitude can be expressed in the following forms by the method of perturbation.

$$\begin{aligned}
\phi(x,z,t) &= a\phi_0(x,z,t)+a^2\phi_1(x,z,t)+\frac{1}{2}a^3\phi_2(x,z,t)+O(a^4) , \\
f(x,t) &= af_0(x,t)+a^2f_1(x,t)+\frac{1}{2}a^3f_2(x,t)+O(a^4) , \\
\sigma &= \sigma_0 + a\sigma_1 +\frac{1}{2}a^2\sigma_2+ O(a^3) ,
\end{aligned} \tag{3.10}$$

where a is the first order amplitude of surface elevation. By applying these perturbation equations to the above conditions, equations are evaluated at z=0 instead of z=f in terms of a.

The results of the third order progressive waves are as follows.

The first order solution is:

$$\phi_0 = \frac{\sigma_0 \sin(kx-\sigma t) \cosh k(z+h)}{k \sinh kh},$$

$$f_0 = \cos(kx-\sigma t), \tag{3.11}$$

$$\sigma_0 = gk \tanh kh .$$

We now define a dimensionless time (argument) τ by

$$\tau = \sigma t = (\sigma_0 + a\sigma_1 + \frac{1}{2} a^2\sigma_2 + \cdots) t . \tag{3.12}$$

The second order solution is:

$$\phi_1 = \sigma_0\alpha_{01}\tau + \sigma_0\beta_{22} \sin 2(kx-\sigma t) \cosh 2k(z+h),$$

$$f_1 = kb_{22} \cos 2(kx-\sigma t), \tag{3.13}$$

$$\sigma_1 = 0,$$

where

$$\alpha_{01} = -\frac{1}{4} (\coth^2 kh - 1),$$

$$\beta_{22} = \frac{3 (\coth^4 kh - 1)}{8 \cosh 2kh}, \tag{3.14}$$

$$b_{22} = \frac{1}{4} (3 \coth^3 kh - \coth kh) .$$

The third order solution is:

$$\phi_2 = k\sigma_0 \beta_{33} \sin 3(kx- \sigma t) \cosh 3k(z+h) ,$$

$$f_2 = k^2\{ b_{11} \cos(kx- \sigma t) + b_{33} \cos 3(kx- \sigma t)\} , \qquad (3.15)$$

$$\sigma_2 = k^2\sigma_0 C_1 ,$$

where

$$\beta_{33} = \frac{(c^2 + 3)(9c^5 - 22c^3 + 13c)}{32 \cosh 3kh} ,$$

$$b_{11} = \frac{1}{8} (3c^4 + 8c^2 - 9) ,$$

$$b_{32} = \frac{3}{32} (9c^6 - 3c^4 + 3c^2 -1) , \qquad (3.16)$$

$$C_1 = \frac{1}{8} (9c^4 - 10c^2 + 9) ,$$

$$c = \coth kh .$$

The solution of the third order progressive waves is written as

$$\frac{k^2\phi}{\sigma_0} = \varepsilon\beta_{11} \sin(kx- \sigma t) \cosh k(z+h) + \varepsilon^2\alpha_{01}\tau$$

$$+ \varepsilon^2\beta_{22} \sin 2(kx- \sigma t) \cosh 2k(z+h)$$

$$+\frac{1}{2}\varepsilon^3 ß_{33} \sin 3(kx- \sigma t) \cosh 3k(z+h) , \tag{3.17}$$

$$kf = [\ \varepsilon+\frac{1}{2}\varepsilon^3 b_{11}] \cos(kx- \sigma t) + \varepsilon^2 b_{22} \cos 2(kx- \sigma t) + \frac{1}{2}\varepsilon^3 b_{33} \cos 3(kx- \sigma t) , \tag{3.18}$$

$$\sigma = \sigma_0[\ 1+ \frac{1}{2}\varepsilon^2 C_1\ ] , \tag{3.19}$$

where $\varepsilon= ka$,

$$ß_{11} = \frac{1}{\sinh kh} . \tag{3.20}$$

From equation (3-18), the crest level of progressive waves is given at x=0 and t=0, such as

$$kf(0,0) = [\ \varepsilon+\frac{1}{2}\varepsilon^3 b_{11}\ ] + \varepsilon^2 b_{22} +\frac{1}{2}\varepsilon^3 b_{33} ,$$

and the trough level of them is given at x=0 and t=T/2, therefore,

$$kf(0,T/2) = -[\ \varepsilon+\frac{1}{2}\varepsilon^3 b_{11}\ ] + \varepsilon^2 b_{22} - \frac{1}{2}\varepsilon^3 b_{33} .$$

The wave height of progressive wave H_I is obtained for the parameter ε as

$$kH_I = kf(0,0) - kf(0,T/2) = 2\varepsilon + \varepsilon^3(b_{11} + b_{33}) . \tag{3.21}$$

The wave number k relates to h and ε, and the following relation is obtained from equations (3.11) and (3.19).

$$\sigma^2 = gk \tanh kh \left[1 + \frac{1}{2} \varepsilon^2 C_1 \right]^2 . \tag{3.22}$$

The first order approximation of wave number k_A is defined by

$$\sigma^2 = gk_A \tanh k_A h .$$

Then the relation between k and k_A is approximated up to third order as

$$k = k_A \left[1 - \frac{1}{2} \varepsilon^2 K_1 \right] , \tag{3.23}$$

where

$$K_1 = \frac{1}{1 + k_A h(\coth k_A h - \tanh k_A h)} . \tag{3.24}$$

The phenomenon of partial standing waves is very complicated and the deformation of surface displacement is associated with the interaction of waves, and energy loss on the wall of structure. The difference due to the deformation makes the secondary effect which is dealt with as bound waves by Hamada (1966). The expressions for the velocity potential and the surface displacement of partial standing waves are

$$\phi = \phi_I + \phi_R + \phi_F , \tag{3.25}$$

where

$$\phi_I = a\phi_{I0} + a^2\phi_{I1} + \frac{1}{2} a^3\phi_{I2} ,$$

$$\phi_R = \lambda a\phi_{R0} + \lambda^2 a^2 \phi_{R1} + \frac{1}{2}\lambda^3 a^3 \phi_{R2} ,$$

$$\phi_F = a^2 \phi_{F1} + \frac{1}{2} a^3 \phi_{F2} ,$$

and

$$f = f_I + f_R + f_F , \tag{3.26}$$

where

$$f_I = af_{I0} + a^2 f_{I1} + \frac{1}{2} a^3 f_{I2} ,$$

$$f_R = \lambda af_{R0} + \lambda^2 a^2 f_{R1} + \frac{1}{2} \lambda^3 a^3 f_{R2} ,$$

$$f_F = a^2 f_{F1} + \frac{1}{2} a^3 f_{F2} ,$$

in which the subscripts I, R and F denote the incident, reflected and bound waves, respectively. The factor λ represents the ratio of reflected to incident wave amplitudes on the first order approximation.

In addition, the angular frequency for a given wave number increases as the wave amplitude increases. In case of partial standing waves produced by wave reflection, no change in wave period will take place, and then the wave length must change instead of wave period. By taking the results of progressive waves into consideration, the perturbation of angular frequency are expressed as

$$\sigma_I = \sigma_0 + \frac{1}{2} a^2 (\sigma_2 + \sigma_{IF}) ,$$

$$\sigma_R = \sigma_0 + \frac{1}{2} a^2 (\lambda^2 \sigma_2 + \sigma_{RF}) . \qquad (3.27)$$

A summary of bound waves by Goda and Abe (1968) is as follows.

The first order solution of bound waves is:

$$\phi_{F1} = \lambda \sigma_0 ß_{20} \sin(I+R) , \qquad (3.28)$$

$$f_{F1} = \lambda k_A b_{02} \cos(I-R) , \qquad (3.29)$$

where

$$ß_{20} = - \frac{(3 + c^2)}{4},$$

$$b_{02} = \frac{(c + c^{-1})}{2}, \qquad (3.30)$$

$$c = \coth k_A h ,$$

$$I \pm R = (k_I \pm k_R)x - (\sigma_I \pm \sigma_R)t .$$

The second order solution of bound waves is:

$$\phi_{F2} = k_A \sigma_0 ß_{31} [\lambda \sin(2I+R) + \lambda^2 \sin(2R+I)] \cosh k_A(z+h)$$

$$+ k_A \sigma_0 ß_{13} [\lambda \sin(2I-R) + \lambda^2 \sin(2R-I)] \cosh 3k_A(z+h) , \qquad (3.31)$$

$$f_{F2} = k_A^2 b_1 [\lambda \cos(R) + \lambda^2 \cos(I)] + k_A^2 b_{31} [\lambda \cos(2I+R)$$

$$+ \lambda^2 \cos(2R+I)] + k_A^2 b_{13} [\lambda \cos(2I-R) + \lambda^2 \cos(2R-I)] , \qquad (3.32)$$

where

$$\beta_{31} = -\frac{9c^5 + 62c^3 - 31c}{32 \cosh kh},$$

$$\beta_{13} = \frac{(1 + 3c^{-2})(3c^5 - 5c + 2c^{-1})}{32 \cosh 3kh},$$

$$b_1 = \frac{(-c^2 + 2 + c^{-2})}{4},$$

$$b_{31} = \frac{(-3c^4 - 18c^2 + 5)}{32},$$

$$b_{13} = \frac{3(9c^4 + 27c^2 - 15 + c^{-2} + 2c^{-4})}{32}, \qquad (3.33)$$

$$I = k_I x - \sigma_I t,$$

$$R = k_R x - \sigma_R t,$$

$$2I \pm R = (2k_I \pm k_R)x - (2\sigma_I \pm \sigma_R)t,$$

$$2R \pm I = (2k_R \pm k_I)x - (2\sigma_R \pm \sigma_I)t.$$

The angular frequency and the wave number are corrected by introducing the bound waves as follows;

$$\sigma_I = \sigma_0 \left[1 + \frac{1}{2} (k_A a)^2 (C_1 - \lambda^2 C_2) \right],$$

$$\sigma_R = \sigma_0 \left[1 + \frac{1}{2} (k_A a)^2 (\lambda^2 C_1 - C_2) \right], \qquad (3.34)$$

and

$$k_I = k_A \left[1 - \frac{1}{2} (k_A a)^2 (K_1 - \lambda^2 K_2) \right] ,$$

$$k_R = -k_A \left[1 - \frac{1}{2} (k_A a)^2 (\lambda^2 K_1 - K_2) \right] , \tag{3.35}$$

where

$$K_2 = \frac{2C_2}{1 + k_A h(\coth k_A h - \tanh k_A h)} . \tag{3.36}$$

In the case of perfect reflection, the amplitude of progressive and reflected waves are equal (λ=1), and then the velocity potential and the surface displacement become

$$\begin{aligned} \frac{k^2 \phi}{\sigma_0} = & \{ 2\beta_0 + 2\varepsilon^2 \alpha_{01} \sigma t - 2\varepsilon \beta_{11} \sin \sigma t \cos kx \cosh k(z+h) \\ & - 2\varepsilon^2 \beta_{22} \sin 2\sigma t \cos 2kx \cosh 2k(z+h) \\ & - \varepsilon^3 \beta_{33} \sin 3\sigma t \cos 3kx \cosh 3k(z+h)\} \\ & - \{ \varepsilon^2 \beta_{20} \sin 2\sigma t + \varepsilon^3 \beta_{31} \sin 3\sigma t \cos kx \cosh k(z+h) \\ & + \varepsilon^3 \beta_{13} \sin \sigma t \cos 3kx \cosh 3k(z+h)\} , \end{aligned} \tag{3.37}$$

$$\begin{aligned} kf = & \{(2\varepsilon + \varepsilon^3 b_{11}) \cos \sigma t \cos kx \\ & + 2\varepsilon^2 b_{22} \cos 2\sigma t \cos 2kx + \varepsilon^3 b_{33} \cos 3\sigma t \cos 3kx\} \\ & + \{ \varepsilon^2 b_{02} \cos 2kx + \varepsilon^3 b_1 \cos \sigma t \cos kx \\ & + \varepsilon^3 b_{31} \cos 3\sigma t \cos kx + \varepsilon^3 b_{13} \cos \sigma t \cos 3kx\} , \end{aligned} \tag{3.38}$$

$$\sigma = \sigma_0 \left[1 + \frac{1}{2} \varepsilon^2 (C_1 - C_2) \right] , \qquad (3.39)$$

where $\varepsilon = ka$.

These results are in complete agreement with equations by Tadjbaksh and Keller (1960), if the first order amplitude of the standing wave is written as twice as the incident wave.

The height of perfect standing waves can be calculated from equation (3.38) for x=0 as

$$H_s = 4a \left[1 + \frac{1}{2} \varepsilon^2 (b_{11}+b_{33}) + \frac{1}{2} \varepsilon^2 (b_1+b_{31}+b_{13}) \right] . \qquad (3.40)$$

Since the height of incident waves denoted with H_I is given by equation (3.18), the standing wave height is expressed with respected to H_I as

$$\frac{H_s}{2H_I} = \frac{1 + \varepsilon^2 (b_1 + b_{11} + b_{13} + b_{31} + b_{33})/2}{1 + \varepsilon^2 (b_{11} + b_{33})} . \qquad (3.41)$$

After the calculation of these coefficients in equation (3.41) by Goda and Abe, they found that the standing wave height H_s is greater than twice the incident wave height by 10 or 15 %.

Finally, the surface displacement of third order partial standing waves is obtained by substituting equations (3.11), (3.13), (3.15), (3.26), (3.29) and (3.32) into equation (3.26).

$$\frac{f}{a} = \lambda \varepsilon b_{02} \cos(k_I - k_R)x + \{ \cos(k_I x - \sigma t) + \lambda \cos(k_R x - \sigma t) \}$$
$$+ \varepsilon b_{22} \{ \cos 2(k_I x - \sigma t) + \lambda^2 \cos 2(k_R x - \sigma t) \}$$

$$+\frac{1}{2}\varepsilon^2 b_{11}\{\cos(k_I x-\sigma t)+\lambda^3\cos(k_R x-\sigma t)\}$$

$$+\frac{1}{2}\varepsilon^2 b_{33}\{\cos 3(k_I x-\sigma t)+\lambda^3\cos 3(k_R x-\sigma t)\}$$

$$+\frac{1}{2}\lambda\varepsilon^2 b_1\{\lambda\cos(k_I x-\sigma t)+\cos(k_R x-\sigma t)\}$$

$$+\frac{1}{2}\lambda\varepsilon^2 b_{31}\{\cos[(2k_I+k_R)x-3\sigma t]+\lambda\cos[(2k_R+k_I)x-3\sigma t]\}$$

$$+\frac{1}{2}\lambda\varepsilon^2 b_{13}\{\cos[(2k_I-k_R)x-\sigma t]+\lambda\cos[(2k_R-k_I)x-\sigma t]\}\ . \qquad (3.42)$$

From equation (3.42) the surface displacement at x=0 is obtained as

$$\frac{f(0,t)}{a}=\lambda\varepsilon b_{02}+[(1+\lambda)+\frac{1}{2}\varepsilon^2(1+\lambda^3)b_{11}$$

$$+\frac{1}{2}\varepsilon^2\lambda(1+\lambda)(b_1+b_{13})]\cos\sigma t+\lambda b_{22}(1+\lambda^2)\cos 2\sigma t$$

$$+\frac{1}{2}\varepsilon^2[(1+\lambda^3)b_{33}+\lambda(1+\lambda)b_{31}]\cos 3\sigma t\ . \qquad (3.43)$$

Therefore, the standing wave height at x=0 is calculated as

$$\frac{H_{sp}}{a}=2(1+\lambda)+\varepsilon^2(1+\lambda^3)(b_{11}+b_{33})+\varepsilon^2\lambda(1+\lambda)(b_1+b_{13}+b_{31})\ . \qquad (3.44)$$

The first and second terms represent the sum of the incident and reflected wave heights. The third term represents the wave

interaction effect and this term is always positive. Hence H_{sp} is greater than the sum of incident and reflected wave heights.

3.2 Wave Profile in Overtopping Condition

In section 3.1, the finite amplitude standing wave theory based on Goda and Abe(1968) was discussed to understand the mechanism of waves in front of a breakwater. The theory was often applied to express the surface displacement of partial standing waves directly in the wave overtopping condition, although it was originally considered to apply only to the standing wave condition with low energy dissipation from the bottom of the channel or the wall of the structure. Use of equations (3.25) and (3.26) might give a good approximation, but we need to review the phenomenon of reflection by the breakwater more precisely here.

The phenomenon of partial standing waves after wave overtopping is a very complicated problem, in which the conservation of mass and energy need to be expressed. The author has developed an equation of wave profile for application to the surface displacement in the wave overtopping condition. Special arrangement need to be taken into account to develop a formulation describing the partial standing wave phenomenon after wave overtopping.

The situation of the problem can be considered in such a way that incident waves strike the structure and reflected waves are generated by the waveward side of the structure. The height of the

reflected waves depends upon the height of incident waves or the height of the structure above the still water level. When the height of the structure is low compared with the crest level of the incident waves, the incident waves affect wave overtopping and change the profile. The height of reflected waves is determined by the height of the structure. On the other hand, when the crest level of incident waves is much lower than the structure, the situation has the opposite characteristics.

As mentioned before, mass transport over the structure makes it difficult to adjust the theory to describe the real phenomenon. The crest level of the waves drops when the height of the structure is decreased. Former investigators have dealt with the physical phenomenon as a decrease of reflection of wave energy, when wave overtopping occurs. It means that they solved this mechanism as only a partial reflection problem.

Let us assume that incident waves travel from right to left toward a vertical breakwater. When the water level changes from trough to crest near the structure, the horizontal velocity component of incident waves is directed to the left. If the height of the structure is lower than the free surface of the partial standing waves, the wave cannot keep the profile of the perfect standing waves, and the water flows over the breakwater to the left. During the wave overtopping period, the velocity component of the incident waves is always directed to the left and that of the reflected waves directed to the right. It may be conceived that water particles from the incident wave component contribute to the overflow, and as a

result, the surface displacement of the original incident waves is considered to be decreased. The surface displacement of partial standing waves is the composition of the left-running incident waves, the height of which is decreased by wave overtopping, and the right-running reflected waves whose wave height is influenced by the crest level of the breakwater or the crest level of incident waves, and the bound wave effect which was introduced in equation (3.26).

The surface displacement of partial standing waves may then be written in a form similar to equation (3.26) as

$$f = f_I + f_R + f_F , \tag{3.45}$$

where

$$f_I = \lambda_1 a f_{I0} + \lambda_1^2 a^2 f_{I1} + \frac{1}{2} \lambda_1^3 a^3 f_{I2} ,$$

$$f_R = \lambda_2 a f_{R0} + \lambda_2^2 a^2 f_{R1} + \frac{1}{2} \lambda_2^3 a^3 f_{R2} ,$$

$$f_F = \lambda_1^2 a^2 f_{F1} + \frac{1}{2} \lambda_1^3 a^3 f_{F2} .$$

The movement of the free surface is assumed to be different in two time periods; when the water level is below the top of the breakwater and above it. When the water level is beneath the top of the breakwater, the conjugation of original incident waves and reflected waves creates a wave profile of partial standing waves. In this case, the calculation of partial standing waves will be carried out with $\lambda_1=1$ in equation (3.45) and the surface displacement at x=0 is obtained from equation (3.43), replacing λ by λ_2.

$$\frac{f(0,t)}{a} = \lambda_2 \varepsilon b_{02} + [(1+\lambda_2) + \frac{1}{2}\varepsilon^2(1+\lambda_2^3)b_{11} + \frac{1}{2}\varepsilon^2\lambda_2(1+\lambda_2)(b_1+b_{13})] \cos \sigma t + \varepsilon\lambda_2 b_{22}(1+\lambda_2^2) \cos 2\sigma t + \frac{1}{2}[\varepsilon^2\{(1+\lambda_2^3)b_{33} + \lambda_2(1+\lambda^2)b_{31}\}] \cos 3\sigma t \ . \quad (3.46)$$

The trough level at z=0 is calculated as

$$\frac{f(0,T/2)}{a} = \lambda_2 \varepsilon b_{02} - [(1+\lambda_2) + \frac{1}{2}\varepsilon^2(1+\lambda_2^3)b_{11} + \frac{1}{2}\varepsilon^2\lambda_2(1+\lambda_2)(b_1+b_{13})] + \varepsilon\lambda_2 b_{22}(1+\lambda_2^2) - \frac{1}{2}\varepsilon^2[(1+\lambda_2^3)b_{33} + \lambda_2(1+\lambda_2)b_{31}] \ . \quad (3.47)$$

If the trough level is obtained from experiments, λ_2 could be calculated explicitly from equation (3.47), and the finite amplitude reflection waves could be expressed in f_R in equation (3.45). The mean water level of reflected waves should not be higher than that of incident waves, because the surface profile of reflected waves oscillates lower in amplitude than that of incident waves. The surface displacement of reflected waves can be expressed by the following equation

$$f_R = \lambda_2 a f_{R0} + \lambda_2^2 a^2 f_{R1} + \frac{1}{2}\lambda_2^3 a^3 f_{R2} + R \ , \quad (3.48)$$

in which R is the shifting of the mean water level from the still water level.

The surface displacement is determined by a similar technique when water level is higher than the structure. In this case we examined the effect of reflected wave on the original incident wave. Using the argument above, but interchanging the role of the incident and reflected waves, a change in the profile of the left-running wave is calculated. The surface displacement in the period can be written by the following equation, after taking $a_* = \lambda_2 a$.

$$f = f_R + f_I + f_F \ , \tag{3.49}$$

where

$$f_R = a_* f_{R0} + a_*^2 f_{R1} + \frac{1}{2} a_*^3 f_{R2} + R \ ,$$

$$f_I = \lambda_1 a_* f_{I0} + (\lambda_1 a_*)^2 f_{I1} + \frac{1}{2} (\lambda_1 a_*)^3 f_{I2} \ ,$$

$$f_F = a_*^2 f_{F1} + \frac{1}{2} a_*^3 f_{F2} \ .$$

The surface displacement at x=0 is written as

$$\begin{aligned} \frac{f(0,t)}{a_*} = {} & \lambda_1 \varepsilon b_{02} + [(1+\lambda_1) + \frac{1}{2} \varepsilon^2 (1+\lambda_1^3) b_{11} \\ & + \frac{1}{2} \varepsilon^2 \lambda_1 (1+\lambda_1)(b_1 + b_{13})] \cos \sigma t + \varepsilon \lambda_1 b_{22} (1+\lambda_1^2) \cos 2\sigma t \\ & + \frac{1}{2} \varepsilon^2 \{(1+\lambda_1^3) b_{33} + \lambda_1 (1+\lambda_1) b_{31}\} \cos 3\sigma t \ . \end{aligned} \tag{3.50}$$

The wave crest level at x=0 is calculated as

$$\frac{f(0,0)}{a_*} = \lambda_1 \varepsilon b_{02} + [(1+\lambda_1) + \frac{1}{2}\varepsilon^2(1+\lambda_1^3)b_{11} + \frac{1}{2}\varepsilon^2\lambda_1(1+\lambda_1)(b_1+b_{13}) + \varepsilon\lambda_1 b_{22}(1+\lambda_1^2) + \frac{1}{2}\varepsilon^2[(1+\lambda_1^3)b_{33} + \lambda_1(1+\lambda_1)b_{31}] \quad . \tag{3.51}$$

If the wave crest level is defined by experiment, λ_1 would be obtained from equation (3.51) with λ_2, which is already calculated by equation (3.47).

Summarizing the results, the surface displacement in the wave overtopping condition is described as follows.

When the water level is lower than the top level of the structure

$$f = f_I + f_R + f_F \quad , \tag{3.52}$$

where

$$f_I = af_{I0} + a^2 f_{I1} + \frac{1}{2} a^3 f_{I2} \quad ,$$

$$f_R = \lambda_2 af_{R0} + \lambda_2^2 a^2 f_{R1} + \frac{1}{2}\lambda_2^3 a^3 f_{R2} + R \quad ,$$

$$f_F = a^2 f_{F1} + \frac{1}{2} a^3 f_{F2} \quad ,$$

or

$$\frac{f}{a} = \lambda_2 \varepsilon b_{02} \cos(k_I - k_R)x + \{ \cos(k_I x - \sigma t) + \lambda_2 \cos(k_R x - \sigma t)\}$$
$$+ \varepsilon b_{22}\{ \cos 2(k_I x - \sigma t) + \lambda_2^2 \cos 2(k_R x - \sigma t)\}$$
$$+ \frac{1}{2}\varepsilon^2 b_{11}\{ \cos(k_I x - \sigma t) + \lambda_2^3 \cos(k_R x - \sigma t)\}$$
$$+ \frac{1}{2}\varepsilon^2 b_{33}\{ \cos 3(k_I x - \sigma t) + \lambda_2^3 \cos 3(k_R x - \sigma t)\}$$
$$+ \frac{1}{2}\lambda_2 \varepsilon^2 b_1\{ \lambda_2 \cos(k_I x - \sigma t) + \cos(k_R x - \sigma t)\}$$
$$+ \frac{1}{2}\lambda_2 \varepsilon^2 b_{31}\{ \cos[(2k_I + k_R)x - 3\sigma t] + \lambda_2 \cos[(2k_R + k_I)x - 3\sigma t]\}$$
$$+ \frac{1}{2}\lambda_2 \varepsilon^2 b_{13}\{ \cos[(2k_I - k_R)x - \sigma t]$$
$$+ \lambda_2 \cos[(2k_R - k_I)x - \sigma t]\} + \frac{R}{a}, \qquad (3.53)$$

where

$$k_I = k_A \left[1 - \frac{1}{2}(k_A a)^2 (K_1 - \lambda_2^2 K_2) \right],$$
$$k_R = -k_A \left[1 - \frac{1}{2}(k_A a)^2 (\lambda_2^2 K_1 - K_2) \right].$$

When the water level is higher than the top of structure.

$$f = f_I + f_R + f_F, \qquad (3.54)$$

where

$$f_I = \lambda_1 a_* f_{I0} + (\lambda_1 a_*)^2 f_{I1} + \frac{1}{2}(\lambda_1 a_*)^3 f_{I2},$$

$$f_R = a_* f_{R0} + a_*^2 f_{R1} + \frac{1}{2} a_*^3 f_{R2} + R,$$

$$f_F = a_*^2 f_{F1} + \frac{1}{2} a_*^3 f_{F2},$$

or

$$\begin{aligned}
\frac{f}{a_*} &= \lambda_1 \varepsilon b_{02} \cos(k_R - k_I)x + \{ \cos(k_R x - \sigma t) + \lambda_1 \cos(k_I x - \sigma t)\} \\
&+ \varepsilon b_{22}\{ \cos 2(k_R x - \sigma t) + \lambda_1^2 \cos 2(k_I x - \sigma t)\} \\
&+ \frac{1}{2}\varepsilon^2 b_{11}\{ \cos(k_R x - \sigma t) + \lambda_1^3 \cos(k_I x - \sigma t)\} \\
&+ \frac{1}{2}\varepsilon^2 b_{33}\{ \cos 3(k_R x - \sigma t) + \lambda_1^3 \cos 3(k_I x - \sigma t)\} \\
&+ \frac{1}{2}\lambda_1 \varepsilon^2 b_1\{ \lambda_1 \cos(k_R x - \sigma t) + \cos(k_I x - \sigma t)\} \\
&+ \frac{1}{2}\lambda_1 \varepsilon^2 b_{31}\{ \cos[(2k_R + k_I)x - 3\sigma t] + \lambda_1 \cos[(2k_I + k_R)x - 3\sigma t]\} \\
&+ \frac{1}{2}\lambda_1 \varepsilon^2 b_{13}\{ \cos[(2k_R - k_I)x - \sigma t] \\
&+ \lambda_1 \cos[(2k_I - k_R)x - \sigma t]\} + \frac{R}{a_*},
\end{aligned} \tag{3.55}$$

where

$$k_R = k_A \left[1 - \frac{1}{2} (k_A a_*)^2 (K_1 - \lambda_1^2 K_2) \right] ,$$

$$k_I = -k_A \left[1 - \frac{1}{2} (k_A a_*)^2 (\lambda_1^2 K_1 - K_2) \right] .$$

3.3 Radiation Stresses and Mean Water Level Changes

Radiation stresses in water waves play an important role in the change in mean water level due to the existence of waves. The radiation stress, which is a pressure force in excess of the hydrostatic pressure force caused by the presence of waves, was defined by Longuet-Higgins and Stewart (1964).

Let us consider how the radiation stress effects the mean water level in linear standing waves by employing Airy theory whose surface displacement is defined by

$$f(x,t) = \frac{H_s}{2} \cos kx \cos \sigma t \ , \tag{3.56}$$

where H_s is the wave height of standing waves. The corresponding velocity components are given by

$$u = \frac{H_s \, gk \cosh k(z+h) \sin kx \sin \sigma t}{2\sigma \cosh kh} \ , \tag{3.57}$$

$$v = - \frac{H_s\, gk \sinh k(z+h) \cos kx \sin \sigma t}{2\sigma \cosh kh} \quad . \tag{3.58}$$

The principal component S_{xx} of the radiation stress is defined the mean value of total flux of horizontal momentum across a plane x=constant with respect to time, minus the mean flux in the absence of waves, as follows

$$S_{xx} = \int_{-h}^{f} \overline{(P + \rho u^2)}\, dz - \int_{-h}^{0} P_0\, dz \,, \tag{3.59}$$

where P is the pressure at any point, P_0 is the hydrostatic pressure, and ρ is the density of water.

The right hand side of equation (3.59) is separated into three parts and described as

$$S_{xx} = S_{xx}^{(1)} + S_{xx}^{(2)} + S_{xx}^{(3)} \,, \tag{3.60}$$

where

$$S_{xx}^{(1)} = \overline{\int_{-h}^{f} \rho u^2\, dz} \approx \int_{-h}^{0} \overline{\rho u^2}\, dz \,, \tag{3.61}$$

$$S_{xx}^{(2)} = \overline{\int_{-h}^{0} (P - P_0)\, dz} \approx \int_{-h}^{0} \overline{(P - P_0)}\, dz \,, \tag{3.62}$$

$$S_{xx}^{(3)} = \overline{\int_{0}^{f} P\, dz} \quad . \tag{3.63}$$

Equation (3.61) expresses an integration of the Reynolds stress and equation (3.62) results from the changes of the mean pressure field.

In the second component $S_{xx}^{(2)}$, the general relation for the vertical flux of momentum was derived by Longuet-Higgins and Stewart as

$$S_{xx}^{(2)} = \rho g h \bar{f} - \int_{-h}^{0} \overline{\rho w^2}\, dz + \frac{\delta}{\delta x} \int_{-h}^{0} \int_{z'}^{0} \overline{\rho u w}\, dz\, dz' \,. \qquad (3.64)$$

The third order component $S_{xx}^{(3)}$ is equal to the pressure P integrated between 0 and f, and then averaged with respect to time. For the first order, the pressure near the free surface equals the hydrostatic pressure.

$$P = \rho g (f - z) \,, \qquad (3.65)$$

so that

$$S_{xx}^{(3)} = \overline{\int_{0}^{f} P\, dz} = \overline{\int_{0}^{f} \rho g (f - z)\, dz}$$

$$= \rho g \left[\bar{f} z - \frac{z^2}{2} \right]_0^{\bar{f}} = \frac{1}{2} \rho g \overline{f^2} \,. \qquad (3.66)$$

Adding this to $S_{xx}^{(1)}$ and $S_{xx}^{(2)}$, we deduce

$$S_{xx} = \rho g h \bar{f} + \int_{-h}^{0} \overline{\rho (u^2 - w^2)}\, dz + \frac{1}{2} \int_{-h}^{0} \int_{z'}^{0} \overline{\rho u w}\, dz\, dz' + \frac{1}{2} \overline{\rho g f^2}$$

. (3.67)

Among the terms on the right hand side of the equation, $\bar{f}$ must be zero and becomes

$$S_{xx} = \int_{-h}^{0} \rho(\overline{u^2 - w^2})\, dz + \frac{1}{2}\int_{-h}^{0}\int_{z'}^{0} \overline{\rho uw}\, dz\, dz' + \frac{1}{2}\overline{\rho g f^2} \quad (3.68)$$

Substituting from equations (3.56), (3.57) and (3.58)

$$S_{xx} = \frac{\rho g H_s^2}{16}\left(\frac{2kh}{\sinh 2kh} + \frac{1}{2} - \frac{kh}{\tanh 2kh}\cos 2kx\right) . \quad (3.69)$$

The local mean level $\bar{f}$ can be found by the conservation of momentum. Let us consider the momentum balance in a slice of water bound by the surface z=f , the bottom z=-h and two vertical planes $x=x_0$ and $x=x_0+dx$, as shown in Figure 4.

The flux of momentum into the slice, closing the slice at plane $x=x_0$, is

$$F(x_0) = S_{xx} + \int_{-h}^{\bar{f}} \rho g(\bar{f} - z)\, dz = S_{xx} + \frac{1}{2}\rho g(\bar{f} + h)^2 . \quad (3.70)$$

Across the plane $x=x_0+dx$, the flow out of the slice will be

$$F(x_0+dx) \approx F(x_0) + \frac{dF}{dx}dx$$

$$= S_{xx} + \frac{\rho g(\bar{f} + h)^2}{2} + \frac{d}{dx}\frac{\{S_{xx} + \rho g(\bar{f} + h)^2\}}{2}dx . \quad (3.71)$$

Bottom friction is neglected here. Momentum balance then gives

$$F(x_0) - F(x_0+dx) = -\frac{dF}{dx}dx = 0 .$$

$$\frac{d}{dx}\{S_{xx}+\frac{\rho g}{2}(\bar{f}+h)^2\}\,dx = 0\,. \tag{3.72}$$

Solving equation (3.72) with equation (3.69), we have

$$\bar{f} = h\{\sqrt{1+\frac{(H_s k)^2}{8kh\tanh 2kh}\cos 2kx} - 1\}\,. \tag{3.73}$$

This equation shows that the local mean level $\bar{f}$ is important when the wave steepness is large in shallow water region.

Longuet-Higgins and Stewart (1964) started from equation (3.67), taking S_{xx} with respect to x over a wave length and substituting equations (3.57) and (3.58), and found the local mean level.

$$\bar{f} = \frac{H_s^2 k}{16}\coth 2kh\cos 2kx\,. \tag{3.74}$$

The mean water level is raised at x=0 and at $x=\pi/k$, and lowered at the nodal points, and the profile of the mean surface has twice the wave number as that of the standing waves.

The mean water level of the partial standing waves (non-linear) is obtained from the equation of Goda and Abe (1968). The mean water level over one time period is equation (3.42) integrated over time and becomes

$$\frac{\bar{f}}{a} = 2\pi\lambda\varepsilon b_{02}\cos(k_I - k_R)x\,. \tag{3.75}$$

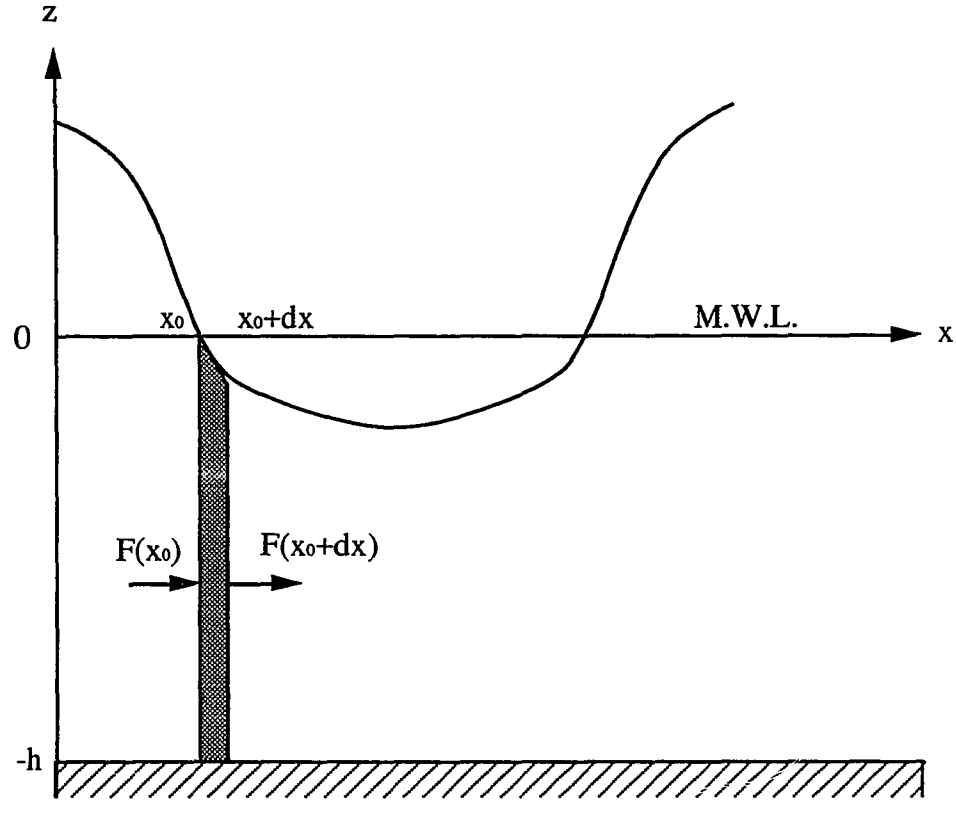

Figure 4, Momentum balance in standing wave condition

The wave numbers of incident and reflected waves are slightly different as expressed in equation (3.35). If the average of $|k_I|$ and $|k_R|$ is defined here as

$$\bar{k} = (|k_I|+|k_R|)/2 = k_A[\, 1 - \varepsilon^2(1+\lambda^2)(k_1-k_2)/4] \,. \qquad (3.76)$$

Equation (3.76) is then expressed with $\bar{k}$ as

$$\frac{\bar{f}}{a} = 2\pi\lambda\varepsilon b_{02} \cos 2\bar{k}x \,. \qquad (3.77)$$

This shows that the mean surface level is raised at $2\bar{k}x=n\pi$ and lowered at $2\bar{k}x=(2n+1)\pi/2$.

The mean water level can be calculated more accurately using the theory of standing waves in higher order approximation. According to the fourth order approximation by Goda and Kakizaki (1966), the mean water level has the fourth harmonic component of oscillation as in the following;

$$\bar{kf} = \left[\frac{1}{8}\varepsilon^2(c^2+c^{-2}) + \frac{1}{6}\varepsilon^4 b^*_{02}\right]\cos 2kx + \frac{1}{6}\varepsilon^4 b^*_{04}\cos 4kx \ , \tag{3.78}$$

where

$$b^*_{02} = \frac{(-27c^{10}+288c^6+168c^2-210c^{-2}-45c^{-6}+18c^{-10})}{512},$$

$$b^*_{04} = \frac{(54c^{14}+243c^{10}+198c^6+6c^2-198c^{-2}+63c^{-6}+18c^{-10})}{512}.$$

Each term of cosine is a positive in equation (3.78). Therefore the fourth order term rises the mean water level at anti-nodal points and lowers it at nodal points. But the quantity of decrease at nodal points is smaller than that of increase at anti-nodal points because of the term of cos 4kx. The concept described by the higher order approximation makes a steeper wave profile.

3.4 Wave Overtopping Model

In theoretical studies of wave overtopping the formula for steady flow over a weir with critical flow has been used by Kikkawa et al (1968), Shi-igai and Kono (1970), Takada (1970), and others. The basic discharge per unit width for critical flow, neglecting friction, is given by

$$q = \frac{2}{3}\sqrt{\frac{2g}{3}}\,E^{3/2}\,, \tag{3.79}$$

where E is the energy head of upstream flow above the crest of the weir. In the case of wave overtopping a vertical wall of breakwater, equation (3.79) may be written by the formula

$$q(t) = \frac{2}{3} C_f \sqrt{2g}\ \{\, f(t) - H_c \,\}^{3/2}\,, \tag{3.80}$$

where f(t) is the surface displacement of waves at the wall and H_c is the height of the vertical wall above the still water level. C_f is a discharge coefficient, which has coorporated the factor $1/\sqrt{3}$. The total amount of wave overtopping per wave period is obtained by the time integration of equation (3.80)

$$Q = \frac{2}{3} C_f \sqrt{2g} \int_{t_0}^{t_1} \{\, f(t) - H_c \,\}^{3/2}\, dt\,, \tag{3.81}$$

in which t_0 and t_1 are the beginning time and the ending time of wave overtopping in one period. If f(t) is explicitly given in equation (3.81), the total amount of wave overtopping can be

calculated with constant C_f. In the formula of equation (3.80), the discharge coefficient C_f should be determined by laboratory tests before the calculation of the total amount of wave overtopping. The value C_f is chosen from 0.5 to 0.7 if the phenomenon is similar to weir overflow. Takada (1970) obtained the discharge coefficient C_f from laboratory tests. He found that the discharge coefficient C_f increases with the increase of height of breakwater H_c and the range of C_f was 0.4 ~ 1.0 in the region $0<H_c/H_I<1.0$.

Tsuchiya and Yamaguchi (1969) defined the relation between the height of incident waves H_I and that of partial standing waves by experimental results

$$H_I = \frac{\{ f(0,0) - f(0,T/2)\}}{2} , \tag{3.82}$$

in which f(0,0) and f(0,T/2) are the crest level and the trough level of partial standing waves at a vertical wall of breakwater, respectively. Some attempts have been made to adapt experimental results to the theoretical surface displacement f(x,t). Takada (1972) applied the surface displacement of finite amplitude standing waves instead of that of standing waves f(x,t) when waves exceed the vertical wall, and replaced a coefficient C_f in equation (3.81) by another overtopping coefficient.

The application of the weir formula to wave overtopping gives relatively good agreement with experimental data. The solution is somewhat relevant in certain conditions where the physical assumptions underlying the formula are very similar to the steady

flow. Therefore, once the discharge coefficient C_f is determined from experiments, the mathematical formula could be used to calculate the volume of wave overtopping no matter how close it is to the physical reality. The approximation of Kikkawa et al (1968) describes only the flow running in one direction and avoids the consideration for the movement of fluid particles by wave motion. Takada (1970) derived further information on the formula and the surface displacement, but the basic assumption of steady flow is retained in his formula.

A different formulation is proposed here, which allows the calculation of quantities of water during wave overtopping at a vertical wall over an entire wave period. The volume of water flowing over breakwater is deduced from the water level in the non-overtopping condition; the rest of the waves retains the characteristics of the standing waves. The phenomenon could therefore be considered in such a way that the fluid keeps an up-and-down motion and water flows through a certain cross section between the free surface and the top level of the breakwater during wave overtopping. The quantity of wave overtopping would be expressed as a function of the water elevations at the wall in both non-overtopping and overtopping conditions. The hypothesis is based on the premise that the energy head related to the overtopping flow is partly converted to kinetic energy of the flow over the breakwater during the wave overtopping period.

The total energy head is generally expressed by a summation of the following heads, according to Bernoulli's law:

1. The head which represents the kinetic energy of the water in motion, called velocity head and is written $v^2(t)/2g$.

2. The head which results directly from elevation representing potential energy, called elevation head and is written z.

3. The head which represents the energy from the internal pressure, called pressure head and written $P/\rho g$.

The total energy head above the bottom of the channel is then

$$E = \frac{v^2(t)}{2g} + z + h + \frac{P}{\rho g} \quad , \tag{3.83}$$

where steady state is assumed to be applicable.

If a vertical hydrostatic pressure distribution is assumed, the pressure at z is described by

$$P = \rho g\{ f(t) - z \} \quad , \tag{3.84}$$

where f(t) is the free surface displacement from z=0.

Substituting equation (3.84) into equation (3.83),

$$E = \frac{v^2(t)}{2g} + f(t) + h \quad , \tag{3.85}$$

where v(t) is the velocity at the surface but is here assumed to represent the average velocity over the weir.

The general expression for the total energy head at time t may be written in the following relation,

$$E = E_F + E_W \quad , \tag{3.86}$$

where E_F and E_W are the energy heads for the flow and the wave, respectively.

In the overtopping condition, the total energy head can be written as

$$E = E_F + E_W = \frac{v(t)^2}{2g} + f_c(t) + h \, . \tag{3.87}$$

On the other hand, the total energy head in non-overtopping condition depends upon the energy head by wave only because of no flow over the wall and therefore the total energy head can be written as

$$E' = E_W' = f_m(t) + h \, . \tag{3.88}$$

Figure 5 shows the sketch of the relationship.

The difference of energy heads for wave motion in both conditions, E_W'- E_W, contributes to the overflow and is equal to the energy head E_F so that

$$f_m(t) = f_c(t) + \frac{v(t)^2}{2g} \, , \tag{3.89}$$

in which v(t) is the mean horizontal velocity over the vertical wall at time t. $f_m(t)$ and $f_c(t)$ are surface displacements in non-overtopping condition and overtopping condition. The velocity v(t) can then be expressed by

$$v(t) = \sqrt{2g \{ f_m(t) - f_c(t) \}} \, , \tag{3.90}$$

The cross section, through which water flows over the breakwater per unit of area, equals $f_c(t) - H_c$, is assumed to be proportional to $f_m(t) - f_c(t)$. This assumption can be demonstrated at

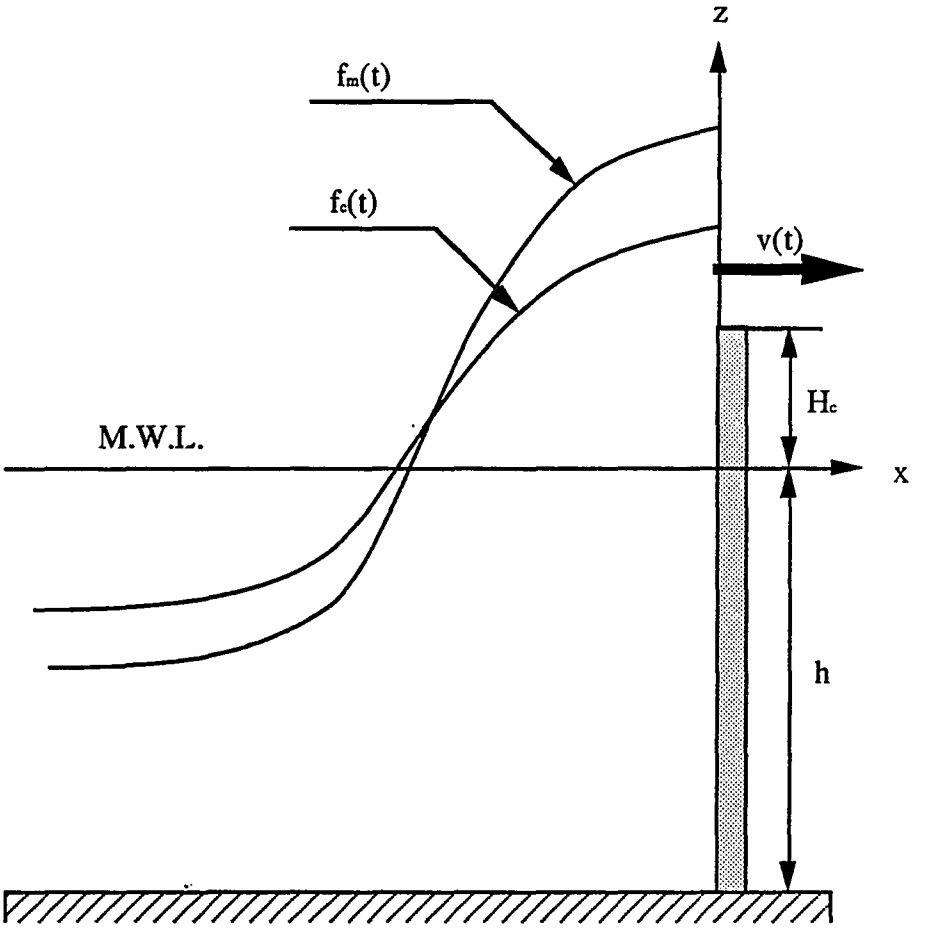

Figure 5, Surface displacement and overtopping flow at time t

the time of maximum crest elevation near the wall, when the surface displacements $f_m(t)$ and $f_c(t)$ turn into η_m and η_c, respectively. At that moment, the ratio $\{f_c(t)-H_c\}/\{f_m(t)-f_c(t)\}$ can be described by applying equation (2.6).

$$\frac{f_c(t)-H_c}{f_m(t)-f_c(t)} = \frac{\eta_c-H_c}{\eta_m-\eta_c} = \frac{0.65\eta_m+0.35H_c-H_c}{\eta_m-0.65\eta_m-0.35H_c} = 1.86 .$$

The discharge per unit width is obtained by a multiplication of the velocity and the section of overtopping flow , and so that

$$q(t) = \sqrt{2g}\ T_f \{ f_m(t) - f_c(t) \}^{3/2}, \qquad (3.91)$$

where T_f is a discharge coefficient to be determined experimentally. The total amount of wave overtopping per wave period can be calculated by the integration of equation (3.91).

$$Q = \sqrt{2g}\ B\ T_f \int_{t_0}^{t_1} \{ f_m(t) - f_c(t) \}^{3/2}\, dt, \qquad (3.92)$$

in which B is the width of the channel.

CHAPTER IV

EXPERIMENTS

4.1 General

A series of experiments for this investigation were conducted in a wave channel of Nihon University shown in figure 6. The channel was 27.60m long, 0.70m wide and 1.0m high. The side walls consisted of glass plates. Wave energy absorbers were installed at both sides of the channel. They were built to reduce wave reflection from both ends of the channel. Each absorber was a horizontal slit type and was 1.0m high and 0.7m thick, as shown in figure 7. Both absorbers consisted of four individual units mounted adjacent to each other.

The wave generator used for this study consisted of a motor, round plates, joint arms and a vertical wave generating board, driven horizontally by a piston. Regular waves were generated as the board through a 5.5kw motor. The motor transmitted the rotation to the round plate. The circular motion by the round plate controlled the wave plate with the rectilinear movement to generate regular waves. The round plate was connected to the wave plate with a steel arm which could change its length easily in order to make different amplitudes of incident waves. A multirevolving potential meter was attached to the wave generating control circuit to regulate the period of the horizontal motion. Wave period could be read on the digital counter with the aid of photoelectric detector which had a measurement capability of 1/1000. The wave generating system can be seen in figure 8.

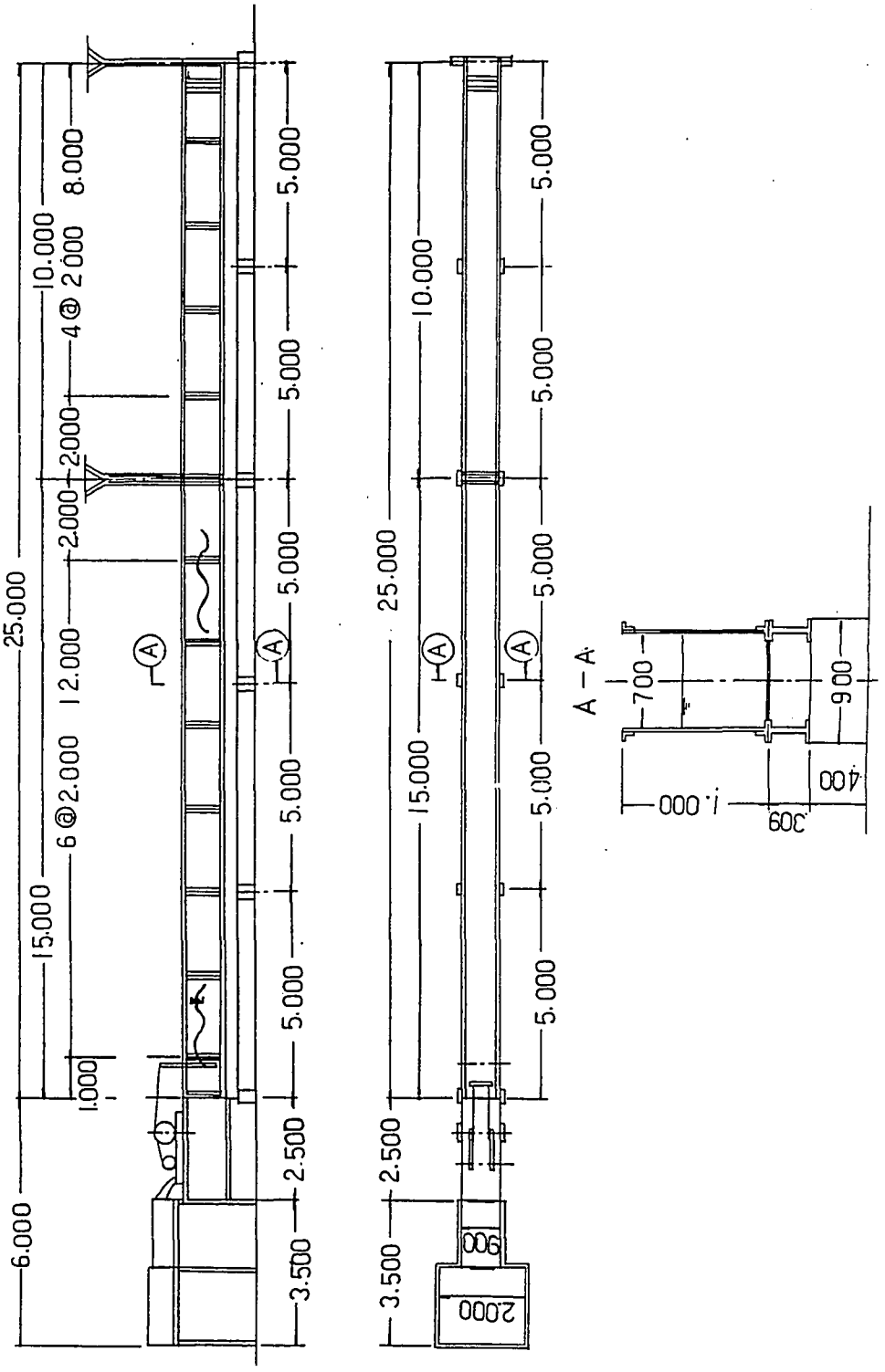

Figure 6, Wave channel

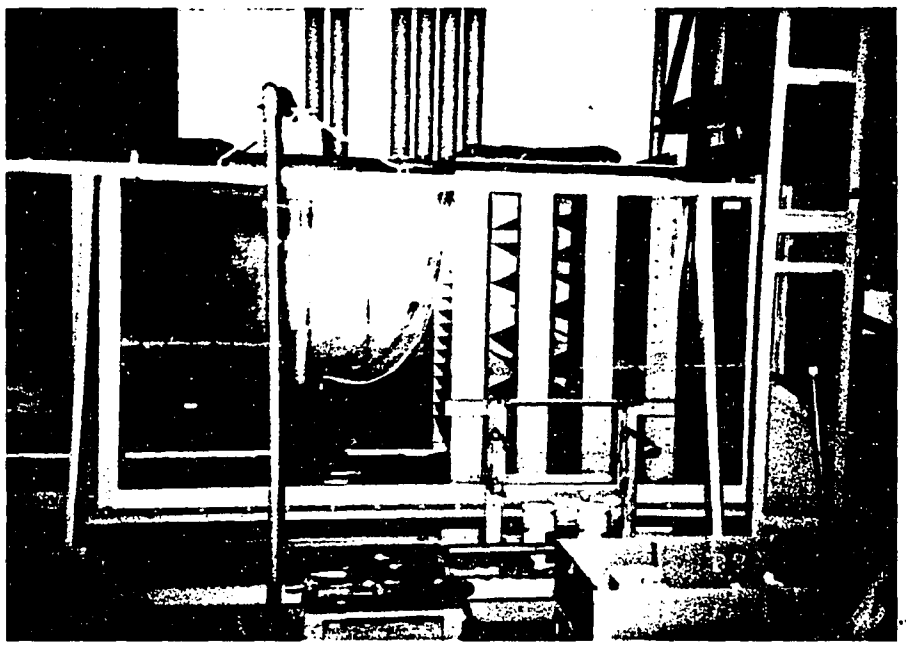

Figure 7, Wave absorber

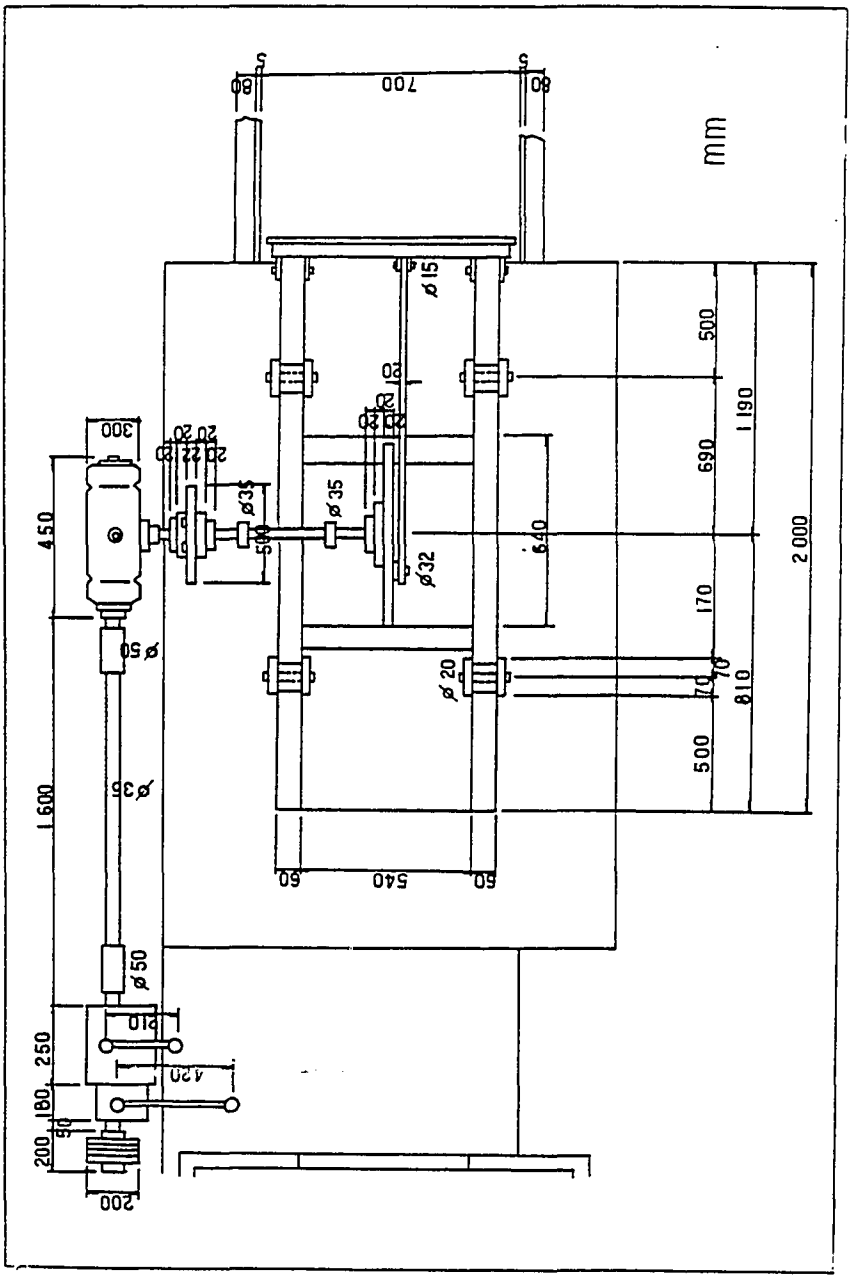

Figure 8, Wave generating system

A capacitance wave gauge was attached to a remotely controlled calibration device which set on a rack across the channel. The calibration device was controlled from a main control panel and moved the wave gauge vertically in 1.0cm intervals. This arrangement allowed quick calibration of the wave gauge before each test. The main controller consisted of control units which allowed a maximum of six wave gauges to be used at the same time.

The wave gauges were used in conjunction with an Analog-to-Digital (A/D) converter (HA-106, Tokyo Keisoku Co.). The A/D converter could indicate the output signal from wave gauges as a voltage or meter reading. The significant figures of A/D converter were three (-999 ~ +999) for a ±2.5 voltage range. A digital data recorder (DR-200 TEAC) was used for recording the surface displacement in centimeters. After processing through the DC-amplifier, the input analog data was converted into digital quantities, and was recorded on a magnetic tape in a format for the digital computer. The sampling frequency available was from 0.1 to 500Hz in 20 different kinds. A multi-channel recording was possible for use with several wave gauges. Real time recording was possible on the tape until 999 day 23 hr 59 min 59 sec. In addition to the recording obtained from the digital data recorder, the rectified signal from the wave gauge was recorded by the digital wave height recorder, which was developed to measure the wave height and the wave period simultaneously. The recorder detected the still water level, the wave crest level and the wave trough level. The detected data was held in the memory circuit and printed out

the crest level, the trough level, the wave height, and the wave period simultaneously. The measuring accuracy was 1/100 cm in wave height and 1/100 second in period.

In this study, measurements were performed to obtain the surface displacement of partial standing waves in front of the structure. The details are described in section 4.2. Other experiments regarding the total amount of wave overtopping were carried out by Horie (1981). The experimental set-up for the analysis of wave overtopping is described in section 4.3.

4.2 Partial Standing Waves

A vertical breakwater model with variable height was used for this investigation. The outer frame was composed of two steel plates of 105.0cm high, 10.0cm wide and 0.5cm thick, and fixed to the glass walls of the channel. The breakwater was made of two pairs of steel plates; each 35.0cm high 69.0cm wide and 0.6cm thick and the other pair 18.0cm high 69.0 cm wide and 0.6cm thick, as shown in figure 9.

Plates of two different sizes were fastened by bolts on the frame, and the other two plates slid vertically along the frame and were fixed by bolts. The height of the wall from the bottom could be regulated in steps of 1.0cm from 38.0cm to 60.0cm. The vertical breakwater was placed nearly at the end of the channel, at a distance of 21.2m from the wave generating board. In the experiment, the height of breakwater was varied from a certain

level up to the height in which no wave overtopping occurred, while the depth of the water in front of the breakwater was 40.0cm and was kept constant.

The wave generator operated with different periods. The periods of the motion were respectively 1.2, 1.4, 1.6, 1.8, 2.0 and 2.2 sec. The wave lengths corresponding to these periods were 193.48 to 411.31cm in Airy's theory. The wave profiles were measured at a horizontal distance of 0.3cm from the vertical wall representing the breakwater and five other points at thirty centimeter intervals from the wall. This setting is shown in figure 10.

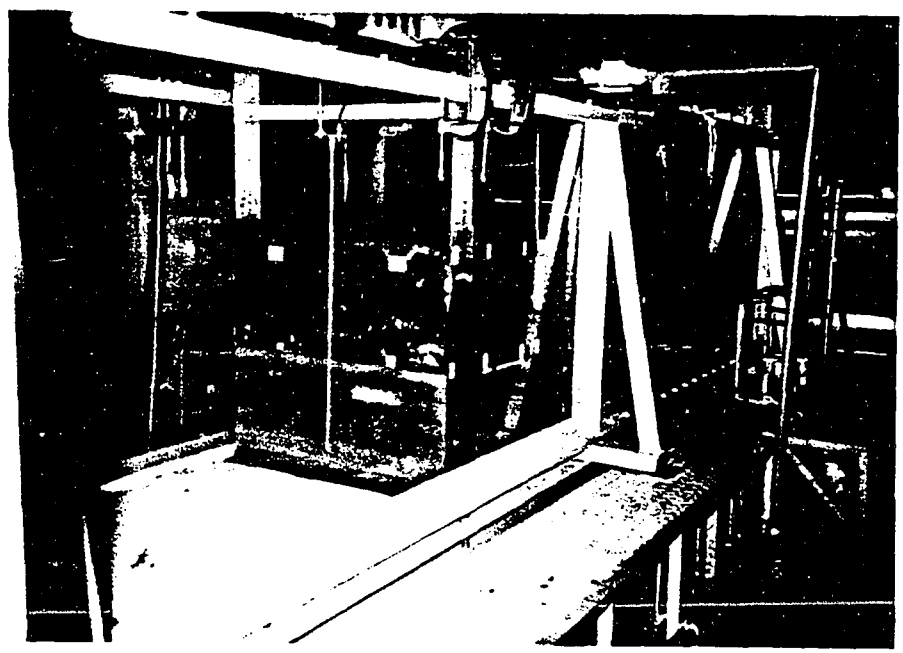

Figure 9, Vertical breakwater model

Figure 10, Setting of wave gauges to measure spatial surface displacement

Experiments were conducted under the conditions listed in Table 1.

Table 1
Incident wave height H_I cm for experiment on surface displacement

Period sec	1.2	1.4	1.6	1.8	2.0	2.2
H_I cm	14.69	12.16	10.26	8.53	7.21	6.48

The heights of the vertical wall were chosen at H_c=4.0cm and 8.0cm above the still water level in the wave overtopping condition. Calibration of wave gauges was performed by the following process. The wave gauges were immersed downward at a distance of 4.0cm from their equibrium position and then raised a total distance of

8.0cm slowly in 1.0 centimeter interval. The calibration curves of these gauges were linear in the range of ±4cm. Before the experiment was started, the wave gauges were returned to their equilibrium position.

After the wave generator was started to generate incident waves, a digital data recorder started to record the signal of the free water surface at each of the wave gauges. The data was transformed by the A/D converter in the recorder with a sampling frequency of 50Hz and was recorded on a casette tape simultaneously. Multi-channel recording from 6 gauges was possible throughout the experiment. The wave generator was turned off before the reflected wave from the breakwater arrived at the wave generating board. A PS-80 microcomputer (TEAC) managed the data and printed out necessary information with an attached printer.

4.3 Amount of Wave Overtopping

The experiments to collect the flow of water of the wave overtopping were conducted in the same wave channel described previously. The type of a vertical wall used for the experiments was the vertical breakwater model which was used for the measurement of partial standing waves and placed nearly in the middle of the channel, 13.00m from the wave generating board.

The amount of water by wave overtopping was collected in a measuring tank which was installed behind the vertical wall. The

size of the outer structure of the tank was 66.20cm x 50.00 cm x 30.00 cm while the inner tank was 66.20cm x 48.10 cm x 29.05 cm and the volume of the measuring tank was 92501.6cm^3. A cover was set on the top of the measuring tank to prevent the inflow from additional waves, after two waves were captured. Figure 11 shows the arrangement of the measuring tank. Wave crest levels and trough levels were measured with a capacitance type wave gauge positioned at 0.3cm from the vertical wall of breakwater.

The water depth was kept 40.0cm throughout the experiment. The wave periods and the corresponding wave heights were varied by shifting the position of the joint of the connecting arm between the round plate and the wave generating board. The wave conditions used in this experiment are listed in Table 2. The wave periods of test waves varied from 1.2 to 2.2 seconds. The corresponding incident waves heights were generated with three different conditions (case 1 to case 3) and the heights were measured at the location of the vertical wall without the wall being present in the channel.

Table 2

Incident wave height H_I cm for experiment on amount of wave overtopping

Period sec	1.2	1.4	1.6	1.8	2.0	2.2
H_I (Case1) cm	12.78	10.68	9.18	7.32	5.96	5.42
H_I (Case2) cm	14.69	12.16	10.26	8.53	7.21	6.48
H_I (Case3) cm	16.47	13.98	11.89	9.64	8.27	7.35

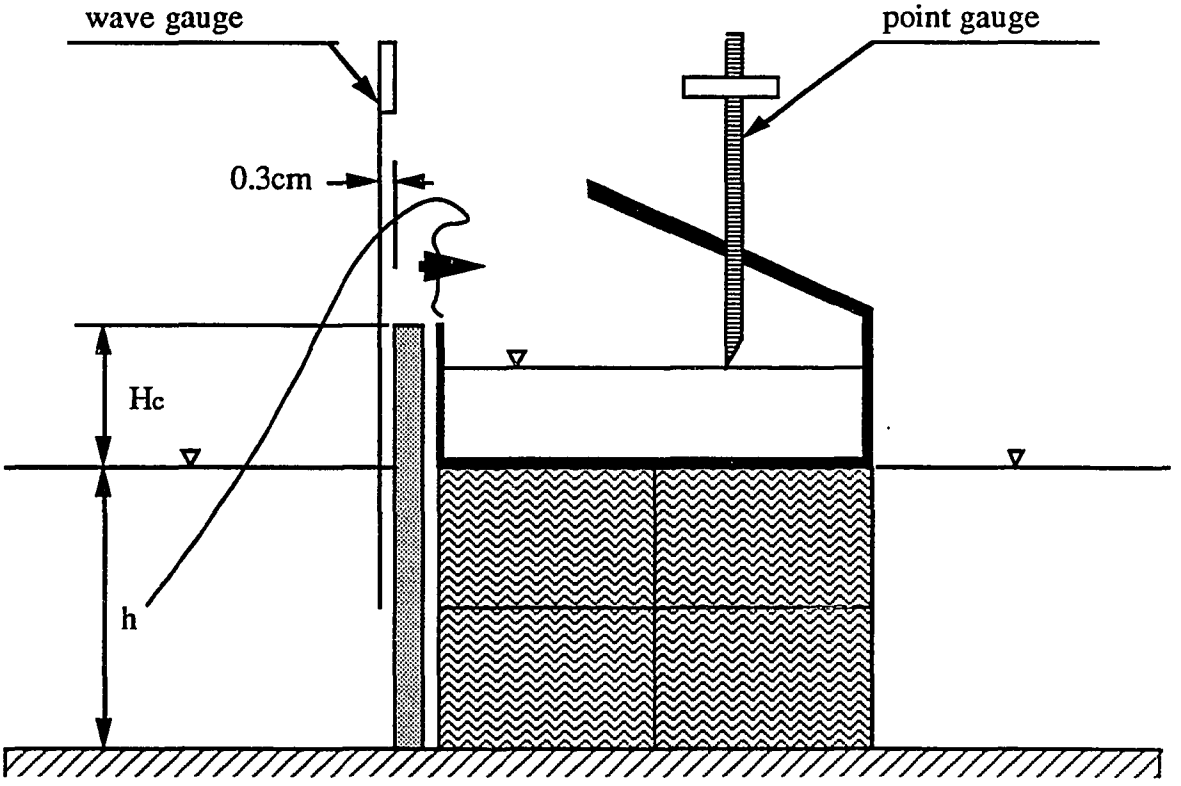

Figure 11, Measureing tank for wave overtopping

The calibration of the wave gauges was performed in the same manner as described in the previous section.

The wave height at the vertical wall became stable after a few periods of wave generation and continued to be stable until reflected waves returned to the vertical plate of the wave generator. However, the volume of wave overtopping in each wave fluctuated a little even after the waves became stable. The following mechanism was considered by Shi-igai and Rong-Chung (1977): soon after a large amount of wave overtopping occurred, the reflected wave energy is decreased so that the wave height near the breakwater is

also decreased. This causes a lesser amount of overtopping than before, which will again be followed by a larger amount of overtopping. The generating system also induces a long wave phenomenon in the tank (seiche) that may affect the mean sea level at the breakwater and thereby influence the rate of overtopping of the incident waves.

For two selected waves the amount of wave overtopping was collected in the measuring tank in each test run after the waves have become stable. The measuring tank was closed with a cover when other waves passed over it. A point gauge was used to measure the water level in the measuring tank after each test. The difference between the water level before and after the test was multiplied by the area of the bottom of the measuring tank, and the volume of the amount of overtopping was obtained. The amount of wave overtopping per wave was defined as half of the volume of water collected in the tank.

Wave crest levels and trough levels were also measured and defined by the averaging of three or four wave levels, depending on the wave period, after the waves became stable.

After each test, water was supplied by a pump to keep the water depth at a constant value.

CHAPTER V

RESULTS AND ANALYSIS

5.1 Introduction

The surface displacements of perfect and partial standing waves and the water volume of wave overtopping were measured in the laboratory to determine the applicability of the theories proposed in Chapter III. The primary topic investigated here is the deformation of the wave profile due to wave overtopping. It is important to compare the predicted results, which were obtained from the newly developed method of finite amplitude standing wave for wave overtopping condition by the author, with experimental results. From such a comparison, one can determine whether the approximations made to develop the theoretical equations are valid. In addition to these wave profiles in time and space, the reflection coefficient and the variation of incident wave height are discussed since the concept underlying this theory is different from work by other authors. The reflection effect is only taken into account in their partial standing wave theories, when they are applied to the overtopping waves. A theoretical equation of mean water level which based on the rate of change of radiation stress in non-overtopping condition is presented here and compared with the other work as well.

The secondary topic deals with the amount of water from wave overtopping over the breakwater, which was collected in a measuring tank; the wave crest level and the wave trough level were measured at the face of the breakwater. Measured crest and

trough levels over the full wave profile are compared with the experimental equations shown in Chapter II, and the capability of these equations to represent actual conditions is investigated from these experiments. An analysis of wave overtopping is made based on the existing as well as the newly developed formulae. The observed water volume of wave overtopping is compared with the results obtained from the theoretical analysis with finite amplitude standing wave theories defined in Chapter III.

5.2 Surface Displacement at Vertical Wall

In order to clarify the applicability of the proposed method for partial standing waves, some results of computational surface displacement by the present method of Goda and Abe for non-overtopping waves and the newly developed method for overtopping waves are compared with the experimental results in this section.

The surface displacements were measured by a wave gauge set at the location of vertical wall x=0.3cm. The breakwater height was chosen in three different levels; H_c=4cm, 8cm and large (no overtopping). In each test between 7 and 10 waves were generated, depending on initial wave conditions, and the test was terminated before the first reflected wave from the vertical wall returned to the wave generating plate and created the re-reflection wave.

The wave profiles are plotted in the following manner. In order to describe a natural profile of standing waves, a surface

displacement of half a wave period was chosen from each test record, after the wave had become stable. Each measured value is plotted from the crest level to the trough level in 0.02sec time intervals. Comparisons of the measured wave profile to the theoretical profile are presented in figures 12 through 17 for H_c=large, in figures 18 through 23 for H_c=4cm and in figures 24 through 27 for H_c=8cm. The abscissa is t/T and the ordinate is $f(t)/H_I$, where t is the time in second, T is the wave period, f(t) is the surface elevation above the still water level and H_I is the incident wave height. The solid curves in these figures show the results calculated by the theory based on the finite amplitude wave approximation, and the circular symbols are the measured data. The measured crest and trough levels at the vertical wall were used to determine these wave profiles as well as the incident wave heights and periods.

The laboratory data of surface dispiacements shown in figures 12 through 17 represent the case of perfect standing waves. It can be seen that the theoretical curves calculated from equation (3.38) predict the profiles with a reasonable degree of accuracy in the range of the conditions tested. There is a small difference between the theoretical wave profile and the experimental data, and this appears to increase with wave periods. Generally the experimental wave profiles are steeper than the theoretical ones and are somewhat higher in both the crest level and the trough level and lower in the region $0.1<t/T<0.4$. We expect to obtain a closer

agreement, if we would calculate the wave profiles with a higher order of approximation.

The surface displacements of overtopping waves for H_c=4cm are presented in figures 18 through 23. From these figures and figures 12 through 17, it is found that as a whole the free surface of perfect standing waves and that of partial standing waves in experiments behave differently in the region higher than the top level of the breakwater. The observed values near the crest for partial standing waves are somewhat flatter than these for the perfect standing waves, while the values near the trough behave similarly in both cases. The pattern of the free surface varies with the function of the wave condition and the height of the vertical wall. A point of inflection exists near the crest level of breakwater. The free surface drops slowly from the crest level until the inflection point and after that, the shape of the free surface becomes closer to the pattern of the perfect standing waves in the same condition. Theoretical equations used to describe these complex phenomena are equation (3.53) for the region lower than the top level of breakwater and equation (3.55) for the region higher than the level. These theoretical equations show experiments to be reasonably correct except in the region around the inflection point.

Figures 24 through 27 show the comparisons of measured surface displacement and theoretical surface displacement for H_c=8cm. When the wave periods were 2.0 and 2.2sec, wave overtopping did not occur in the laboratory tests, and no figures are shown for these conditions. The agreement between the theory and

measured values is fairly good. Even near the inflection point, the agreement of these surface elevations is quite satisfactory. The discrepancy appears to be a little less than that for the case of H_c=4cm. These results imply that overall the theoretical surface displacement describes the measured values reasonably well. The surface displacement near the inflection point becomes smoother with the increase in the height of vertical wall.

5.3 Spatial Surface Displacement

The surface displacements of waves as a function of time were measured by a series of six wave gauges fixed at x=0.3, 30, 60, 90, 120 and 150cm, and are compared with theoretical surface displacements in figures 28 through 43. The experimental data are plotted at two different times, corresponding to the times of crest level and trough level at station x=0.3cm. It should be noted that the time difference between the profiles was not exactly equal to one half wave period, T/2, but it was the closest possible value to allow comparison with the theory. These figures show the free surface variation normalized by the incident wave height H_I as a function of the horizontal distance from the location of vertical wall.

Figures 28 through 33 compare measured surface displacements with theoretical ones for the perfect standing waves (no overtopping). It can be seen that the measured crest level is somewhat lower than predicted by theory, when a trough occurs at the vertical wall. This is presumably due to an effect of the position

of the wave gauge at the vertical wall and therefore the free surface takes the highest value at the wall. Since the theoretical equation is calculated to obtain the surface displacement with the standing wave height H_s, which might be measured at the vertical wall in laboratory and includes the wall effect described above, the free surface can not raise the theoretical crest level at antinodal points. This phenomenon is noticeable in the shorter wave period and the higher wave height. The agreement with theoretical equation (3.38) for perfect standing waves is quite good in T=1.6, 1.8, 2.0 and 2.2sec.

Comparisons of measured spatial surface displacements with theoretical ones for H_c=4cm are shown in figures 34 through 39. Theory and measurements deviate at one or two locations in each case; this is x=60 and 120cm for T=1.2 and 1.4sec, x=30 and 150cm for T=1.6 and 1.8sec and x=30cm for T=2.0 and 2.2sec. This deviation is remarkable; it occurs when wave overtopping takes place at x=0, especially as the difference between measured values and theoretical profile at x=60cm for T=1.2 and 1.4sec and at x=30cm for T=1.8, 2.0 and 2.2sec during the stage of wave overtopping.

Finally surface displacements for the case H_c=8cm are shown in figures 40 through 43 comparing the measured and theoretical data. As can be seen, the differences between the measured data and the theory are small compared to the previous two cases; H_c=large, and H_c=4cm. The experimental data show better

agreement with the finite amplitude theory as modified by the author.

5.4 Reflection Coefficient and Variation of Incident Wave Height

When the reflected wave height is equal to the incident wave height, a perfect standing waves will be formed no matter what theory is applied in the phenomenon. Since $\lambda=1$ for perfect reflection in equations (3.25) and (3.26), the wave numbers k_I and k_R are equal to $\bar{k}$. The surface displacement is given by equation (3.38) for $k=\bar{k}$. The calculated surface displacement for $\lambda=1$ showed good agreement with the measured data in the case of perfect standing waves in figures 12 through 17 for time dependent surface displacement and in figures 28 through 33 for spatial displacement.

When the height of breakwater is lower than the crest height of the perfect standing waves, the standing wave facing the vertical wall exceeds the crest of the breakwater and the wave is deformed in front.

The surface displacement of reflected waves is obtained by substituting equations (3.11), (3.13) and (3.15) into equation (3.48). Thus the final result of f_R becomes

$$f_R = \lambda_2 a \cos(k_R x-\sigma t) + \lambda_2^2 a^2 k b_{22} \cos 2(k_R x-\sigma t)$$

$$+ \frac{1}{2}\lambda_2^3 a^3 k^2 \{ b_{11} \cos(k_R x-\sigma t)$$

$$+ b_{33} \cos 3(k_R x-\sigma t)\} + R \,. \qquad (5.1)$$

The reflected wave height is calculated at x=0 as

$$H_R = 2\lambda_2 a + \lambda_2^3 a^3 k^2 (b_{11} + b_{33}) + R \,. \qquad (5.2)$$

Similarly, the surface displacement of incident wave after wave overtopping is obtained by substituting equations (3.11), (3.13) and (3.15) into f_I in equations (3.52) and (3.54).

When free surface is higher than H_c, the surface displacement of incident waves becomes

$$f_I = \lambda_1 a_* \cos(k_I x-\sigma t) + \lambda_1^2 a_*^2 k b_{22} \cos 2(k_I x-\sigma t)$$

$$+ \frac{1}{2} \lambda_1^3 a_*^3 k^2 \{b_{11} \cos(k_I x-\sigma t)+b_{33} \cos 3(k_I x-\sigma t)\} \,. \qquad (5.3)$$

When the free surface is lower than H_c, the surface displacement of incident waves near the wall becomes

$$f_I = a \cos(k_I x-\sigma t) + a^2 k b_{22} \cos 2(k_I x-\sigma t)$$

$$+ \frac{1}{2} a^3 k^2 \{b_{11} \cos(k_I x-\sigma t)+b_{33} \cos 3(k_I x-\sigma t)\} \,. \qquad (5.4)$$

The incident wave height at the wall due to wave overtopping is obtained by subtracting trough level from crest level at x=0 as

$$H_I' = \lambda_1 a_* + a + (\lambda_1^2 a_* - a^2) k b_{22} + (\lambda_1^3 a_*^3 + a^3) k^2 (b_{11}+b_{33}) \,. \qquad (5.5)$$

The wave crest level and the wave trough level facing the vertical wall were measured by model study and experimental equations (2.6) and (2.7) were suggested as a function of H_c by Endo

and Miura (1983). These values will be used on the calculation of reflection coefficient and the variation of incident wave height.

The reflection coefficient K_R and the ratio K_I on incident wave heights before and after wave overtopping, are shown in figures 44 through 49 for the initial wave conditions given in Table 1. In these figures, the axis of abscissas indicates the ratio H_c/H_I and the axis of ordinate indicates the reflection coefficient $K_R(=H_R/H_I)$ and the coefficient K_I $(=H_I'/H_I)$. The solid curves in these figures show the reflection coefficient K_R, while the dashed curves indicate the coefficient K_I. The reflection coefficient K_R is about 0.35 when the crest of breakwater is at the still water level, $H_c=0$. The reflection coefficient increases linearly in the region $0<H_c/H_I<0.6$. This is caused by the increase of height of vertical wall and in this region the reflection is proportional to the height H_c from the mean water level as explained in Chapter III. In the region $H_c/H_I>0.6$, the reflection coefficient also varies linearly as a function of H_c but in a different way, since it depends on the crest level of the incident wave. The variation of these levels are not so remarkable with the changing of H_c. As expected, the coefficient K_I corresponding to the region $0<H_c/H_I<0.6$ decreases, being proportional to the height of vertical wall. The coefficient K_I becomes smaller than the reflection coefficient K_R in the region $0.4<H_c/H_I<0.6$. In the region near $H_c/H_I=0.5$, the coefficient K_I increases again, but it is less than the reflection coefficient K_R.

5.5 Wave Crest Level and Trough Level

The crest level and the trough level were measured at a location x=0.3cm very near the breakwater, when the water volume of wave overtopping was measured. The results of the laboratory measurements are compared with the experimental equations (2.6) and (2.7) in figures 50 through 55. The results show that these experimental equations can predict the crest level and trough level well. The measured crest levels for T=1.2 and 1.6sec and the trough level of T=2.2sec, however, are somewhat higher than the predicted values according to the experimental equations (2.6) and (2.7). The reason for the discrepancy may be due to the process of averaging the measured data. The measured data are averaged for three or four consecutive waves after the wave height had become almost stable. As explained in Chapter IV, each wave level fluctuates even after the stable condition; therefore the average values obtained may deviate from the predicted ones. The presence of low amplitude long period oscillations (seiches) may also appear the results.

5.6 Mean Water Level

In section 3.3, analytical equations were derived to estimate the change of mean water levels when standing waves were created in front of a vertical breakwater. Figures 56 between 61 compare shapes of the mean water level which were obtained by equations (3.73), (3.74), and (3.77) for λ=1. The abscissa is x/L, where x is the

distance from the vertical breakwater and L is the wave length in Airy's theory. The ordinate is $f(x)/H_I$, where f(x) is the value of the mean water level at x, and H_I is the incident wave height. The results are shown as solid curves with triangle symbols for the newly derived equation (3.73), with square symbols for Longuet-Higgins and Stewart's equation (3.74), and with circle symbols for Goda and Abe's equation (3.77). The profile of the mean water level solved by equation (3.73) has the same period as solved by equation (3.74). The period of the formula in equation (3.77) is larger than the ones calculated from equations (3.73) and (3.74), since it was obtained using an average wave number $\overline{k}$.

The relative amplitudes of mean water level have larger values for larger h/L and H/L and smaller values for smaller h/L and H/L. Therefore the relative water depth and the wave steepness are important factors for the change of the mean water level. There seems to be little difference in the values of the mean water level between equations (3.73) and (3.74) in all cases, although equation (3.77) has an amplitude smaller than these values for larger h/L and larger for smaller h/L.

5.7 Wave Overtopping Model Test

The experimental results of the amount of wave overtopping are shown in figures 62 through 64 for variable wall height and different wave conditions defined in Table 2. As may be noted from these figures, each curve for a specified wave period is part of

general family of curves. It also can be shown that the measured values of wave overtopping normalized by $H_I L/(2\pi)$ are affected by the initial wave condition H_I and T. This means that the amount of wave overtopping is related to the wave steepness.

The discharge coefficient C_f for finite amplitude wave was calculated by the numerical integration of equation (3.81) with the measured values of wave crest and trough levels and of the total amount of wave overtopping. The results are shown in figures 65 through 67.

The equation (3.86) was applied to determine a value T_f on the basis of a series of laboratory tests. The comparison of predicted values and measured values will primarily investigate the transfer coefficient T_f to compute the quantity of wave overtopping associated with the height of vertical wall. Equation (3.86) was integrated with the help of Simpsom's method after the surface displacements of standing wave $f_m(t)$ and $f_c(t)$ were determined from equation (3.38) and equation (3.55) for x=0, respectively. Figures 68 through 70 show the ratio of measured quantity of wave overtopping Q_{exp} to predicted wave overtopping Q_a with unit transfer coefficient, which is responsible for H_c/H_I. The transfer coefficient T_f is almost equal to one in the major region $H_c/H_I<1.0$. The greater the normalized wall height, $H_c/H_I>1.0$, the more T_f deviates from one. It is uncertain whether such a difference mentioned above is caused by the imperfection of the hypothesis or by the inaccuracy of the measuring technique. It should be noted that in the region the measured value of wave overtopping is very small and the quantity

of water cannot be measured with high accuracy. However, these quantities are not important for practical designing. Another interesting result is that in every wave condition, the value T_f is smaller than one when the wall level is at the still water level (H_c/H_I=0).

The following figures will evaluate the model's ability to describe the physical phenomenon of wave overtopping. The relationship between the measured quantities Q_{exp} and the calculated values Q_a for T_f=1 is shown in figures 71 through 73. In all cases the predicted values Q_a are in reasonably good agreement with the measured ones Q_{exp}, until they reach the value of 170~200cm^2. Thereafter, the theory overpredicts the total amount of wave overtopping. The following reason for this is considered. This tendency is thereupon influenced by the value T_f which was assumed constant throughout wave overtopping condition. The transfer coefficient T_f is not necessarily equal to one as was used in figures 71 through 73, because it depends on the height of the breakwater.

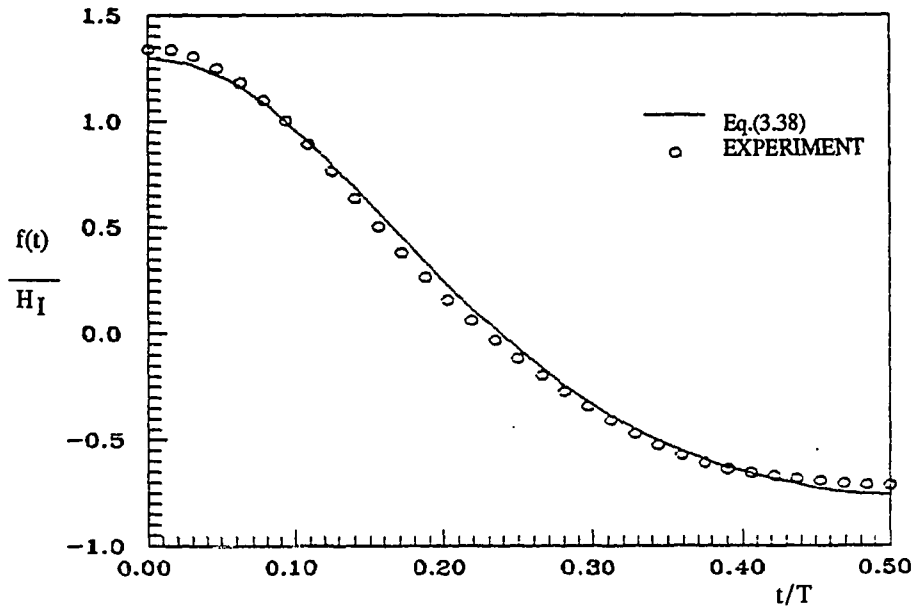

Figure 12 , Time surface displacement (x=0.3cm)
H_c=Large, H_I=14.69cm, T=1.2sec

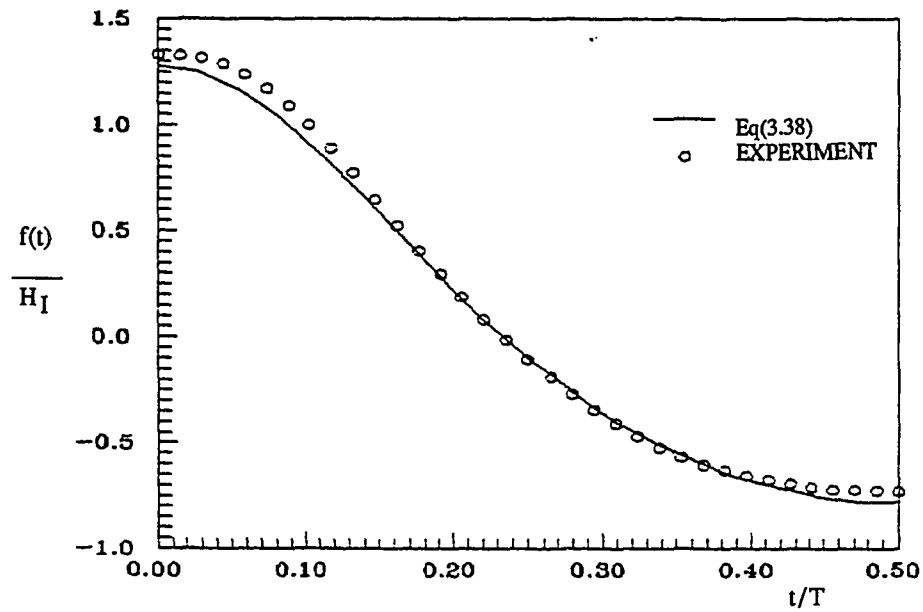

Figure 13 , Time surface displacement (x=0.3cm)
H_c=Large, H_I=12.16cm, T=1.4sec

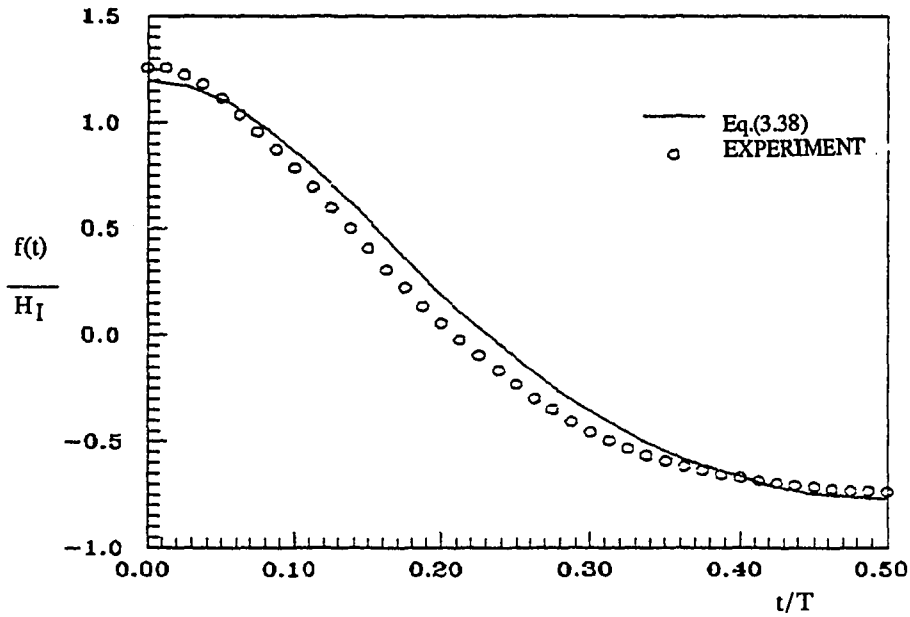

Figure 14 , Time surface displacement (x=0.3cm)
H_c=Large, H_I=10.26cm, T=1.6sec

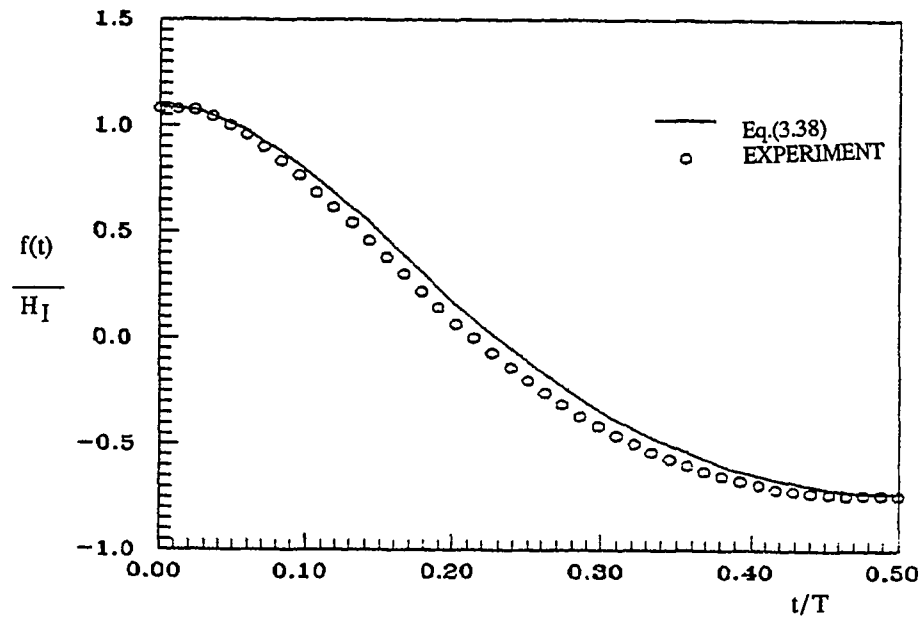

Figure 15 , Time surface displacement (x=0.3cm)
H_c=Large, H_I= 8.53cm, T=1.8sec

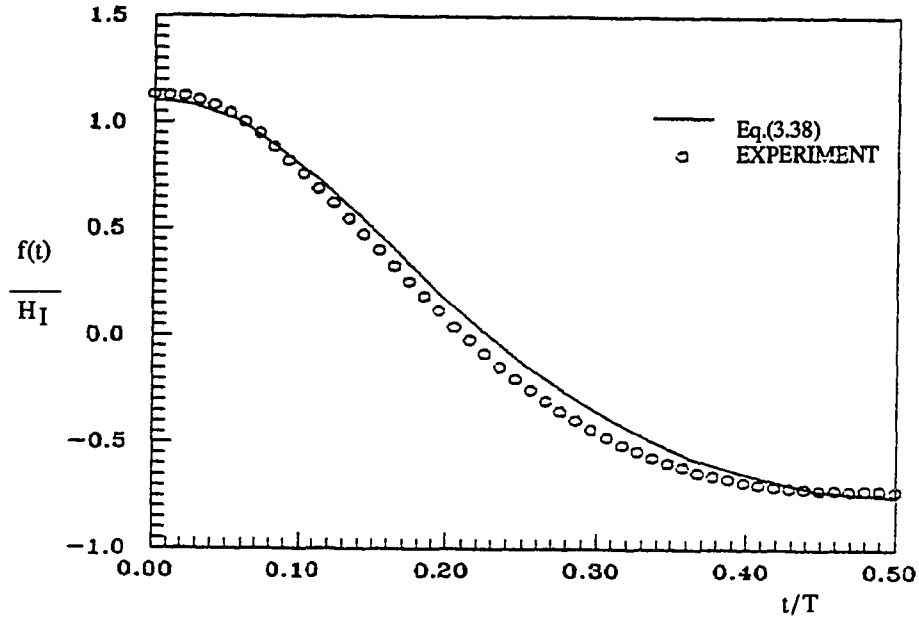

Figure 16 , Time surface displacement (x=0.3cm)
H_c=Large, H_I= 7.21cm, T=2.0sec

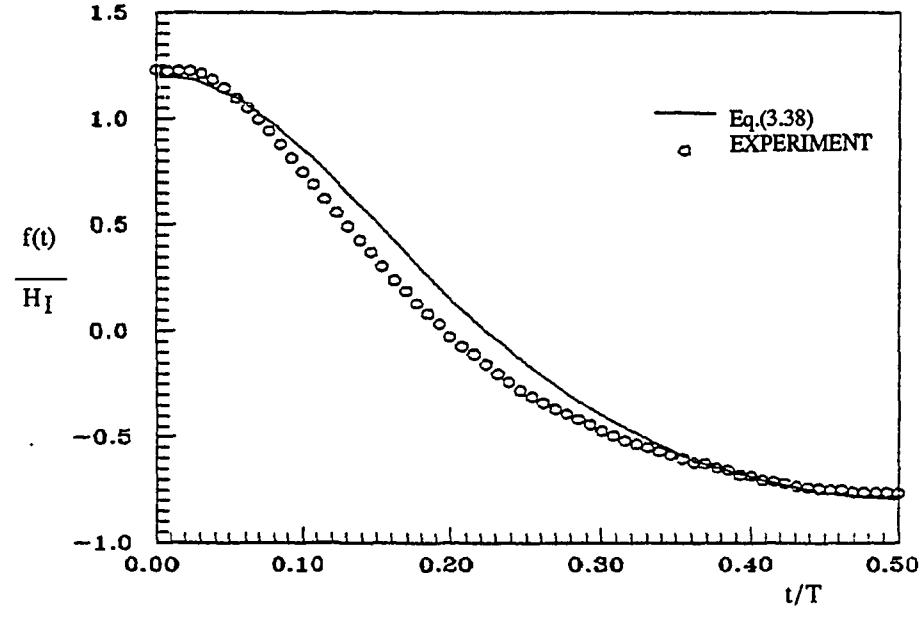

Figure 17 , Time surface displacement (x=0.3cm)
H_c=Large, H_I= 6.48cm, T=2.2sec

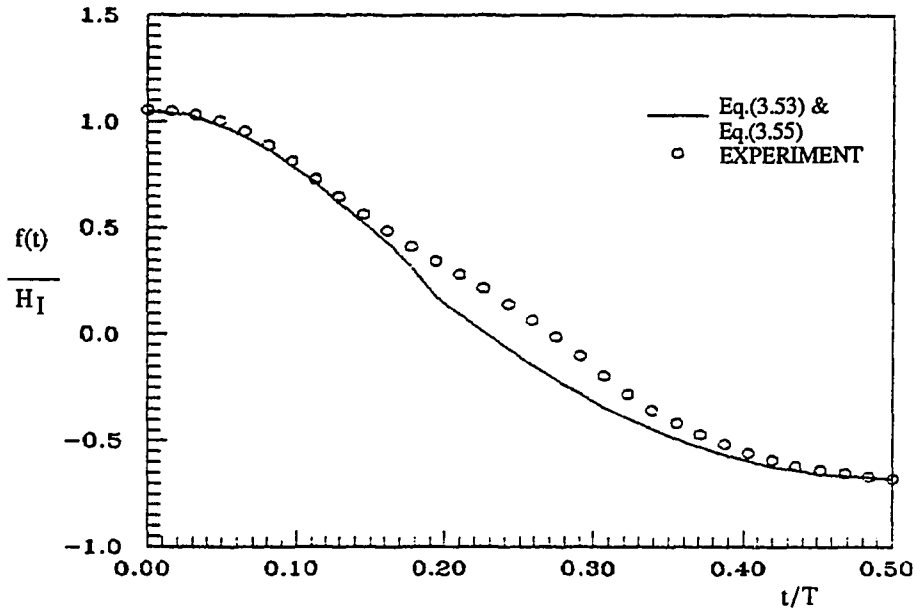

Figure 18 , Time surface displacement (x=0.3cm)
H_c=4.0cm, H_I=14.69cm, T=1.2sec

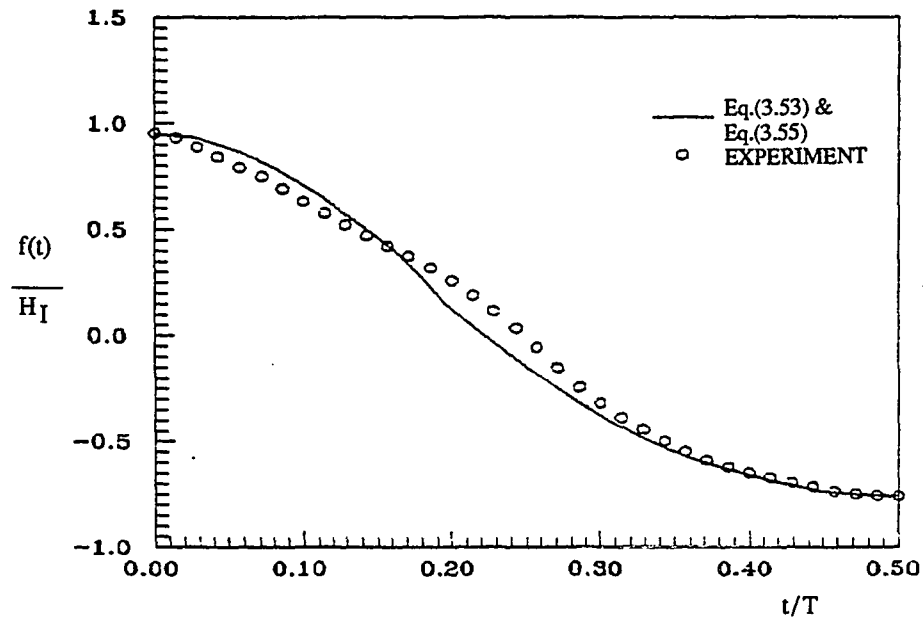

Figure 19 , Time surface displacement (x=0.3cm)
H_c=4.0cm, H_I=12.16cm, T=1.4sec

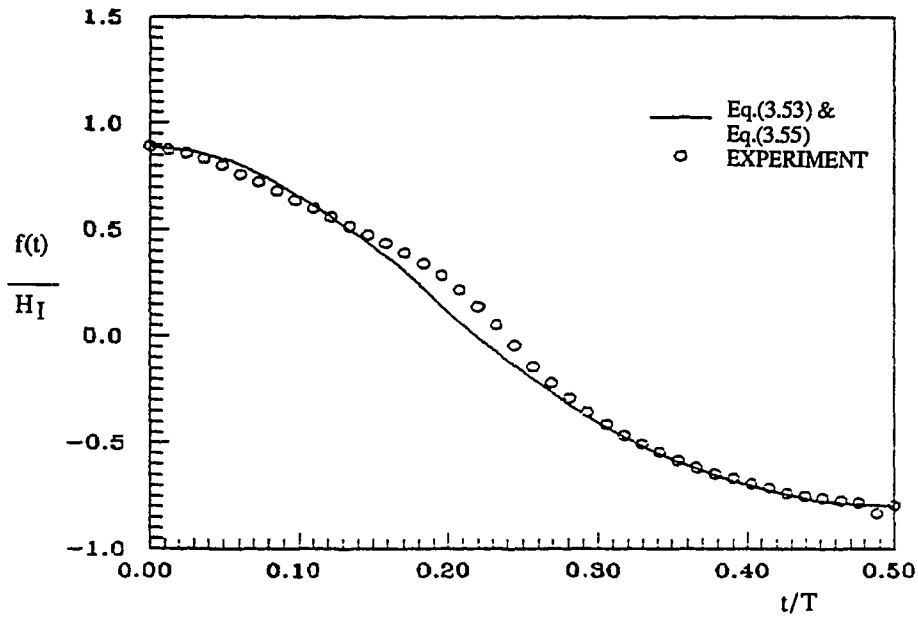

Figure 20 , Time surface displacement (x=0.3cm)
H_c=4.0cm, H_I=10.26cm, T=1.6sec

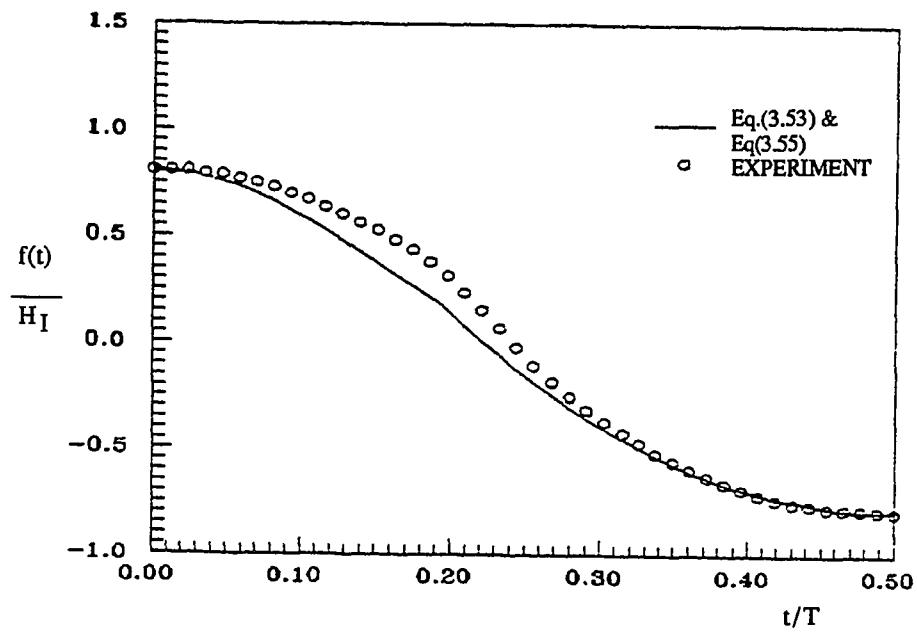

Figure 21 , Time surface displacement (x=0.3cm)
H_c=4.0cm, H_I= 8.53cm, T=1.8sec

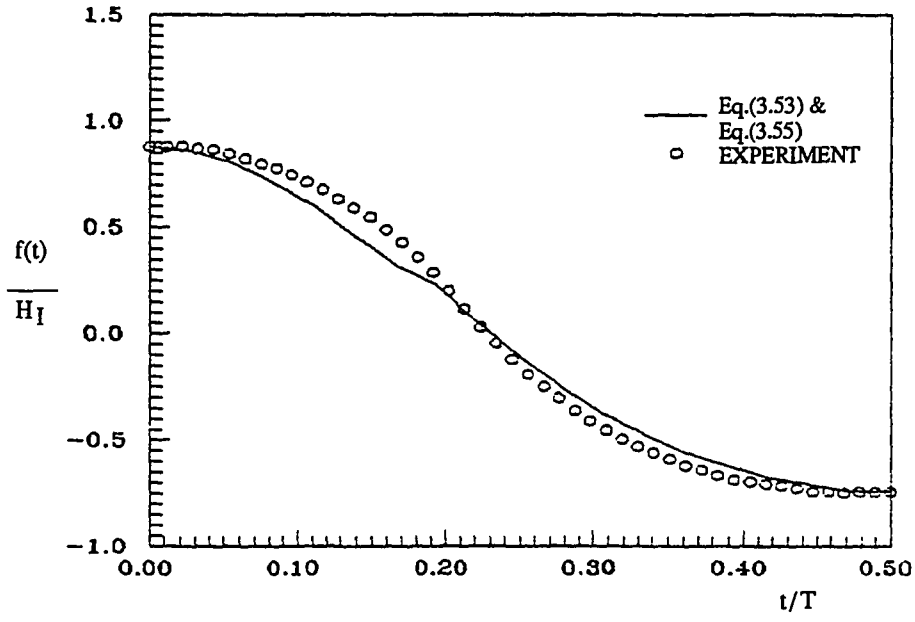

Figure 22 , Time surface displacement (x=0.3cm)
H_c=4.0cm, H_I= 7.21cm, T=2.0sec

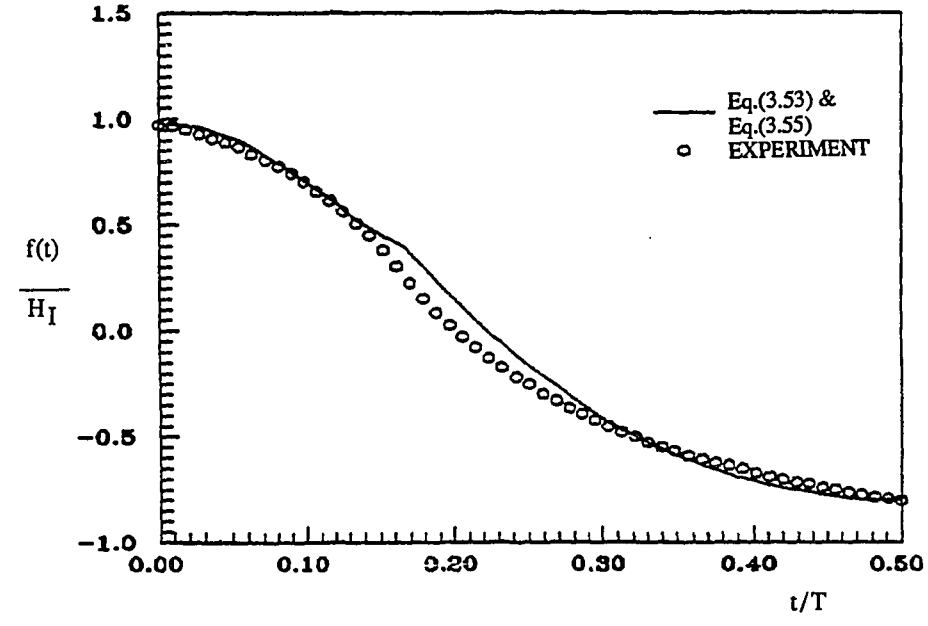

Figure 23 , Time surface displacement (x=0.3cm)
H_c=4.0cm, H_I= 6.48cm, T=2.2sec

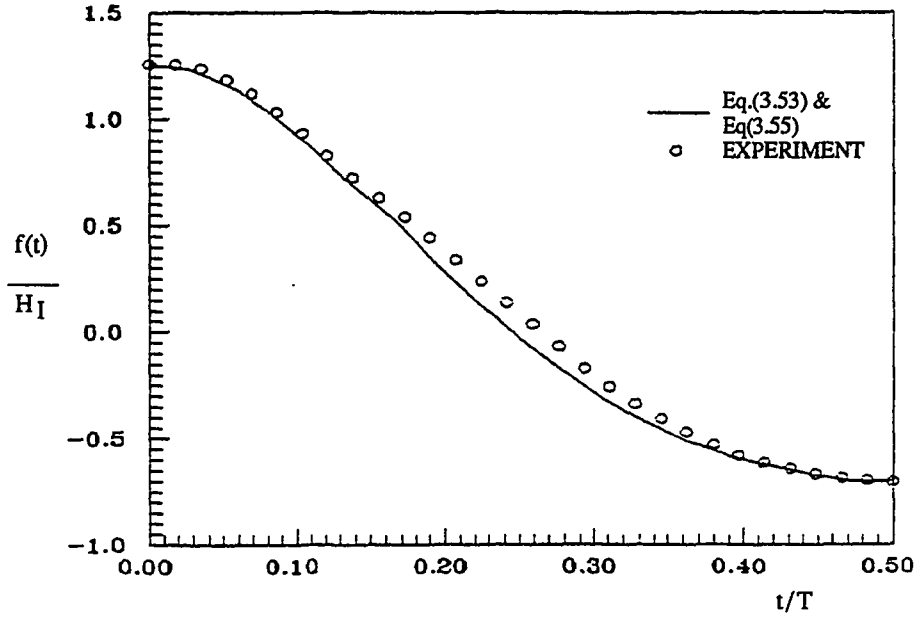

Figure 24 , Time surface displacement (x=0.3cm)
H_c=8.0cm, H_I=14.69cm, T=1.2sec

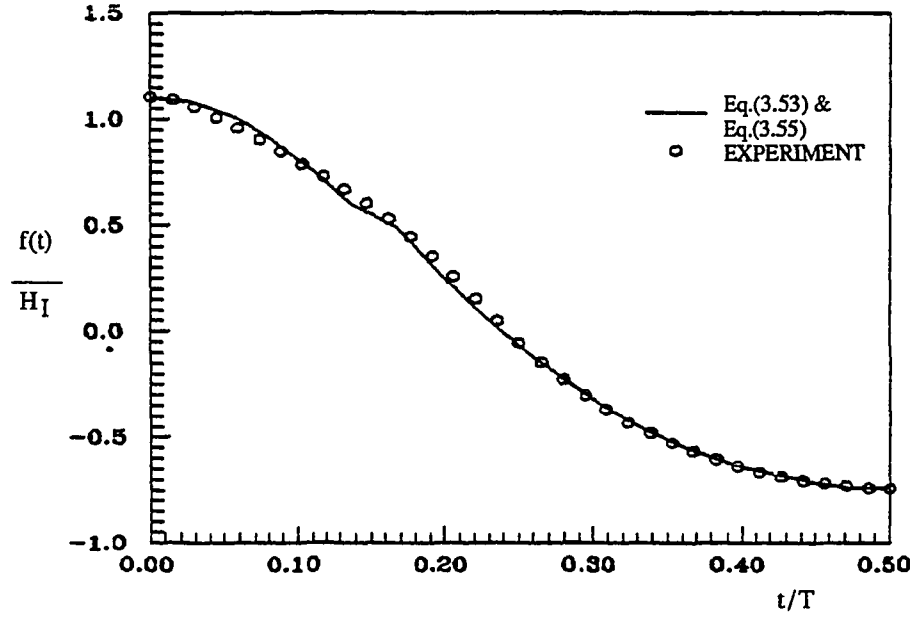

Figure 25 , Time surface displacement (x=0.3cm)
H_c=8.0cm, H_I=12.16cm, T=1.4sec

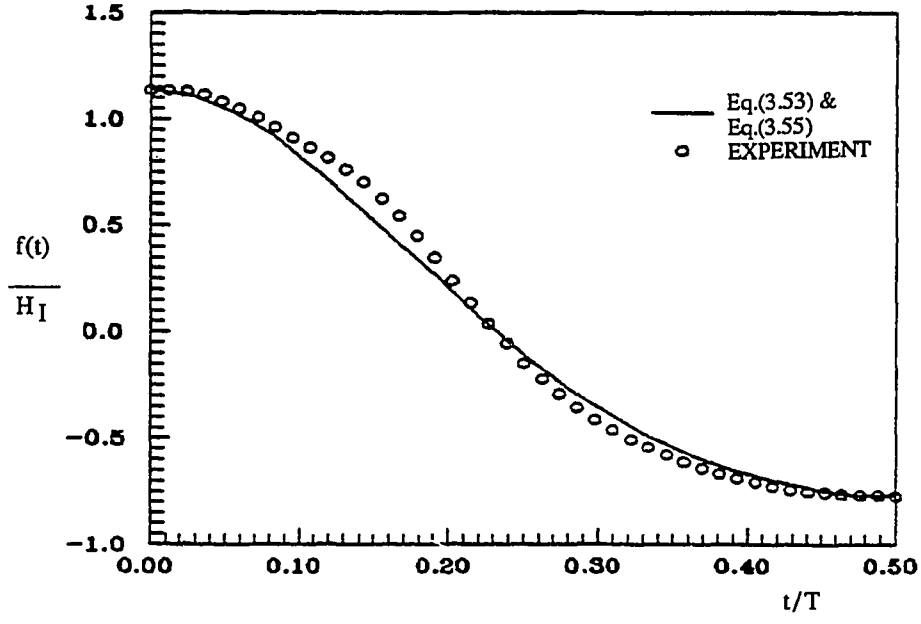

Figure 26 , Time surface displacement (x=0.3cm)
H_c=8.0cm, H_I=10.26cm, T=1.6sec

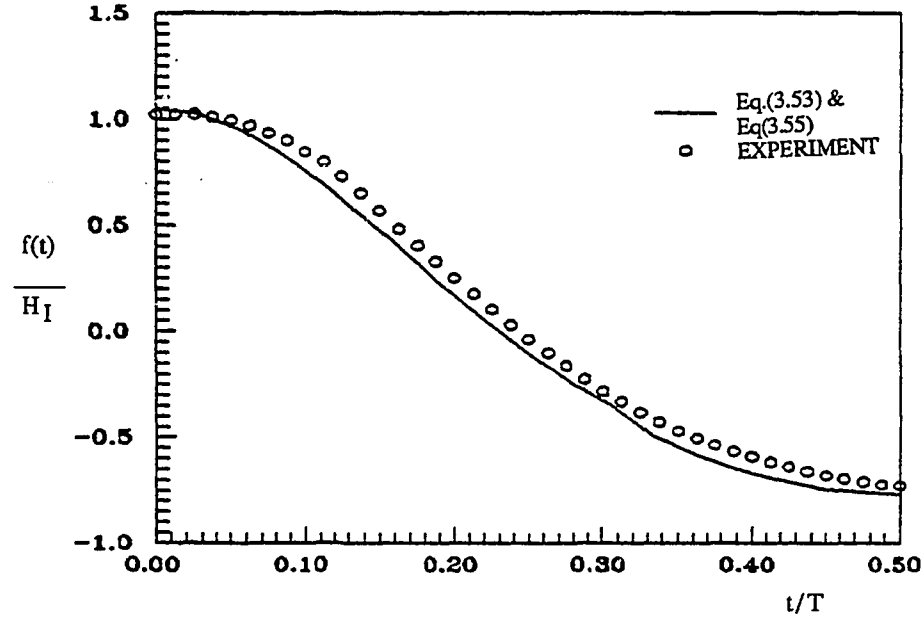

Figure 27 , Time surface displacement (x=0.3cm)
H_c=8.0cm, H_I= 8.53cm, T=1.8sec

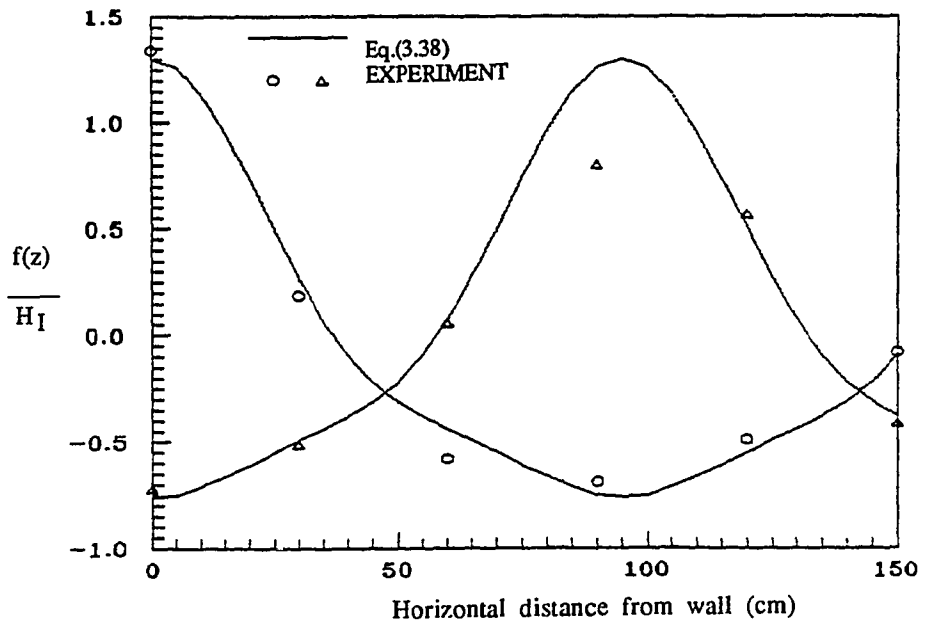

Figure 28 , Spatial surface displacement
H_c=Large, H_I=14.69cm, T=1.2sec

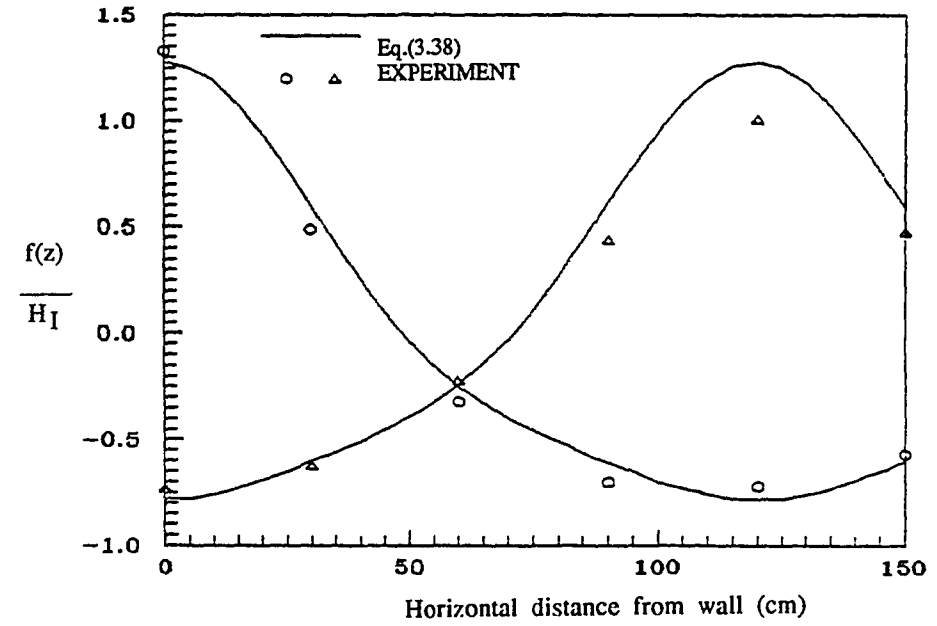

Figure 29 , Spatial surface displacement
H_c=Large, H_I=12.16cm, T=1.4sec

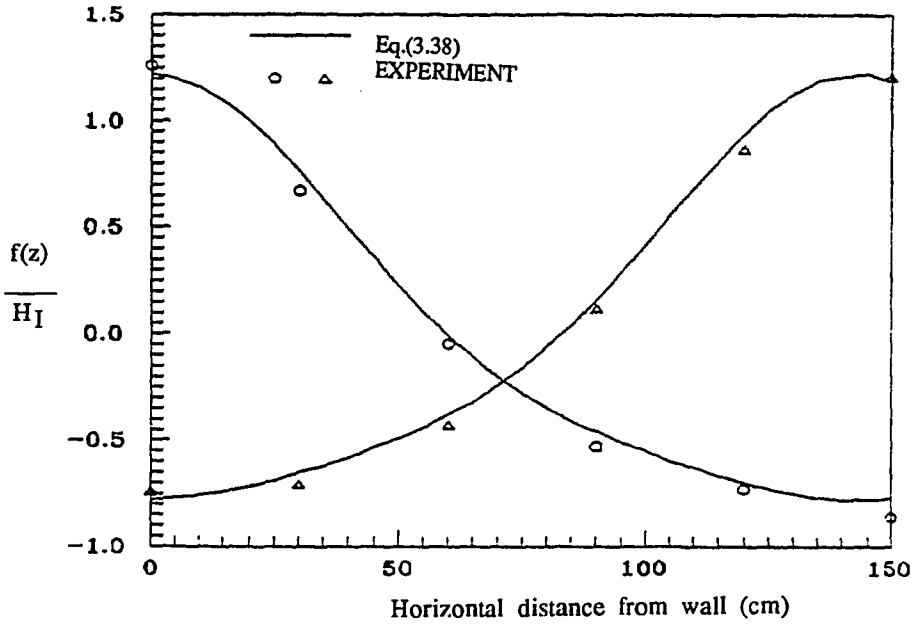

Figure 30 , Spatial surface displacement
H_c=Large, H_I=10.26cm, T=1.6sec

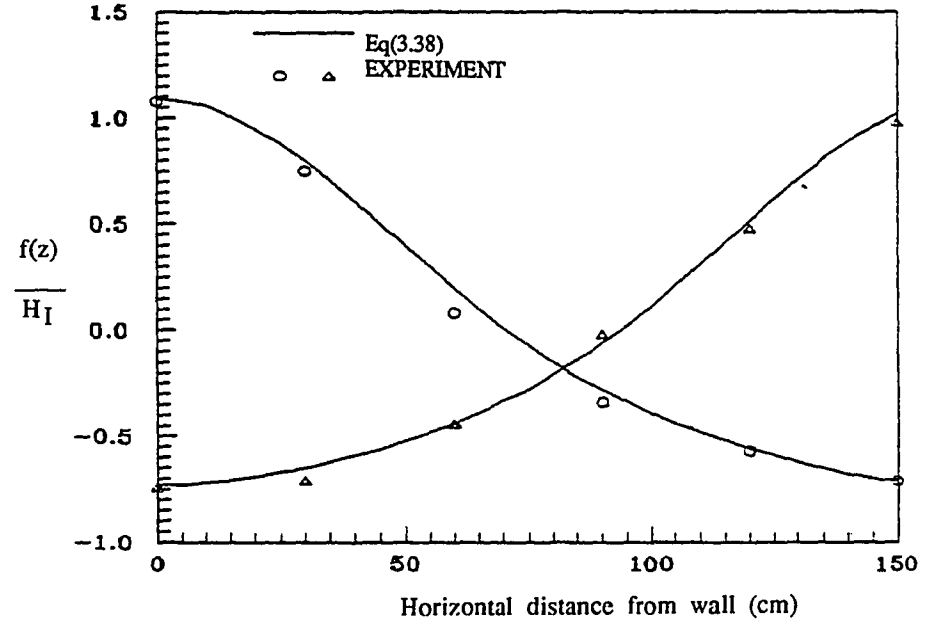

Figure 31 , Spatial surface displacement
H_c=Large, H_I= 8.53cm, T=1.8sec

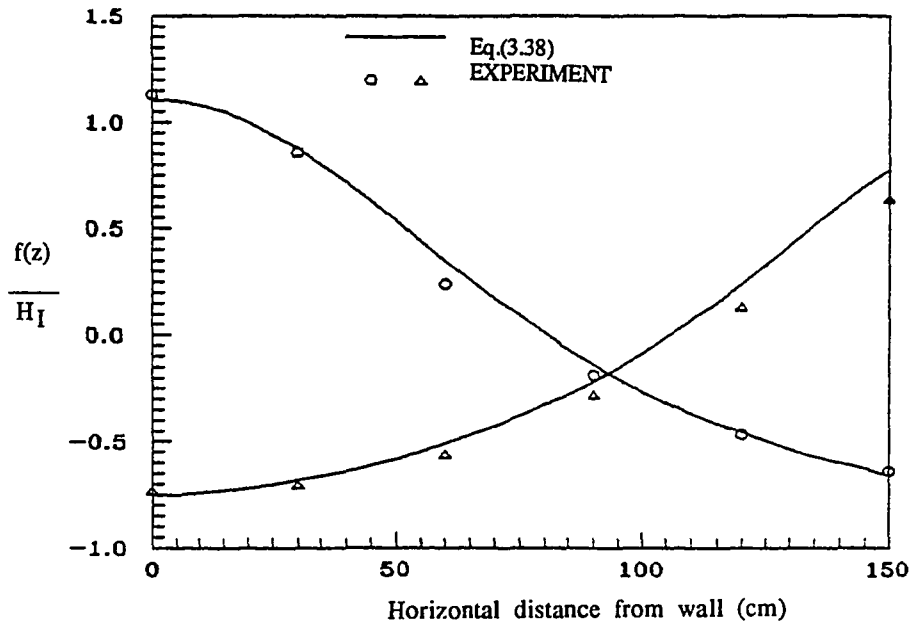

Figure 32 , Spacial surface displacement
H_c=Large, H_I= 7.21cm, T=2.0sec

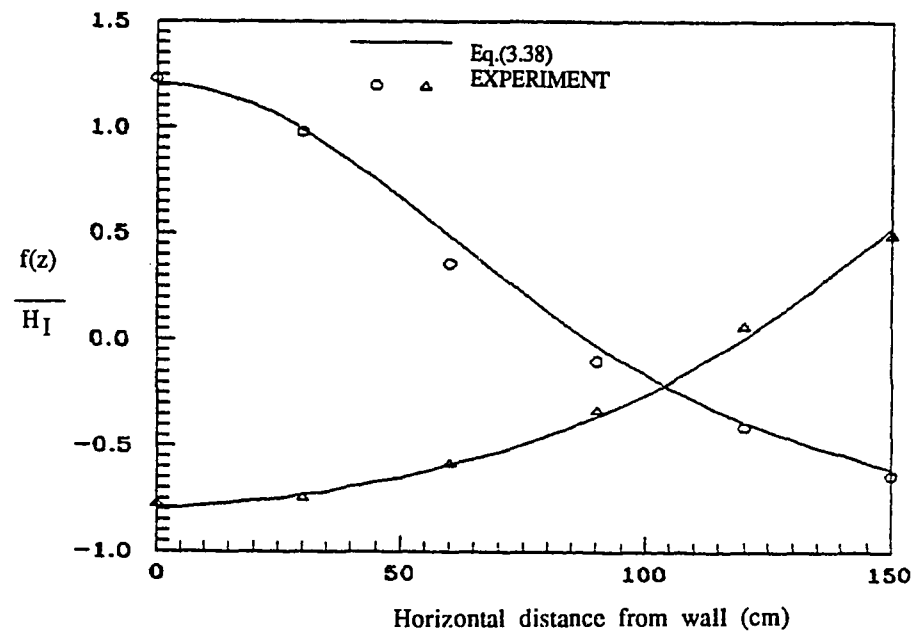

Figure 33 , Spatial surface displacement
H_c=Large, H_I= 6.48cm, T=2.2sec

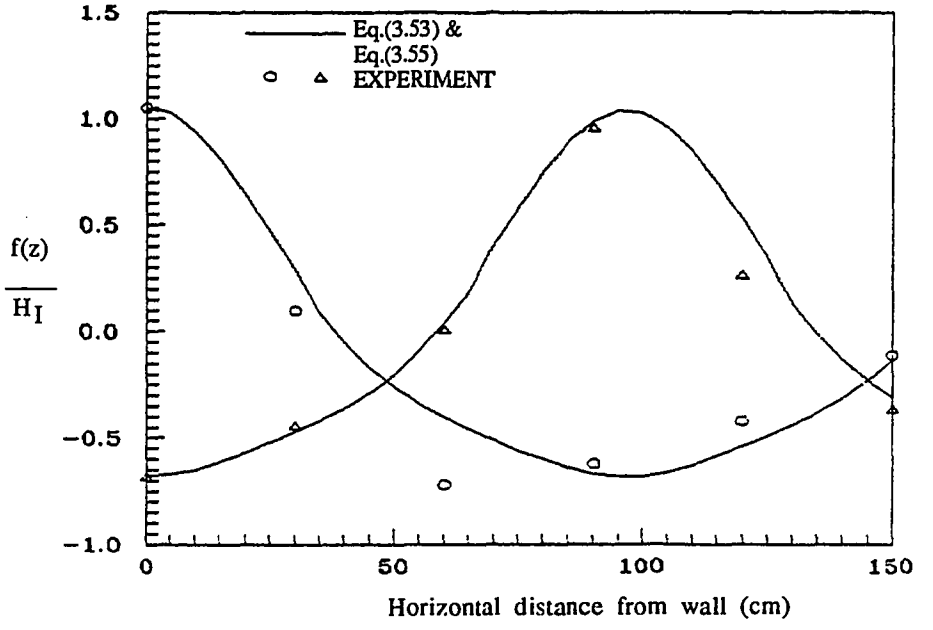

Figure 34 , Spatial surface displacement
H_c=4.0cm, H_I=14.69cm, T=1.2sec

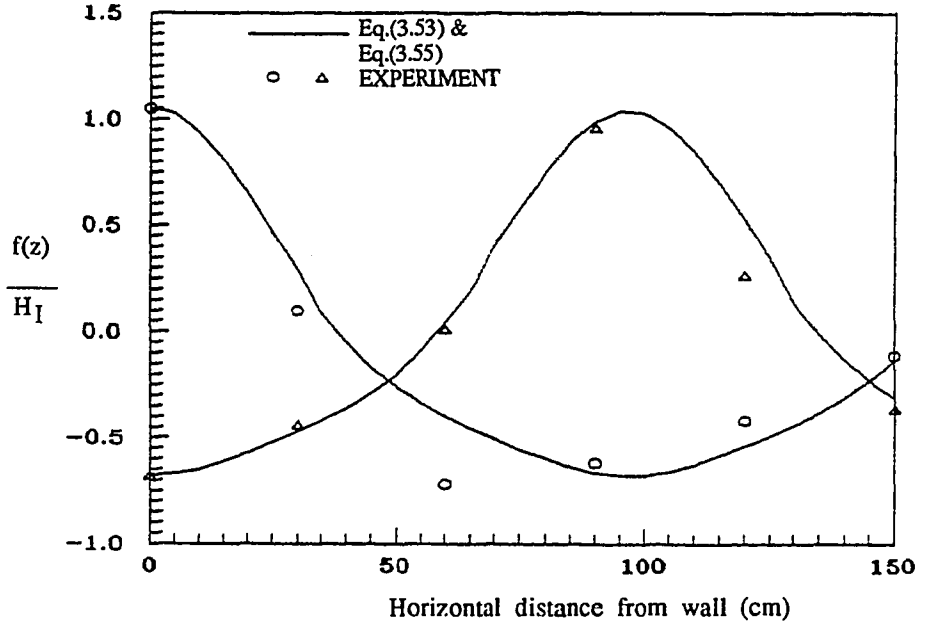

Figure 35 , Spatial surface displacement
H_c=4.0cm, H_I=12.16cm, T=1.4sec

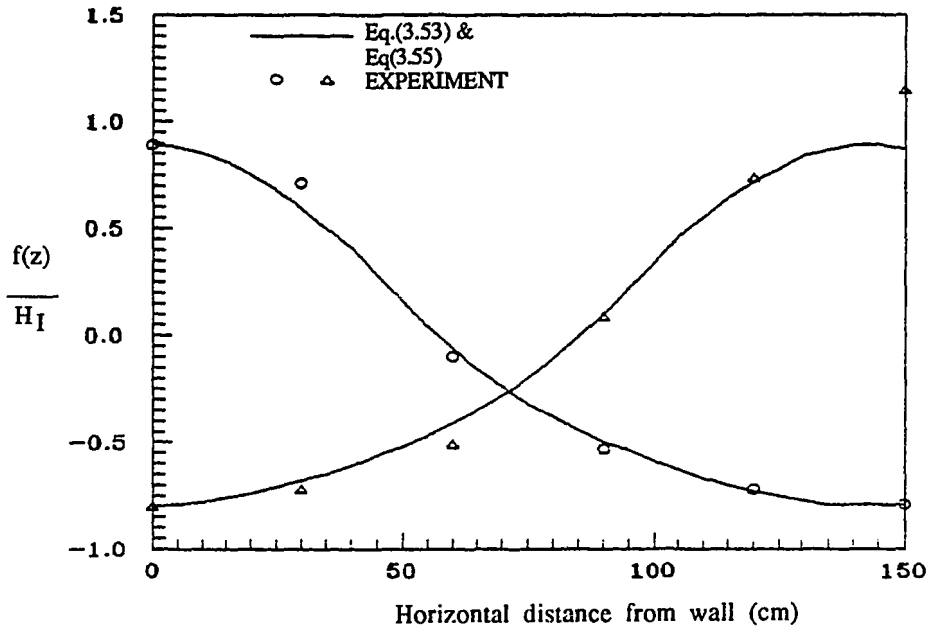

Figure 36 , Spatial surface displacement
H_c=4.0cm, H_I=10.26cm, T=1.6sec

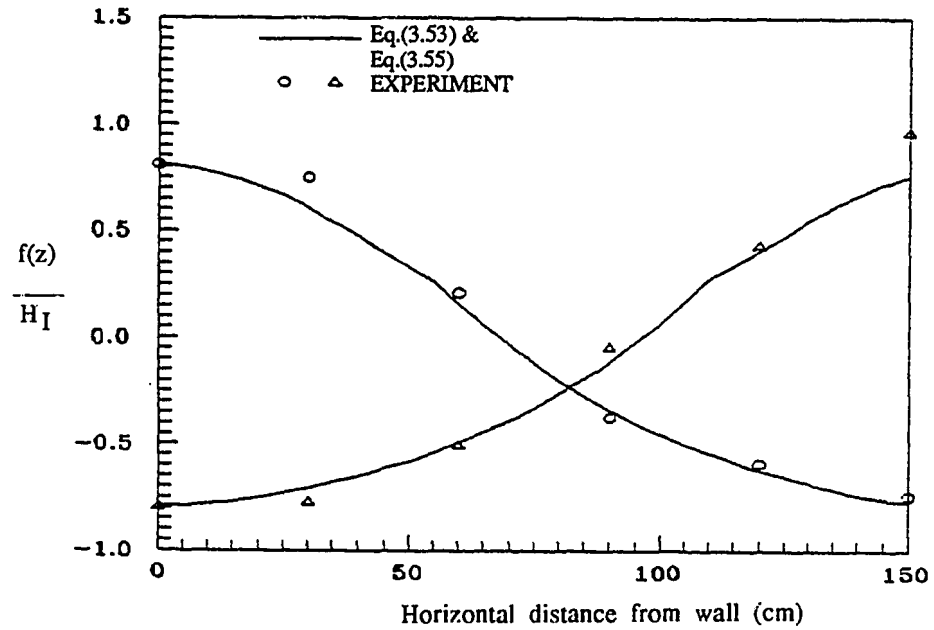

Figure 37 , Spatial surface displacement
H_c=4.0cm, H_I= 8.53cm, T=1.8sec

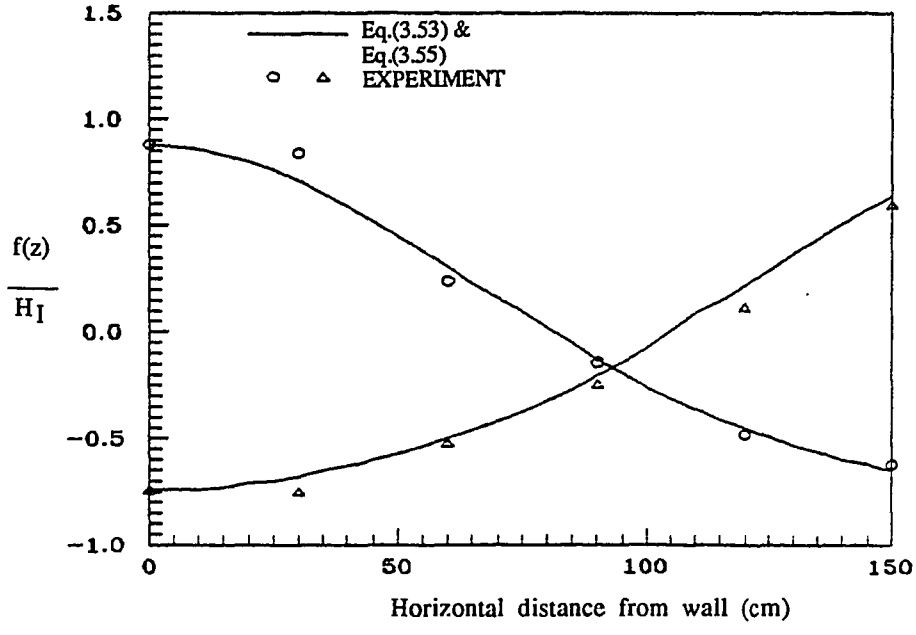

Figure 38 , Spatial surface displacement
H_c=4.0cm, H_I= 7.21cm, T=2.0sec

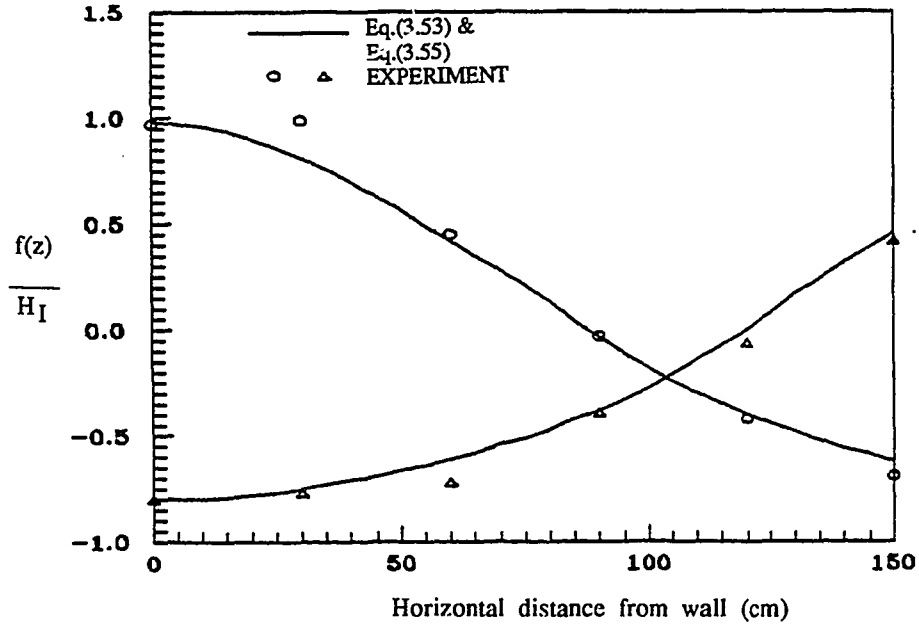

Figure 39 , Spatial surface displacement
H_c=4.0cm, H_I= 6.48cm, T=2.2sec

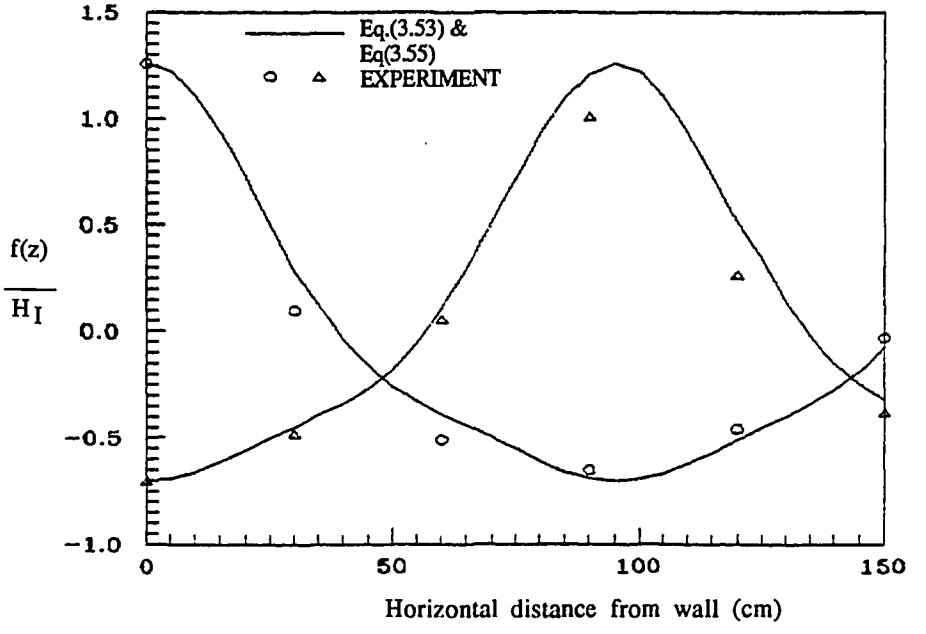

Figure 40 , Spatial surface displacement
H_c=8.0cm, H_I=14.69cm, T=1.2sec

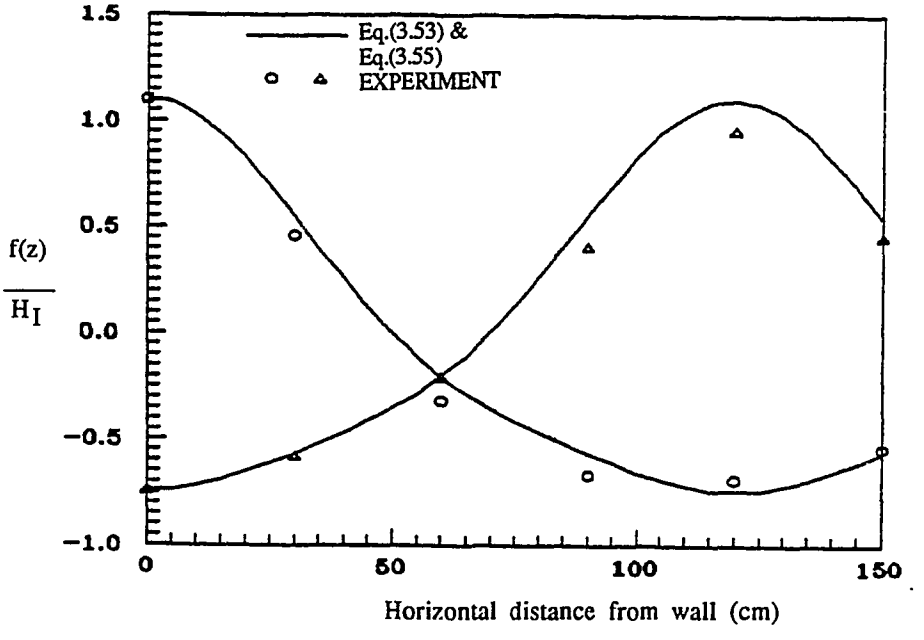

Figure 41 , Spacial surface displacement
H_c=8.0cm, H_I=12.16cm, T=1.4sec

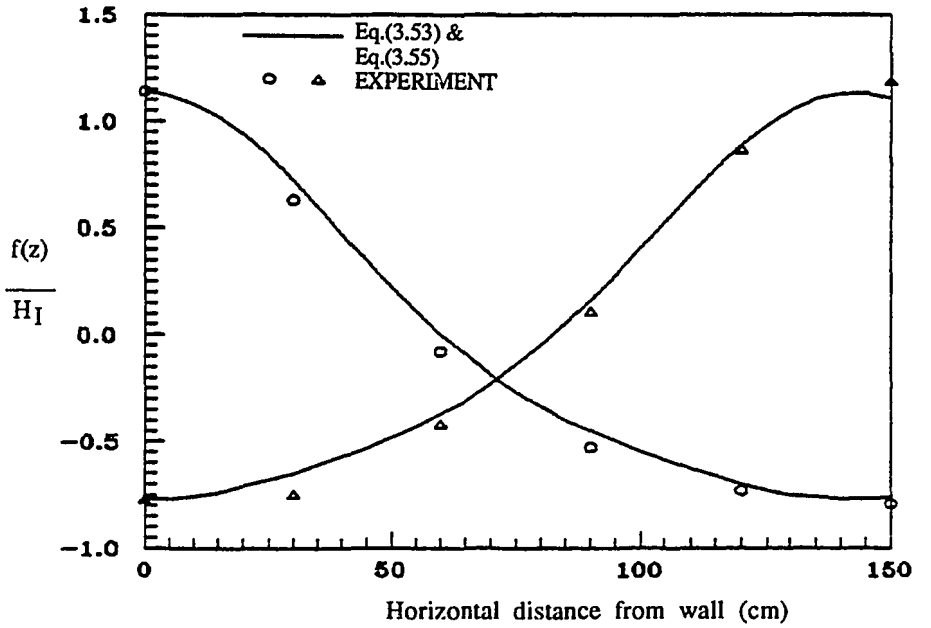

Figure 42 , Spacial surface displacement
H_c=8.0cm, H_I=10.26cm, T=1.6sec

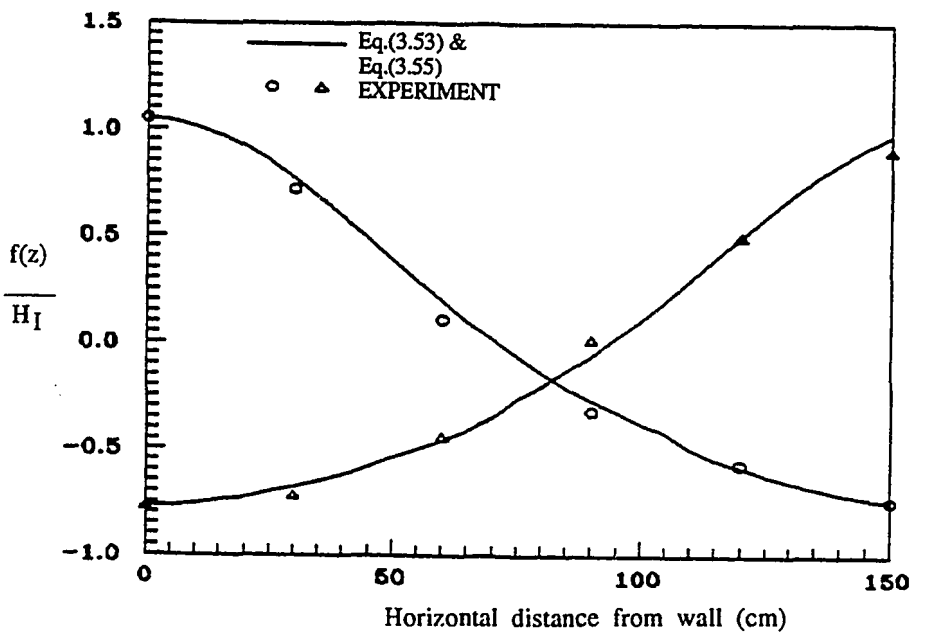

Figure 43 , Spatial surface displacement
H_c=8.0cm, H_I= 8.53cm, T=1.8sec

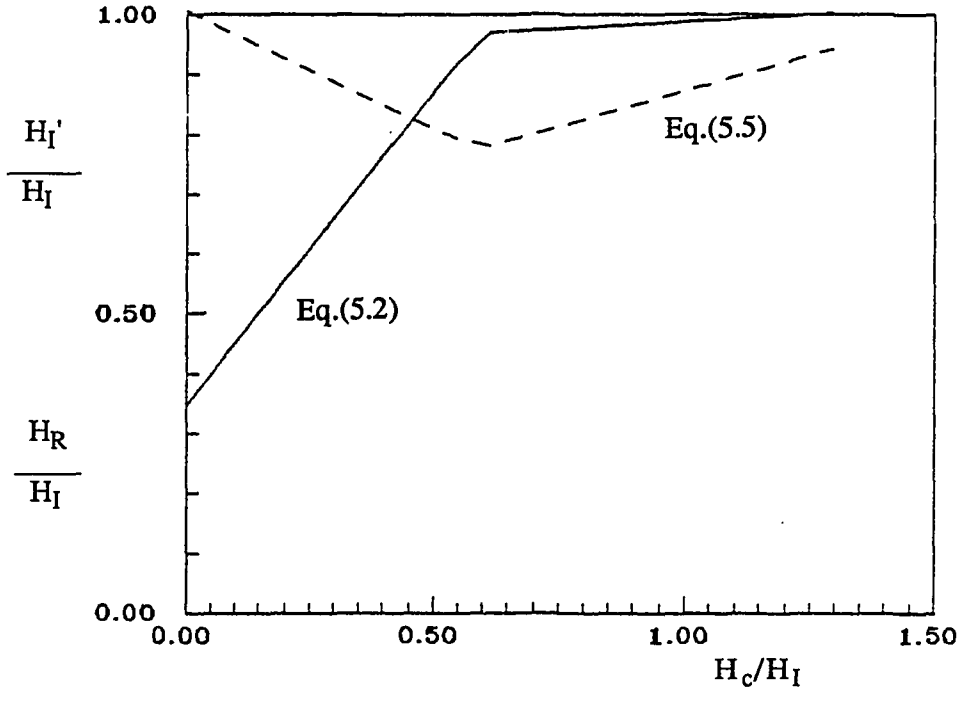

Figure 44 , Reflection coefficient and change of incident wave height H_I=14.69cm, T=1.2sec

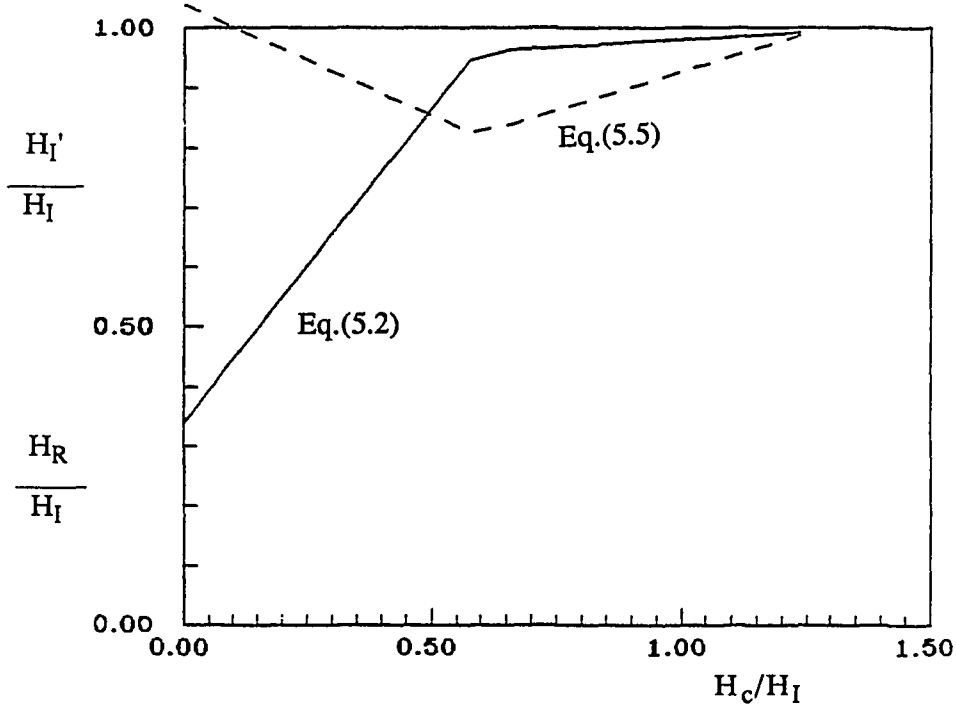

Figure 45 , Reflection coefficient and change of incident wave height H_I=12.16cm, T=1.4sec

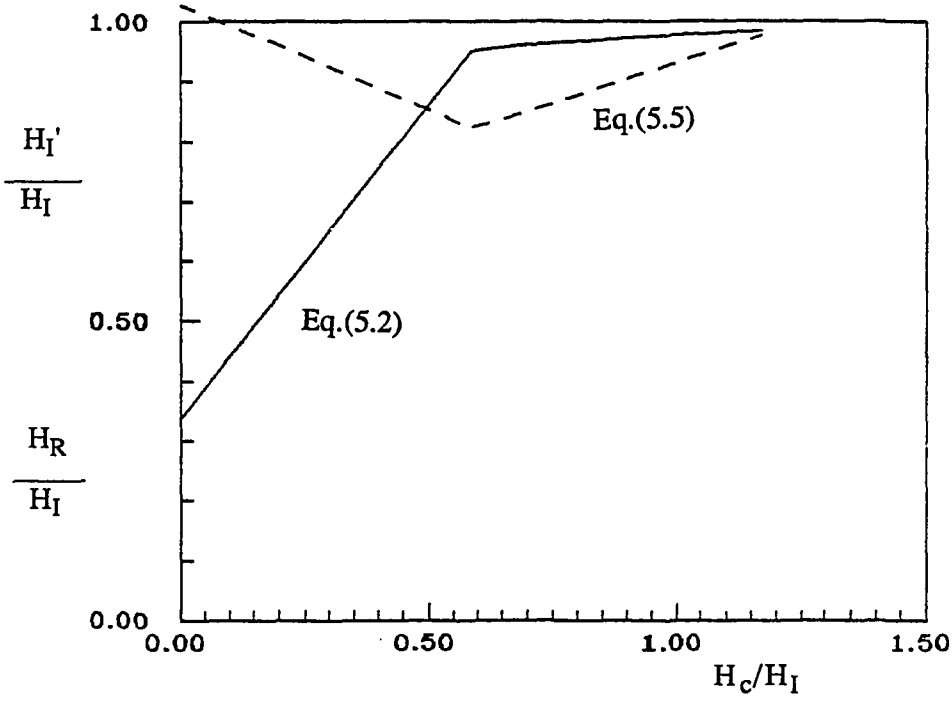

Figure 46 , Reflection coefficient and change of incident wave height H_I=10.26cm, T=1.6sec

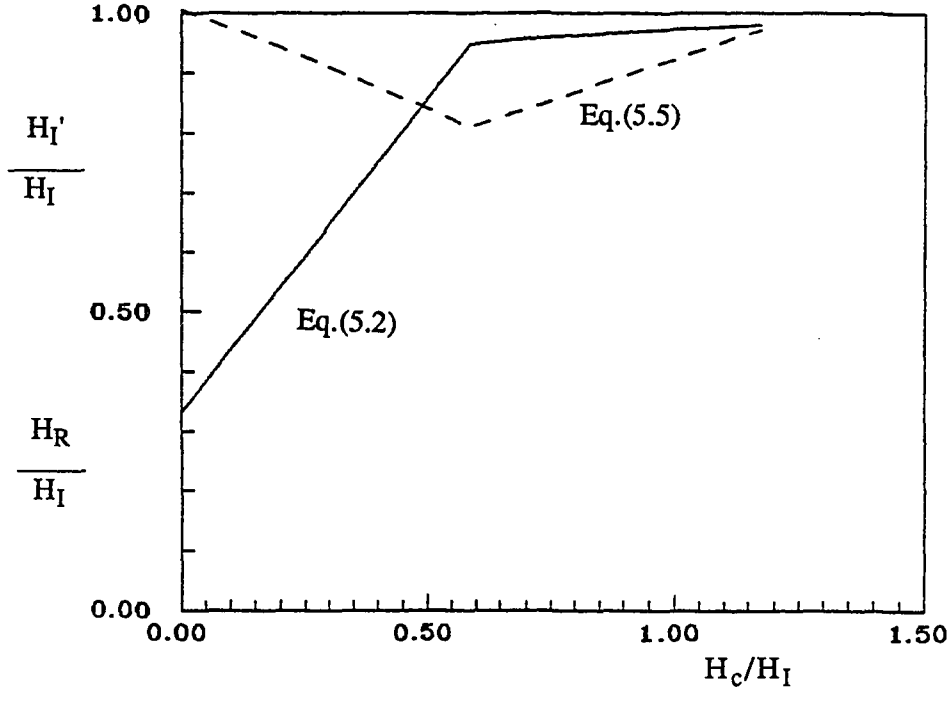

Figure 47 , Reflection coefficient and change of incident wave height H_I= 8.53cm, T=1.8sec

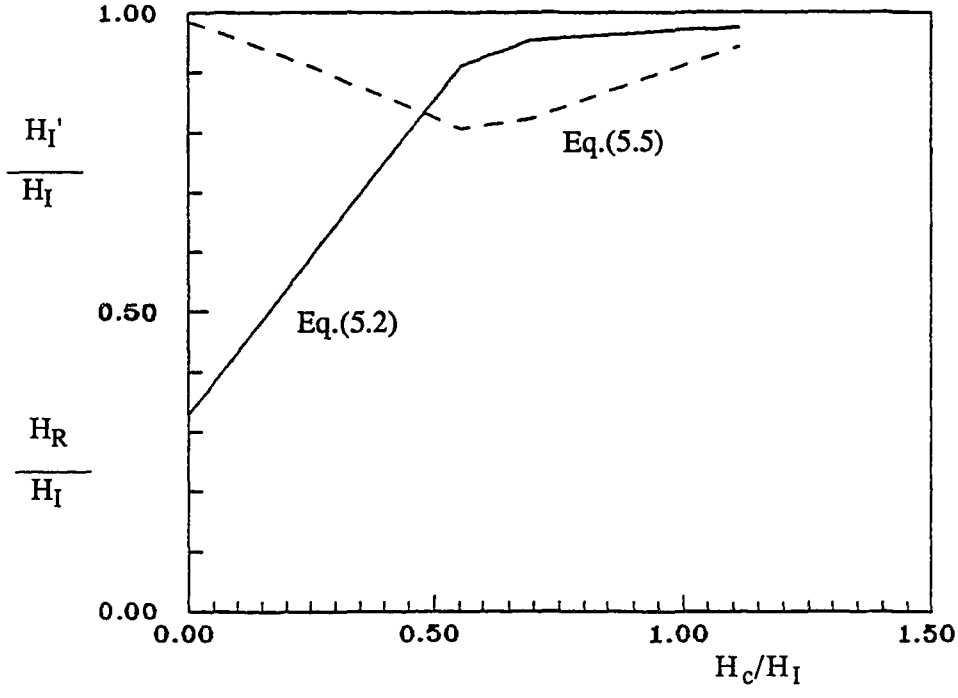

Figure 48 , Reflection coefficient and change of incident wave height H_I= 7.21cm, T=2.0sec

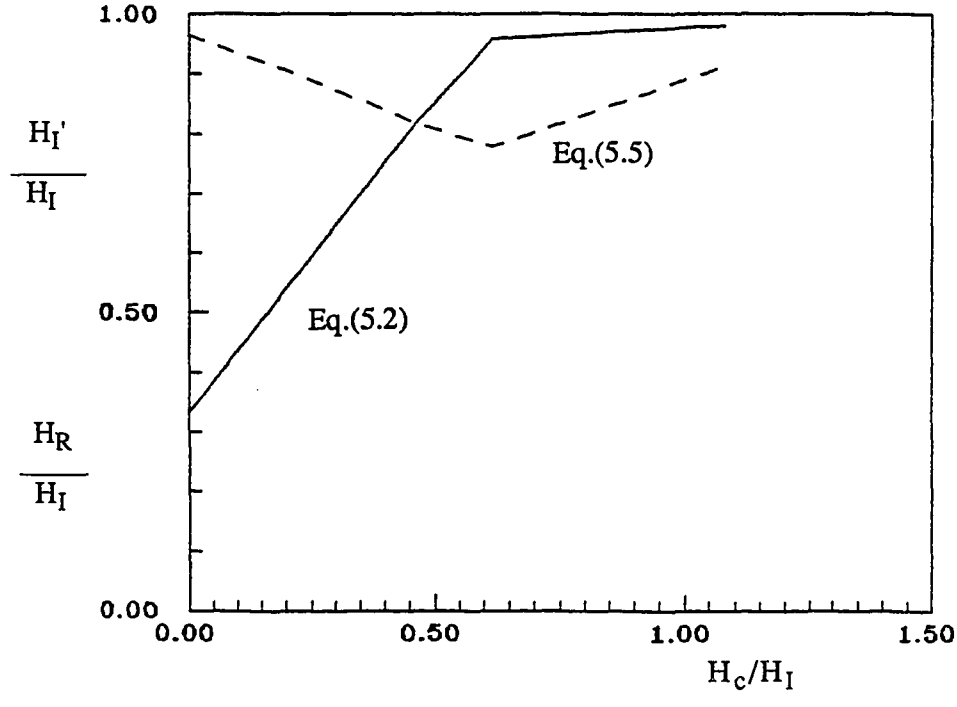

Figure 49 , Reflection coefficient and change of incident wave height H_I= 6.48cm, T=2.2sec

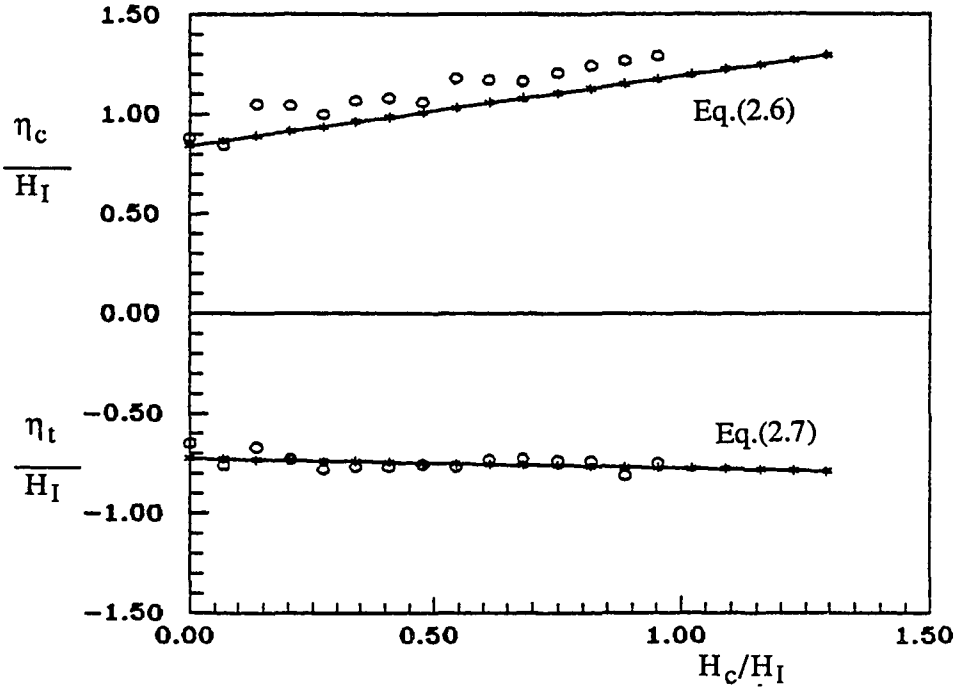

Figure 50 , Wave crest and trough levels
H_I=14.69cm, T=1.2sec

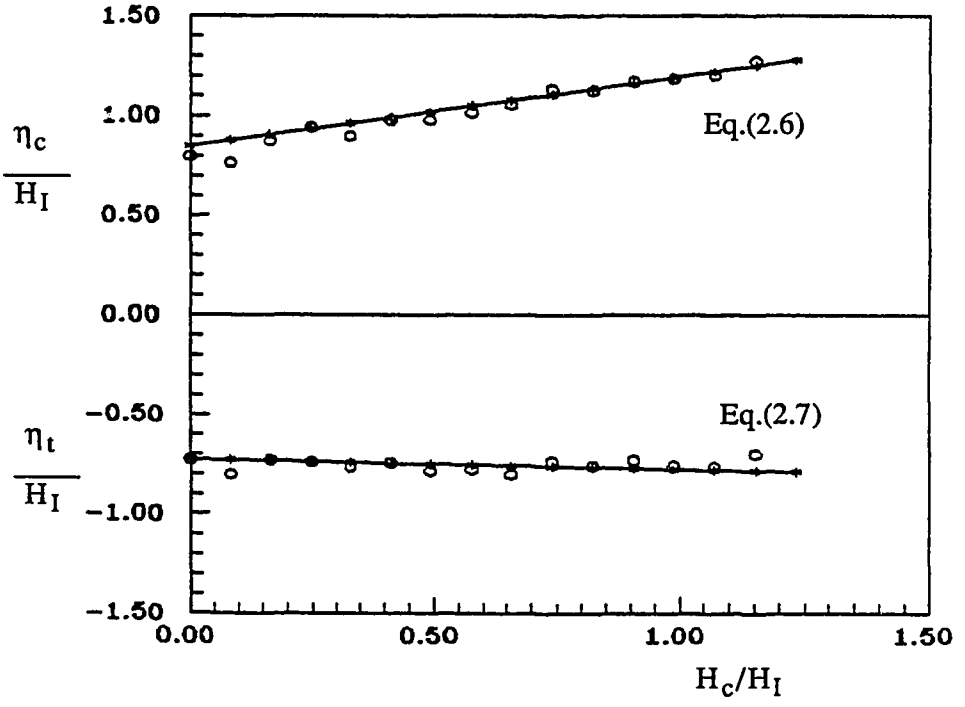

Figure 51 , Wave crest and trough levels
H_I=12.16cm, T=1.4sec

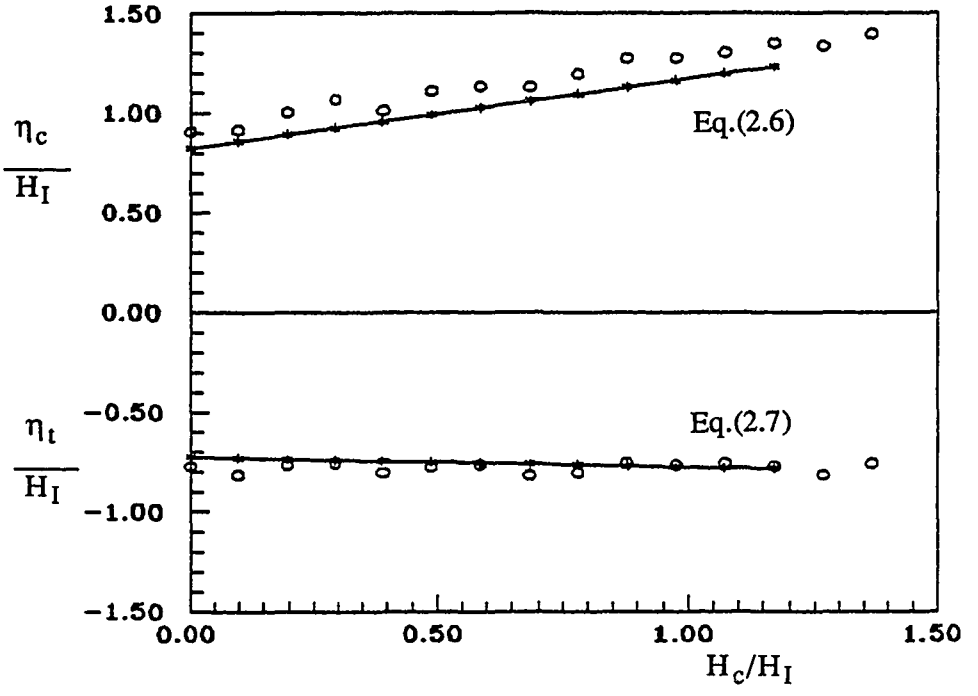

Figure 52 , Wave crest and trough levels
H_I=10.26cm, T=1.6sec

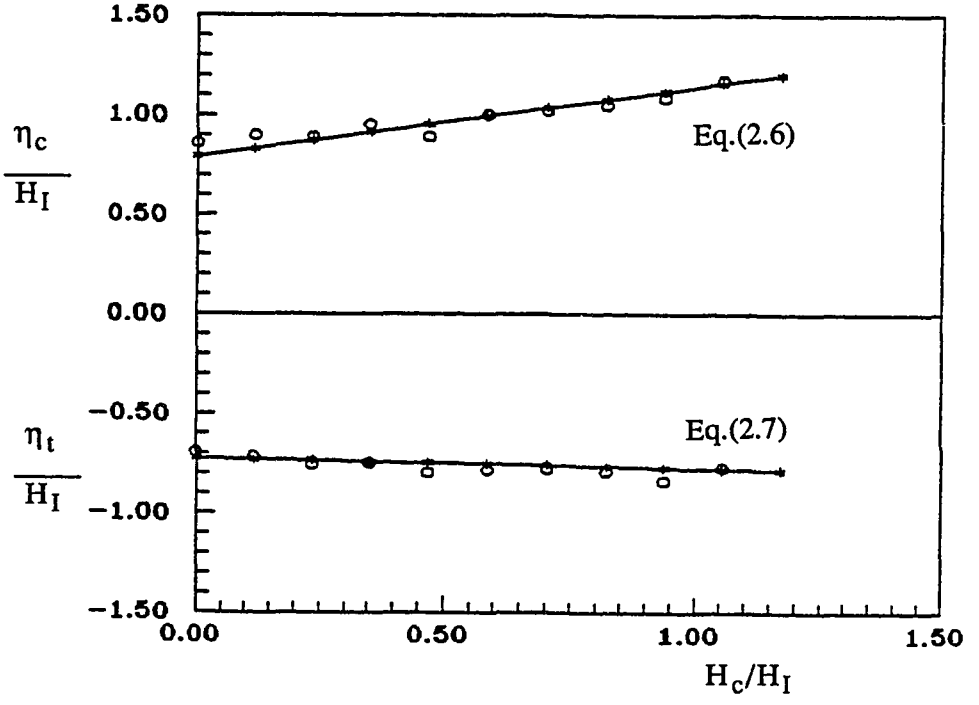

Figure 53 , Wave crest and trough levels
H_I= 8.53cm, T=1.8sec

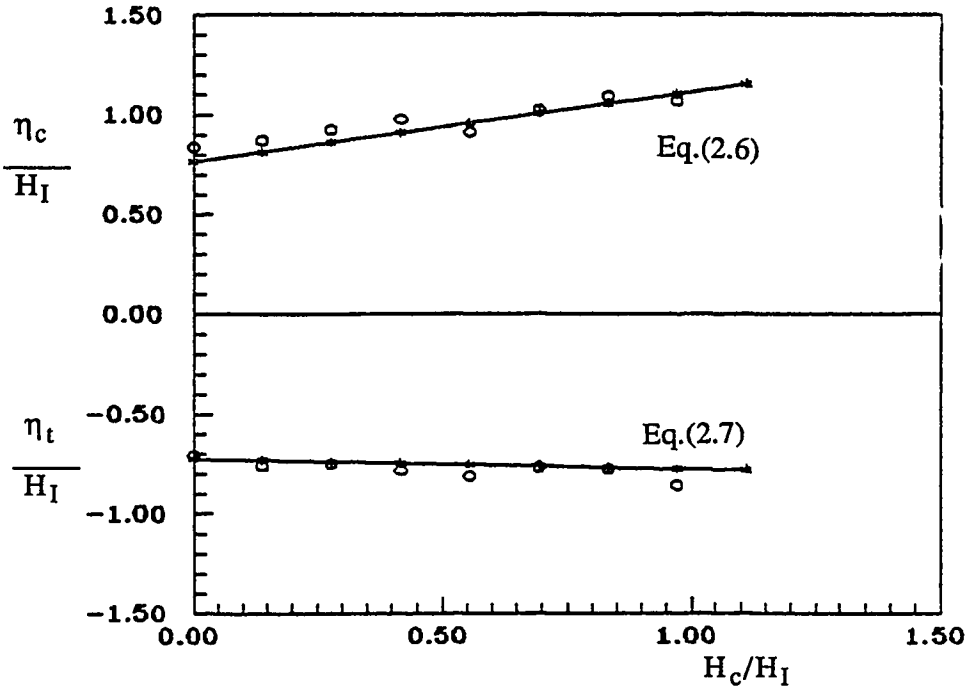

Figure 54 , Wave crest and trough levels
H_I= 7.21cm, T=2.0sec

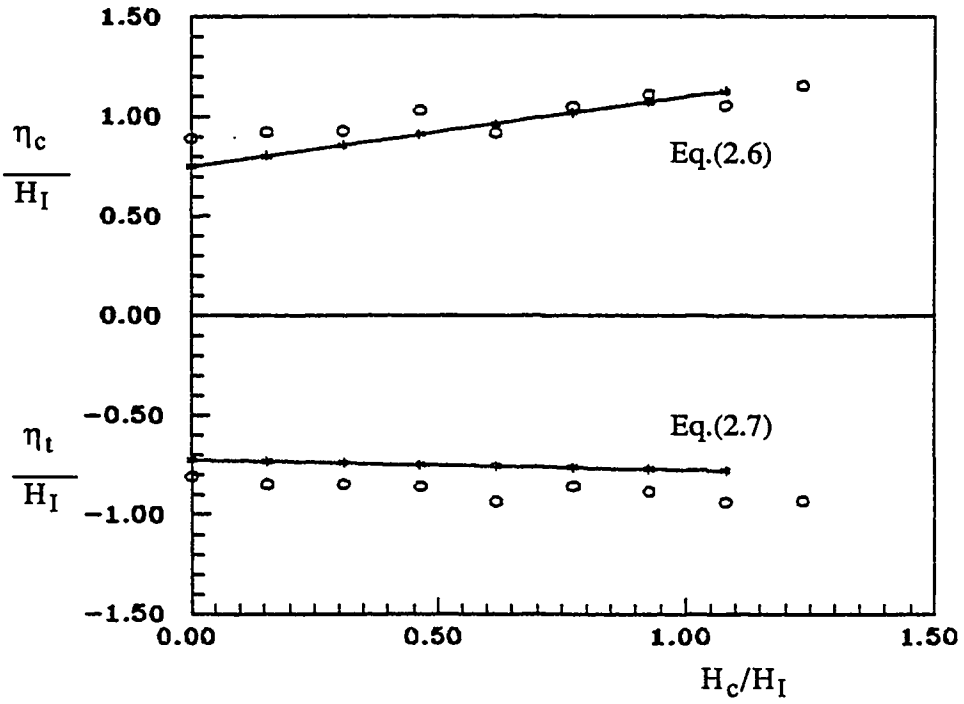

Figure 55 , Wave crest and trough levels
H_I= 6.48cm, T=2.2sec

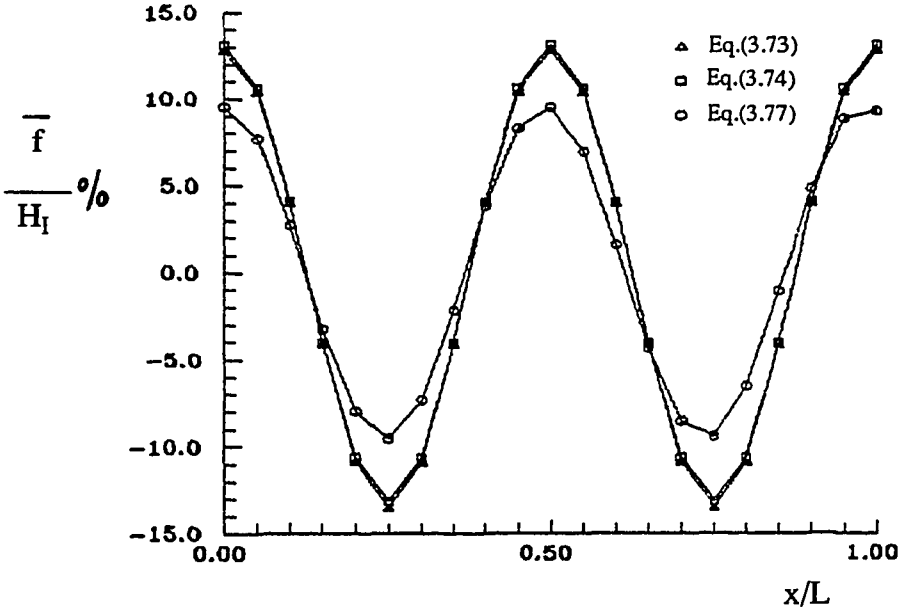

Figure 56 , Distribution of mean water level
H_I=14.69cm, L=193.48cm, h=40cm

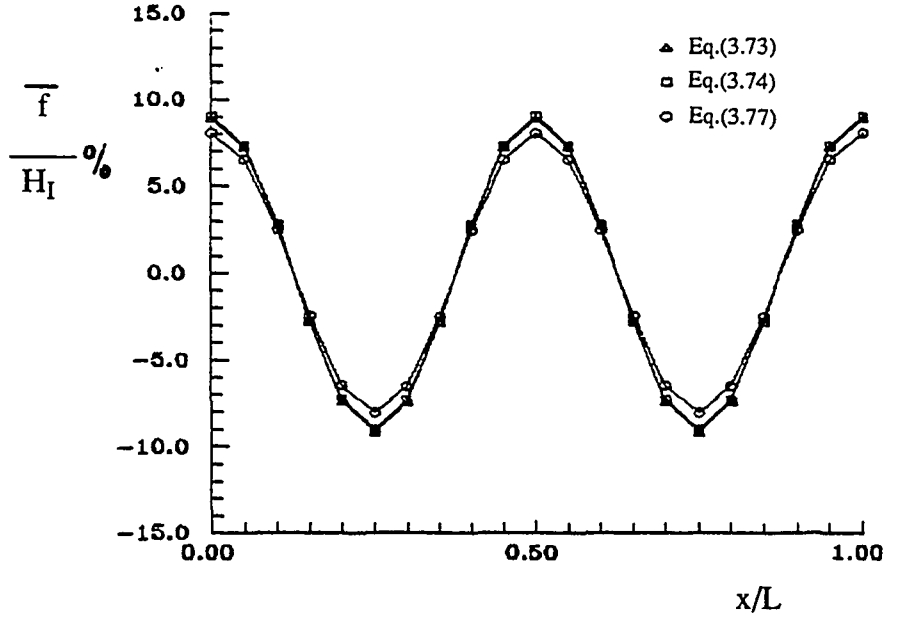

Figure 57 , Distribution of mean water level
H_I=12.16cm, L=239.12cm, h=40cm

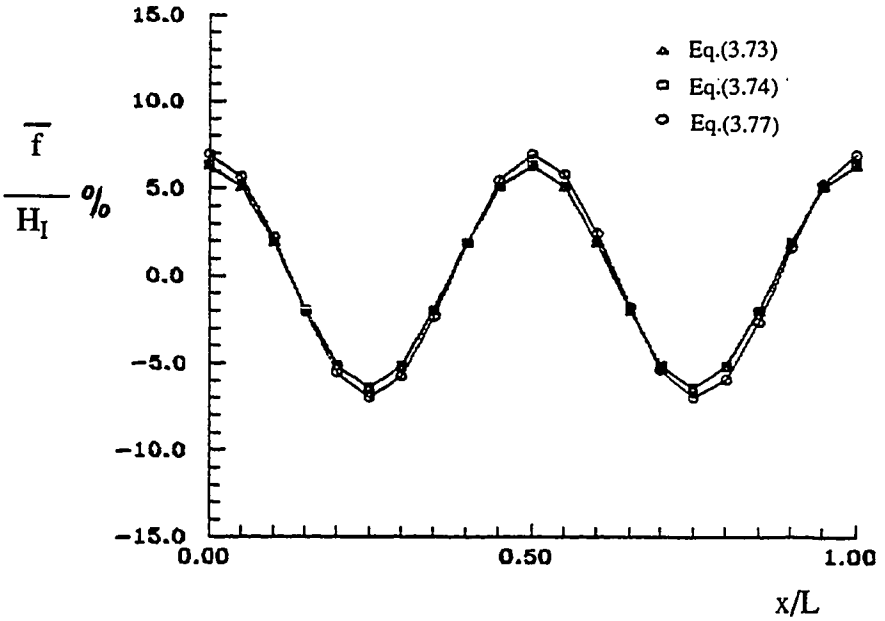

Figure 58 , Distribution of mean water level
H_I=10.26cm, L=283.42cm, h=40cm

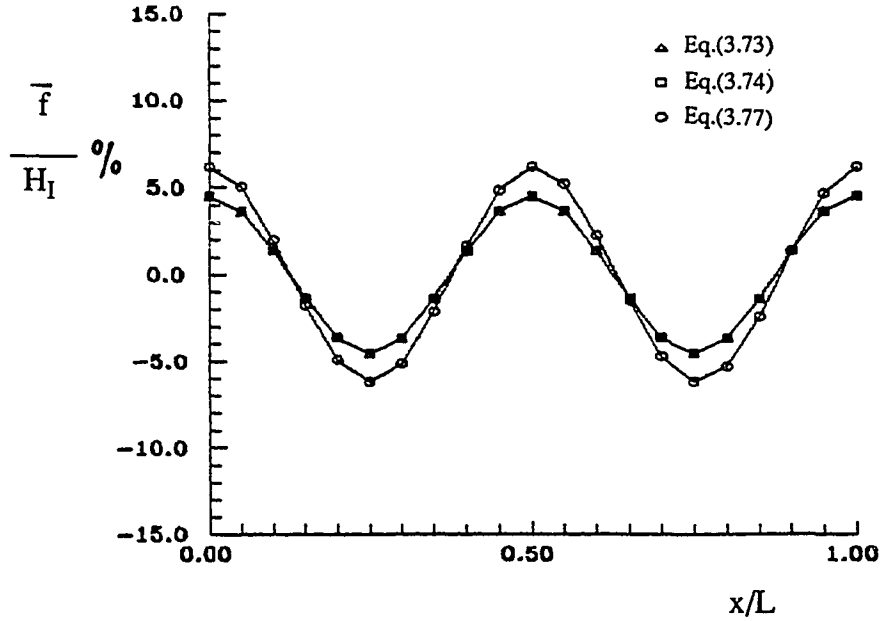

Figure 59 , Distribution of mean water level
H_I= 8.53cm, L=326.71cm, h=40cm

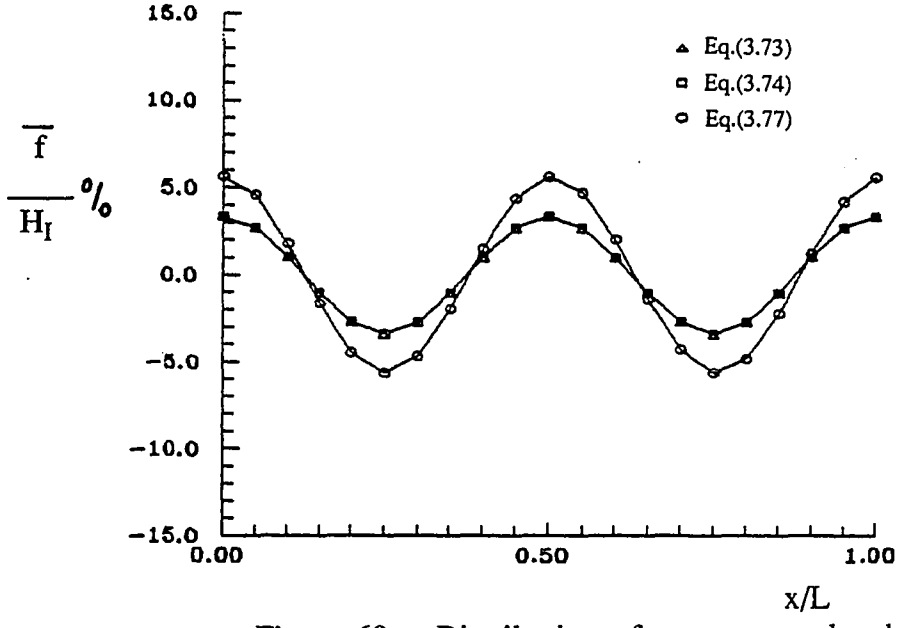

Figure 60 , Distribution of mean water level
H_I= 7.21cm, L=369.28cm, h=40cm

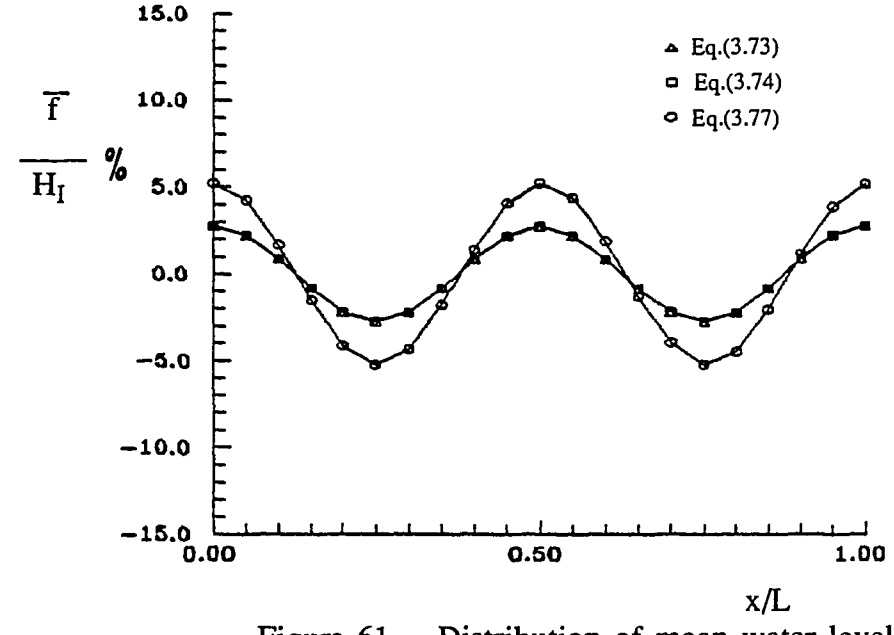

Figure 61 , Distribution of mean water level
H_I= 6.48cm, L=411.31cm, h=40cm

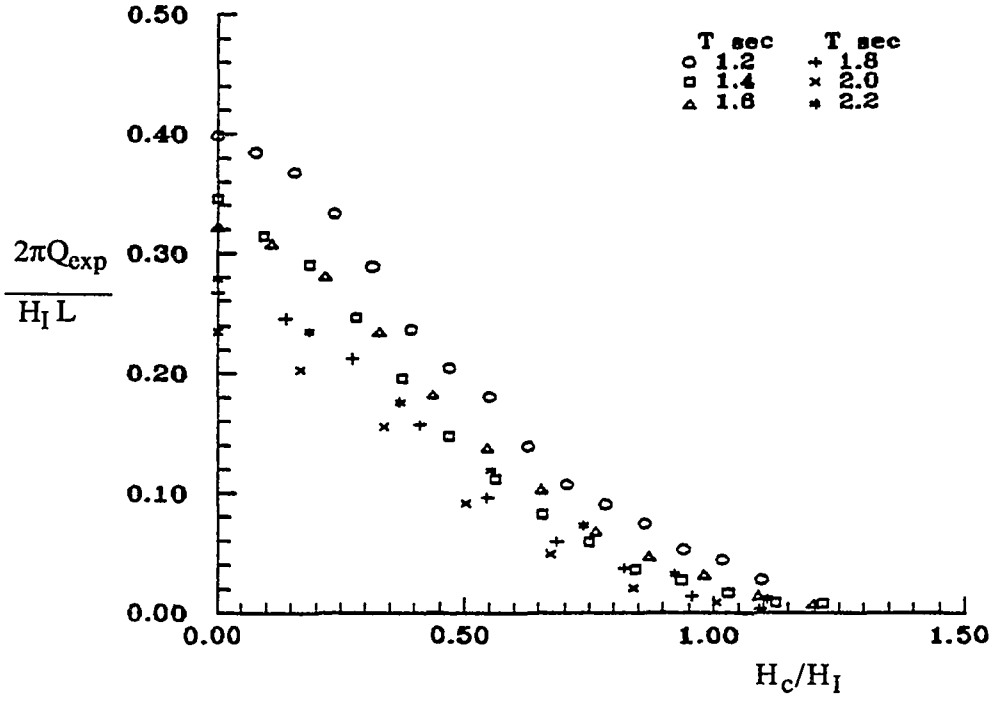

Figure 62 , Volume of overtopping in variable H_c (Case 1)

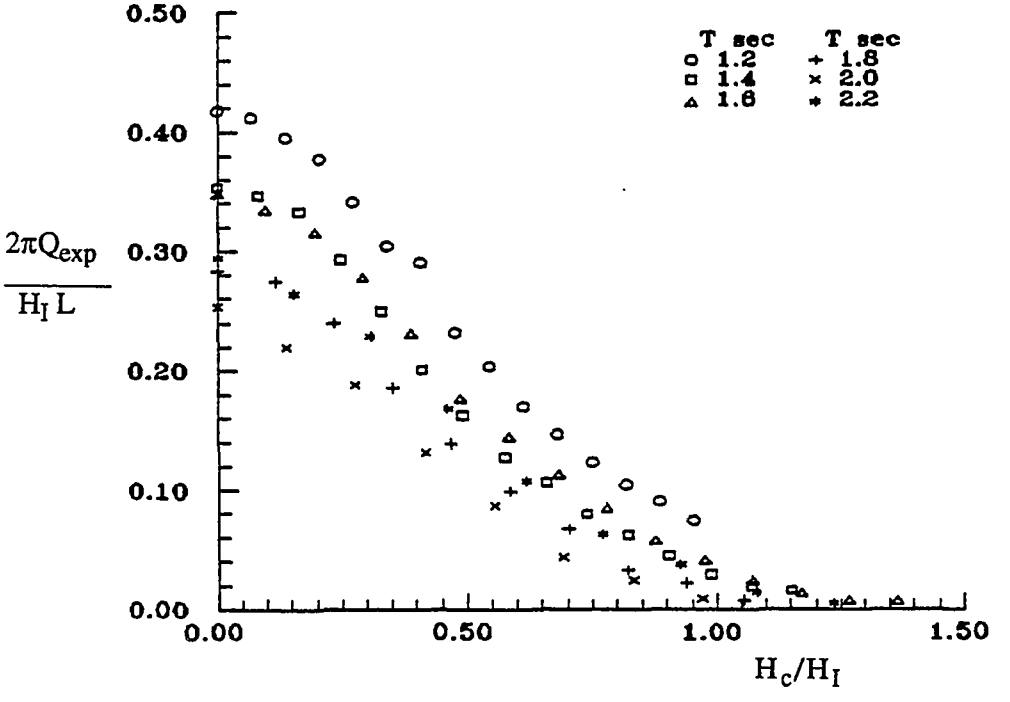

Figure 63 , Volume of overtopping in variable H_c (Case 2)

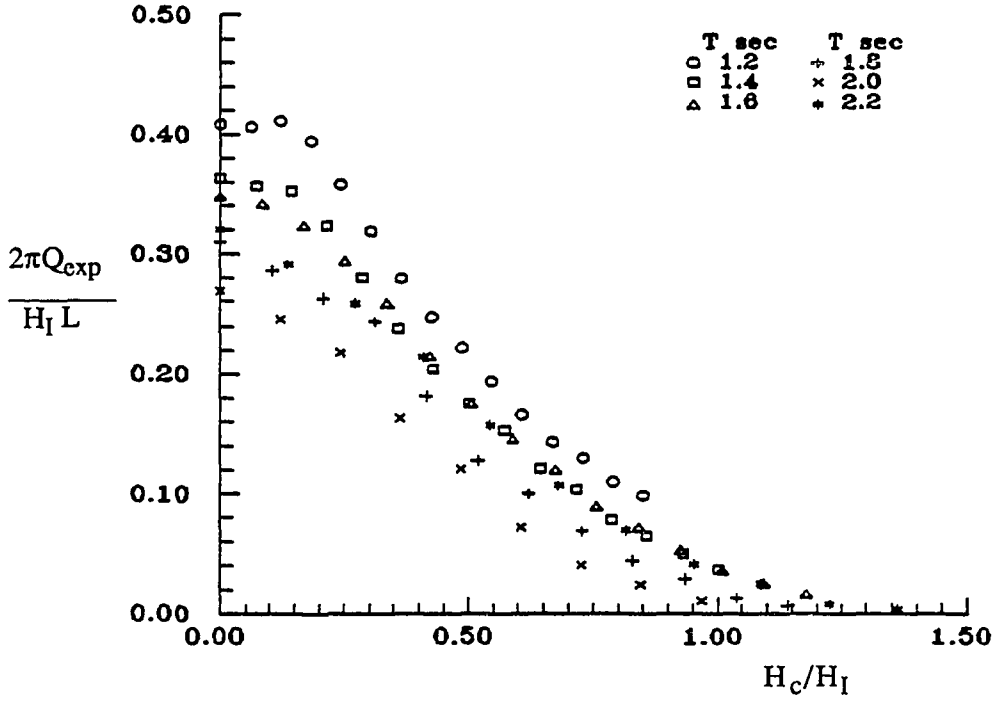

Figure 64 , Volume of overtopping in variable H_c (Case 3)

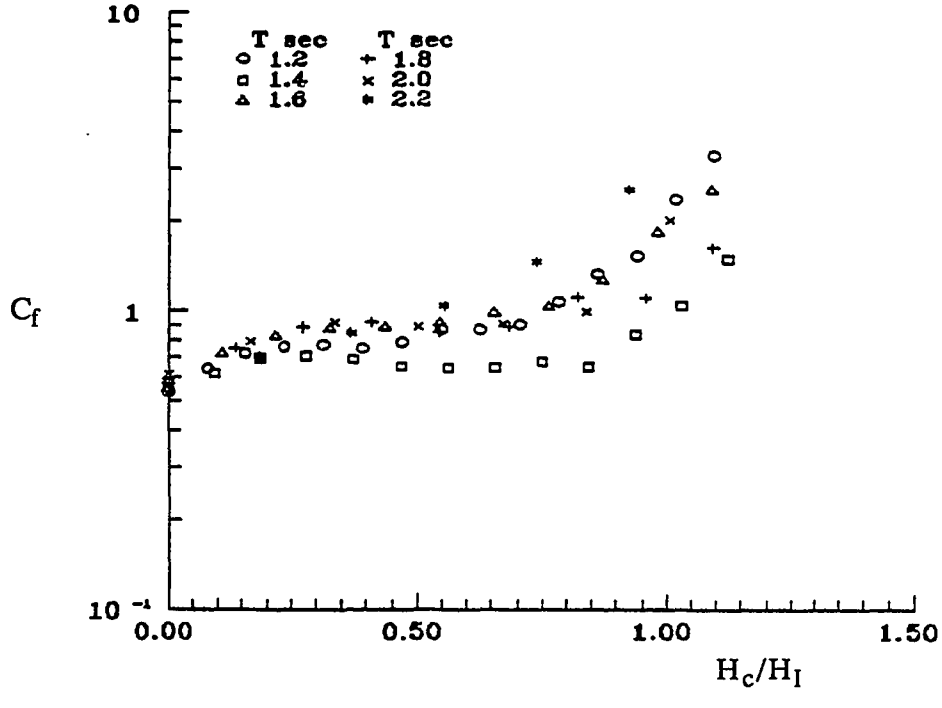

Figure 65 , Discharge coefficient C_f for H_c/H_I (Case 1)

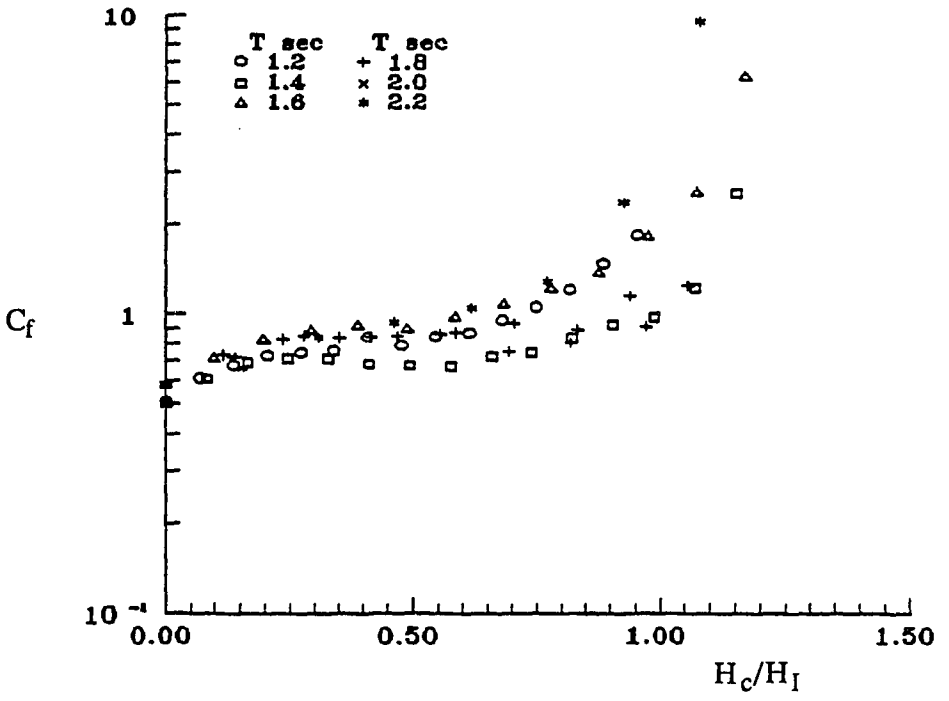

Figure 66 , Discharge coefficient C_f for H_c/H_I (Case 2)

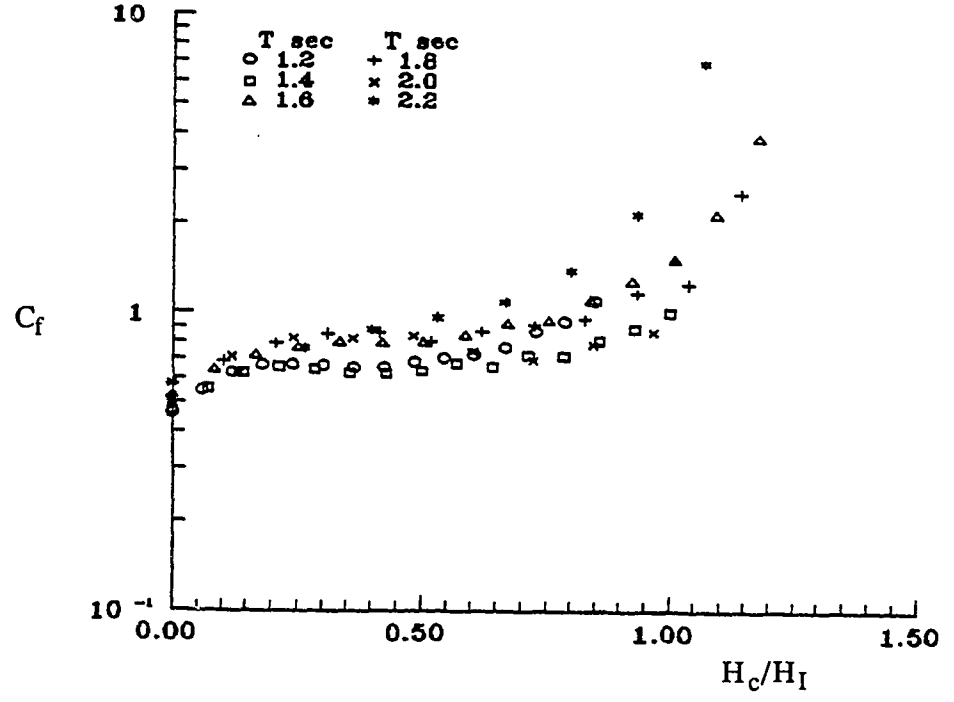

Figure 67 , Discharge coefficient C_f for H_c/H_I (Case 3)

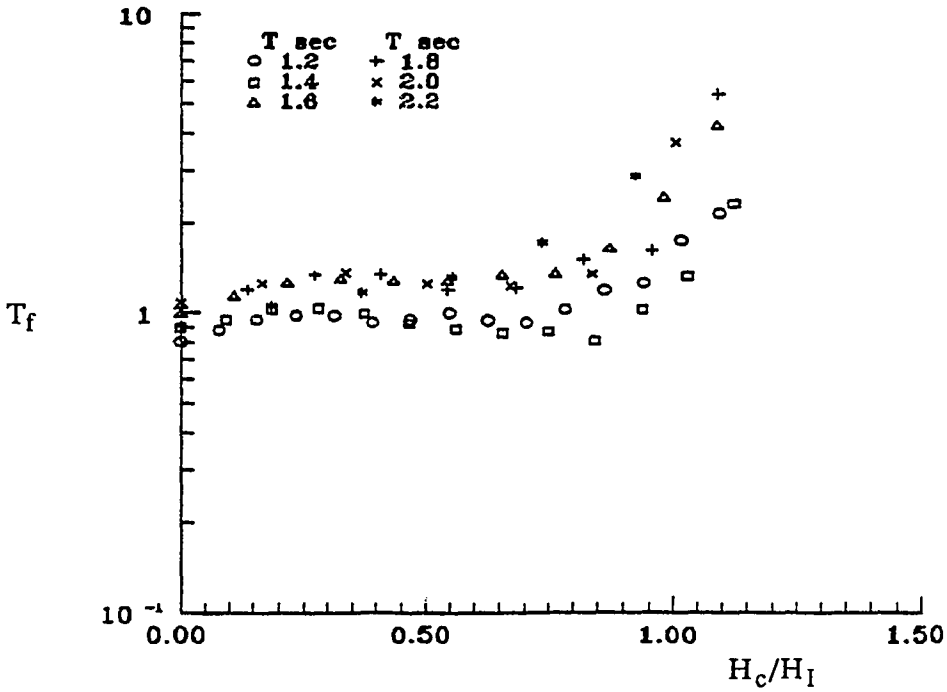

Figure 68 , Transfer coefficient T_f for H_c/H_I
(Case 1)

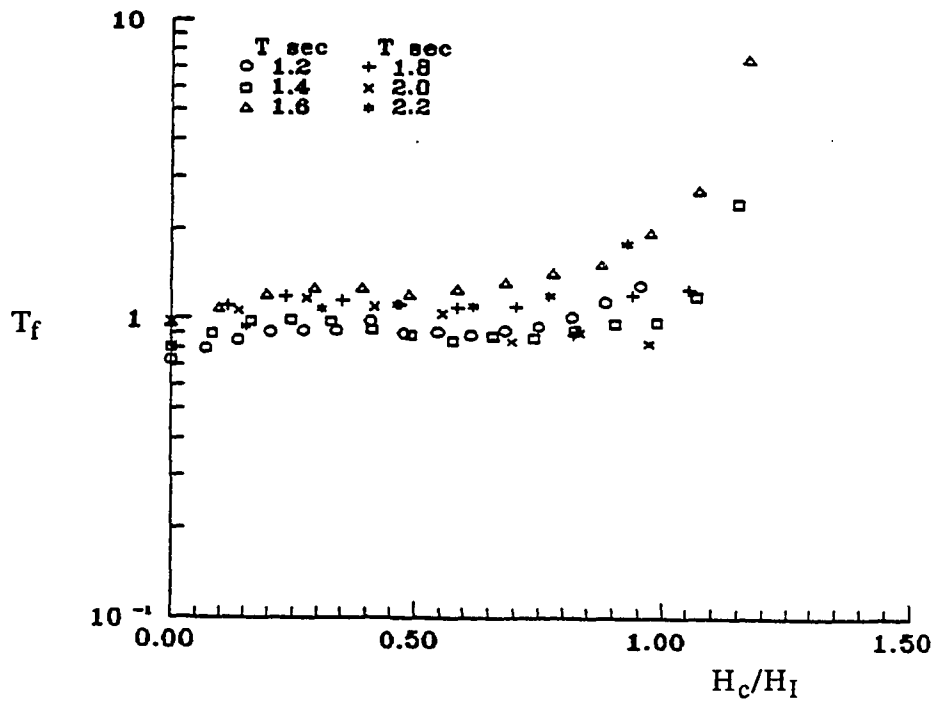

Figure 69 , Transfer coefficient T_f for H_c/H_I
(Case 2)

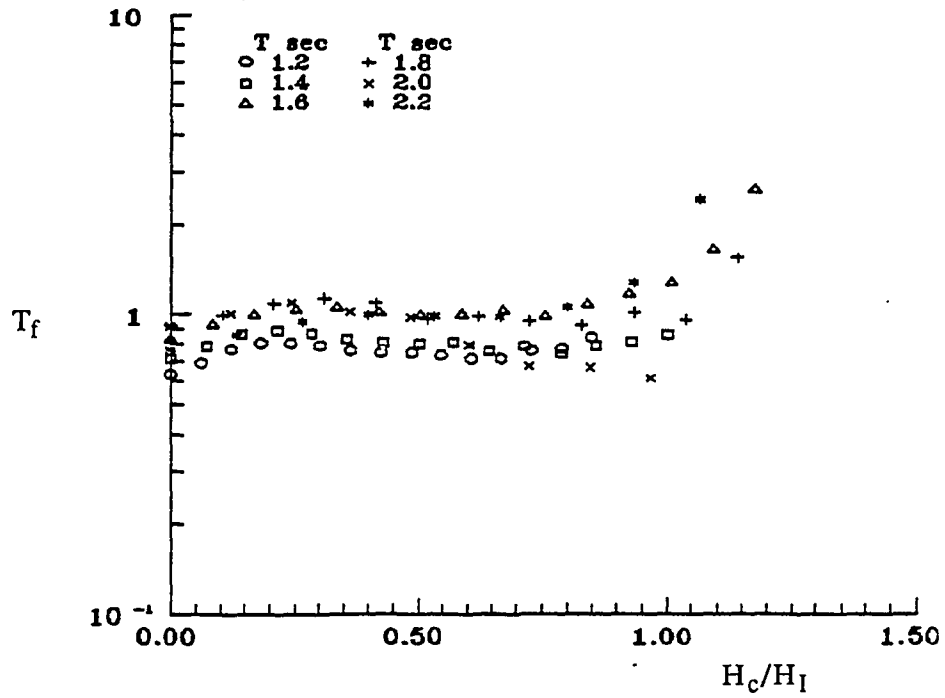

Figure 70 , Transfer coefficient T_f for H_c/H_I (Case 3)

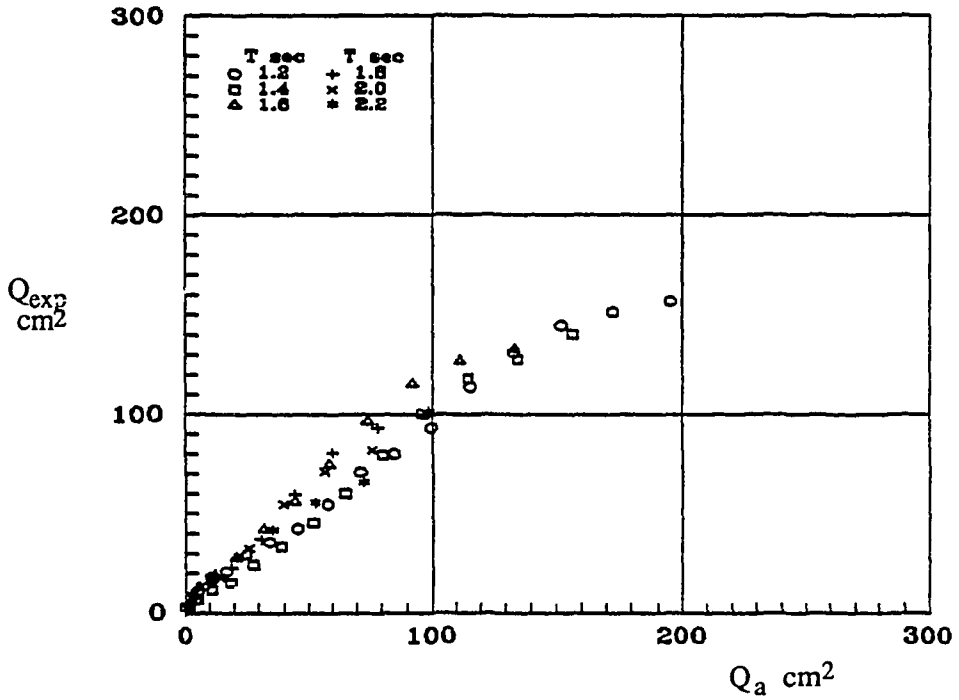

Figure 71 , Volume of overtopping (Case 1) Theory Q_a and Measurement Q_{exp}

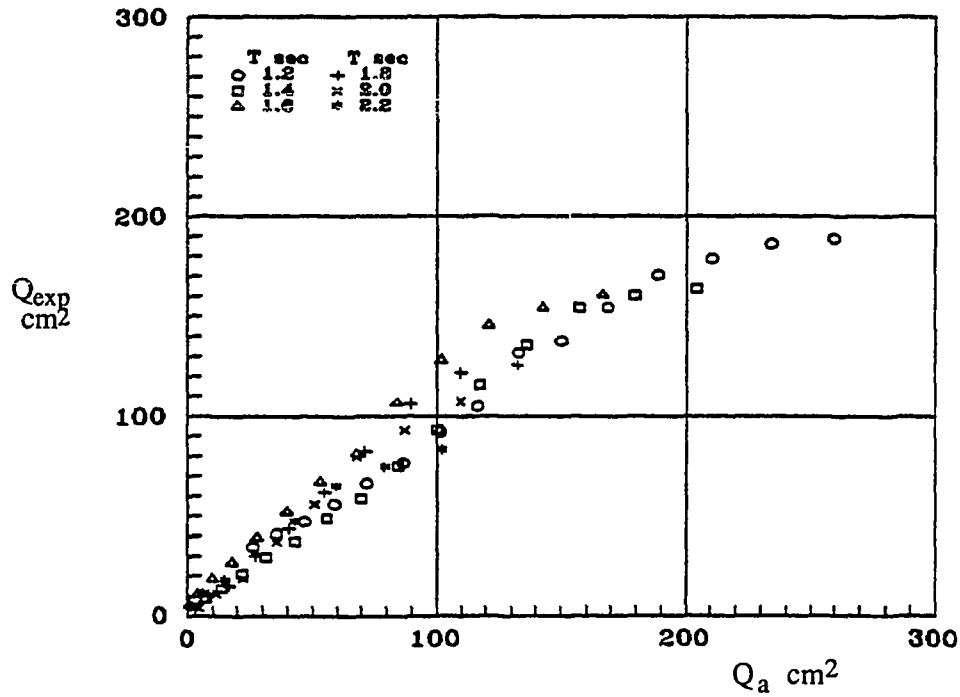

Figure 72 , Volume of overtopping (Case 2)
Theory Q_a and Measurement Q_{exp}

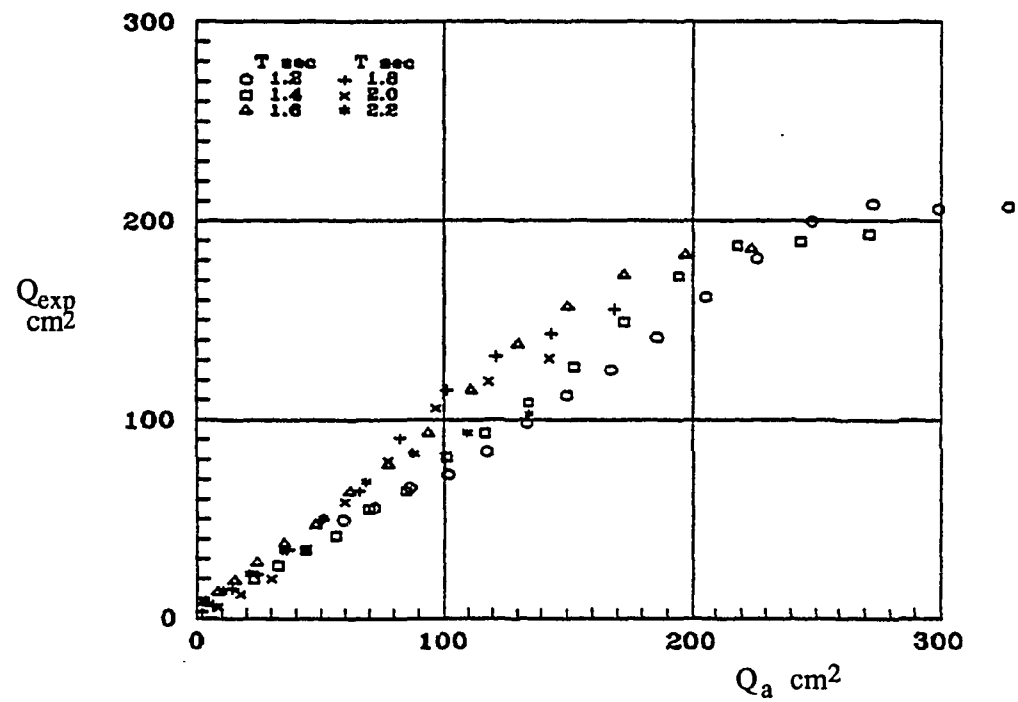

Figure 73 , Volume of overtopping (Case 3)
Theory Q_a and Measurement Q_{exp}

CHAPTER VI
CONCLUSIONS

6.1 General

The major objective of this investigation was to study the influence of wave overtopping on the waves facing a vertical breakwater and to develop a prediction model for the total amount of wave overtopping. Some theories have been developed related to the phenomena of partial standing waves and wave overtopping, and compared with experimental results from hydraulic models. The study consisted of: (a) a review of finite amplitude partial standing wave theories and their application to wave overtopping conditions, and a comparison with laboratory data of free surface elevations measured in a wave channel; (b) an investigation of the mean surface level, the wave reflection and the effect on incident wave height by the influence of wave overtopping; (c) a comparison of obserbed wave crest and wave trough levels with predictions by Endo and Miura; (d) an establishment of a method to calculate the total amount of wave overtopping which will be in correspondence with laboratory experiments.

This investigation included two major areas of emphasis; the partial standing waves and the amount of wave overtopping.

6.2 Partial Standing Waves

The theory of partial standing waves by Goda and Abe was reviewed to be adapted to the use in the overtopping condition and applied to some specific wave conditions with a different height of breakwater. The following are the conclusions that were drawn from this study.

1. The theoretical formula of the partial standing waves by Goda and Abe (1968) describes the surface displacement reasonably well when wave overtopping does not occur (λ=1), except near crest and trough level. This formula is in perfect agreement with the third order approximation by Tadjbaksh and Keller (1960). The higher order approximation (fourth order) by Goda and Kakizaki (1966) draws the wave profile more accurately in no overtopping (perfect standing wave) condition.

2. The experimental free surface profile changes abruptly when wave overtopping occurs over the crest of the breakwater. This tendency becomes more prominent for lower values of H_c. No existing theory was available to describe the surface profile in the overtopping condition, and therefore a new method has been suggested to express the influence of wave overtopping on the wave profile. The resultant equation of surface displacement agreed reasonably well with experimental results during wave overtopping tests.

3. The reflection coefficient K_R and the ratio between the initial wave height to the incident wave height affected by overtopping K_I can be predicted from the proposed wave equation,

for different crest levels of the breakwater. When the crest of the breakwater is at the still water level, the coefficients K_R and K_I are about 0.35 and 1.0, respectively. The reflection coefficient K_R tends to increase linearly and the coefficient K_I to decrease linearly with the increase of H_c. Finally the reflection coefficient K_R slowly approaches 1.0 for higher crest elevations of the breakwater and the coefficient K_I starts increasing again after $H_c/H_I=0.6$.

4. The wave crest level in the overtopping condition can be expressed by an experimental equation as a function of the wave height in the non-overtopping condition and the height of the breakwater H_c. The height of the breakwater has a strong influence on the wave crest level and a weak influence on the wave trough level at the vertical wall. The wave crest level increases in proportion to the rising height H_c while the wave trough level decreases with the increase of H_c and the initial wave height H_I. These results well describe the experimental results which were measured at the wall of the breakwater in the channel.

6.3 Wave Overtopping Quantities

A model to predict the total amount of wave overtopping was developed, based on an energy consideration, which relates the mean velocity of the overtopping flow to surface elevations in the non-overtopping and overtopping conditions. Based on the results of this analysis, the following conclusions and recommendations for future study can be drawn.

1. It is suggested that equation (3.92) describes the rate of flow in the overtopping condition.

2. This equation can not be solved analytically and therefore numerical calculations were carried out by the use of Simpson's method.

3. The agreement between measurements of overtopped water quantities and computed values using equation (3.92) for T_f=1 is reasonable in most cases, suggesting that the model can be used to determine the total amount of wave overtopping.

4. It was assumed in the model that the discharge at the vertical wall can be responsible for both the mean waver velocity defined in equation (3.90) and the cross section. Therefore it is recommended that further investigations be made to measure the velocity distribution in overtopping flow at the vertical wall in order to have a better understanding of the mechanism.

5. The measurement of the quantity of wave overtopping for higher values of H_c, when the amount of wave overtopping is very small, has a higher degree of inaccuracy because a point gauge is used to determine the water level in the measuring tank. Future work to measure this quantity in greater detail would be beneficial.

6. This investigation did not treat the case of wave breaking; however this aspect of the process is of great importance and further work to incorporate this aspect into a wave overtopping model is recommended.

REFERENCES

Airy,G.B: Encyc. Metrop. "Tides and Waves", 1845.

Dean,R.G. and Dalrymple,R.A.: Water Wave Mechanics for Engineers and Scientists, Prentice-Hall, 1984, 353pp.

Endo,S. and Miura,A.: "Experimental Study on Sea Wave Movement Facing a Vertical Wall", Report of Res. Inst. of Industrial Tech., Nihon Univ., No.14,1983, 20pp.

Fultz,D.: "An Experimental Note on Finite-Amplitude Standing Gravity Waves", J. Fluid Mech., Vol.13, 1962, pp.193-212.

Goda,Y.: "The Fourth Order Approximation to The Pressure of Standing Waves", Coastal Eng. in Japan, Vol.10, 1967, pp.1-11.

Goda,Y. and Abe,Y.: "Apparent Coefficient of Partial Reflection of Finite Amplitude Waves", Report of Port and Harhour Res. Inst., No.3, 1968, 58pp.

Goda,Y. and Kakizaki,S.: "Appearance of Double Crest Pressure on Standing Waves (in Japanese)", Coastal Eng. Japan, 12th, 1965, pp99-105.

Goda,Y. and Kakizaki,S.: "Study on Finite Amplitude Standing Waves and Their Pressure upon A Vertical Wall", Report of Port and Harbour Res. Inst., No.10, 1966, 57pp.

Hamada,T.: "The Secondary Interactions of Surface Waves", Report of Port and Harbour Res. Inst., No.10, 1965, 28pp.

Hamada,T.: "The Secondary Effect of Surface Wave (in Japanese)", Coastal Eng. Japan, 11th, 1965, pp.12-14.

Hom-ma,M. and Aki,K.: Mononobe Hydraulics (in Japanese), Iwanami, 1962, 660pp.

Horie,M.:"The Volume of Wave overtopping exceeds a vertical wall of upright breakwater (in Japanese)", B.Eng. thesis, Dept. of Civil Eng., Nihon Univ., Industrial Tech., 1981.

Horikawa,K.: Coastal Engineering, Tokyo Univ. Press., 1973.

Iwagaki,Y., Shima,A. and Inoue,M.: "Effects of Wave Height and Sea Water Level on Wave Overtopping and Wave Run-up", Coastal Eng. in Japan, Vol.8, 1965, pp.141-151.

Kikkawa,H., Shi-igai,H. and Kono,T.: "Experimental Study on Wave Overtopping over A Vertical Wall (in Japanese)", Proc. Ann. Conf. JSCE, 1966, 118/1-118/3.

Kikkawa,H., Shi-igai,H. and Kono,T.: "Foundmental Study of Wave Overtopping on Levees", Coastal Eng. in Japan, Vol.11, 1968, PP.107-114.

Longuet-Higgins,M.S. and Stewart,R.W.: "Radiation Stress in Water Waves; A Physical Discussion with Application", Deep Sea Res., Vol.2, 1964, pp.529-562.

Masuda,S.: "Characteristics of Waves on Wave Overtopping (in Japanese)", B.Eng. thesis, Dept. of Civil Eng., Nihon Univ., Industrial Tech., 1981.

McCormick,M.E.: Ocean Engineering Wave Mechanics, John Wiley & Sons, 1973.

Miche,M.: "Mouvements Ondulatoires de la Mer en Profondeur Constante on Dicroissante", Annales des Ponts et Chaussee, 1944.

Penney,W.G. and Price,A.T.: "Finite Periodic Stationary Gravity Waves in A Perfect Liquid", Phil. Trans., Series A, Vol.244, 1952, pp.254-284.

Sainflou,G.: "Essai sur Les Diques Maritimes Verticales", Annales des Ponts et Chaussee, 1928.

Saville,T. and Caldwell,J.M.: "Experimental Study of Wave Overtopping on Shore Structures", Proc. IAHR., 1953, pp.261-269.

Shi-igai,H. and Kono,T.: "Analytical Approach on Wave Overtopping on Levees", Proc. Conf. Coastal Eng., 12th, 1970.

Shi-igai,H. and Rong-Chung,H.: "An Analytical and Computer Study on Wave Overtopping", Coastal Eng., Vol.1, 1977, pp.221-241.

Sibul,O.J.: "Flow over Structure by Wave Action", Trans.A.G.U., 36(1), 1955, pp.61-69.

Stokes,G.G.: "On the Theory of Oscillatory Waves", Cambridge Trans. Vol.8, 441, 1847.

Stokes,G.G.: " Supplement to a Paper on the Theory of Oscillatory Waves", Mathematical and Physical papers, I, Cambridge University Press., 1880, pp.314-326.

St.Venant,B. and Flamant,A.: "Du la houle et du clapotis", Annales des Ponts et Chaussee, 1888.

Tadjbaksh,I. and Keller,J.B.: "Standing Surface Waves of Finite Amplitude", J. Fluid Mech., Vol.8, 1960, pp.442-451.

Takada,A.: "On Relations among Wave Run-Up, Overtopping and Reflection (in Japanese)", Proc. JSCE, 182, 1970.

Takada,A.: "Relevancy between Run-Up of Wave Overtopping and Reflection (the third report, in Japanese)", Coastal Eng., 18th, 1971, pp.249-258.

Takada,A.: "Wave Overtopping Quality Correlated to The Surface Elevation of Finite Amplitude Clapotis (in Japanese)", JSCE, Vol.201, 1972, pp.61-76.

Takada,A.: "Wave Overtopping Quantity correlated to the Special Profile of Run-Up Waves (in Japanese)", Proc. JSCE, Vol.212, 1973, pp.25-39.

Technical Advisory Committee on Protection against Inundation: Wave Run-Up and Overtopping, Goverment Publishing Office, the Hague, 1974, 176pp.

Tsuchiya,Y. and Yamaguchi,M.: "Basic Study of Finite Amplitude Standing Waves(3) (in Japanese)", Bull. Disas. Prev. Res. Inst., Kyoto Univ., No.13B, 1973, pp.391-407.

Tsuchiya,Y. and Yamaguchi,M.: "Characteristics of Standing Waves in Overtopping Condition (in Japanese)", Coastal Eng. Japan, 17th, 1970, pp.79-84.

Tsuruta,S. and Goda,A.: "Expected Discharge of Irregular Wave Overtopping", Proc. Conf. Coastal Eng., 11th,1969, pp.833-952.

U.S.Army, Coastal Engineering Research Center: Shore Protection Manual, U.S. Goverment Printing Office, Washington D.C., 1983.

Umeyama,M. Endo,S. and Gerritsen,F.: "Wave Overtopping on Coastal Structure", Natural and Man-Made Coastal Hazards, Proceedings, pp.160-165, 1988.

Urabe,K.: "Characteristics of Waves by Wave Overtopping (in Japanese)", B. Eng. thesis, Dept. of Civil Eng., Nihon Univ, Industrial Tech., 1980.

Weggel,J.R.: "Wave Overtopping Equation", Proc. Conf. Coastal Eng., 15th, 1976.

Wiegel,R.L.: Oceanographical Engineering. Prentice-Hall, 1964, 527pp.